BIOGEOGRAPHY AND GENETIC VARIATION OF TRIATOMINE CHAGAS DISEASE VECTORS AND *Trypanosoma cruzi* ISOLATES FROM TEXAS

A Dissertation

by

SONIA ALANE KJOS

Submitted to the Office of Graduate Studies of
Texas A&M University
in partial fulfillment of the requirements for the degree of

DOCTOR OF PHILOSOPHY

May 2007

Major Subject: Entomology

BIOGEOGRAPHY AND GENETIC VARIATION OF TRIATOMINE CHAGAS DISEASE VECTORS AND *Trypanosoma cruzi* ISOLATES FROM TEXAS

A Dissertation

by

SONIA ALANE KJOS

Submitted to the Office of Graduate Studies of
Texas A&M University
in partial fulfillment of the requirements for the degree of

DOCTOR OF PHILOSOPHY

Approved by:

Co-Chairs of Committee,	Jimmy K. Olson
	Craig J. Coates
Committee Members,	Thomas M. Craig
	Karen F. Snowden
	Pete D. Teel
Head of Department,	Kevin M. Heinz

May 2007

Major Subject: Entomology

ABSTRACT

Biogeography and Genetic Variation of Triatomine Chagas Disease Vectors and *Trypanosoma cruzi* Isolates from Texas. (May 2007)

Sonia Alane Kjos, B.S., University of Minnesota;

M.S., The University of Texas School of Public Health

Co-Chairs of Advisory Committee: Dr. Jimmy K. Olson
Dr. Craig J. Coates

Trypanosoma cruzi is endemic in the U.S., infecting humans, dogs, and wildlife. This study identified a new geographic distribution for triatomine species within Texas based on 2,449 records obtained from published data and new field studies. Triatomine vectors of *T. cruzi* were reported from 97 counties covering all ecological zones. *Triatoma gerstaeckeri* was the most commonly collected species followed by *T. sanguisuga*. New field collections resulted in 233 specimens from 37 counties and a 52% *T. cruzi* infection rate. A second trypanosome, *Blastocrithida triatomae* was found in two specimens from different locations. A habitat suitability model for *T. gerstaeckeri* was developed using GIS and remote sensing applications. Forest and rangeland were the predominant land cover classes found within *T. gerstaeckeri* habitat, where as water and agriculture proved to have little influence on habitat suitability.

Genetic variation of seven triatomine species from Texas was evaluated using cytochrome *b* DNA sequences from 61 new specimens. This is the first study of the taxonomic status of *T. gerstaeckeri, T. indictiva*, and *T. neotomae* using molecular

markers. Intraspecific variation for *T. sanguisuga* and *T. gerstaeckeri* suggests significant gene flow across their ranges within Texas.

Genetic variation of *T. cruzi* isolates from Texas was evaluated using SSU rRNA gene sequences. Included were 63 new sequences from five triatomine species, canine, baboon, and human isolates. Sequences partitioned into two groups in agreement with previous studies on U.S. isolates. Genetic variation of *T. cruzi* did not occur according to host, geographic location, or collection site.

The extent of Chagas disease in domestic canines of Texas is described by geographic distribution, signalment, and clinical presentation and histopathology. Based on data from 553 cases, the geographic distribution in Texas is widespread (46 counties) and closely matches the distribution of the Triatomine vectors. Chagas disease was diagnosed in 33 breeds, primarily sporting/working dogs.

This study represents the most comprehensive characterization of components of the Chagas disease transmission cycle in the U.S. to date. These findings should raise awareness among physicians, veterinarians, and public health practitioners regarding *T. cruzi*, its vectors, canine infection, and human risk for Chagas disease in Texas.

To my parents

who gave me a wonderful sense of home to carry with me through all my journeys

ACKNOWLEDGMENTS

I am grateful to my committee members for giving me the flexibility and support to create a project with broad coverage of an area largely unfamiliar to all of us. My hope is that our efforts will raise awareness (especially among funding agencies) that there are “neglected diseases” of public health concern within our own national boundaries. I am thankful to Craig Coates for providing overall direction for the molecular studies and for his confidence in my ability to master a new skill set. I am thankful to Pete Teel for providing helpful input on spatial modeling, assisting me with securing a position as a teaching assistant, and for promoting a positive working environment within the department. I am thankful to Tom Craig for providing me with a long list of contacts which proved to be invaluable to my field studies. I will be forever grateful for his gift of the out-of-print Lent and Wygodzinsky key to Triatominae of North America and for letting me invade the peace and quiet of his office space to microscopically explore the amazing world of the triatomine hindgut. I am thankful to Karen Snowden for opening her research laboratory and budget to support me. She provided a very supportive environment that facilitated my training in a long list of molecular and non-molecular techniques and allowed me to explore areas outside the original scope of my project. I greatly appreciate her efforts in pursuing a funded position for me at TAMU and always maintaining an air of optimism about my future prospects. Finally, I am very thankful to Jim Olson, the reason I came to TAMU. I am fortunate to have observed his skills in organismal and field entomology practices and the application of these components to understanding and preventing vectorborne

disease transmission. His dedication to service whether it be to students or the public or private sectors is truly admirable and a testament to a style where understanding human nature is as important as understanding mother nature when pursuing scientific advances in the prevention of vectorborne disease.

I have many people to thank for contributing their time or resources to my project. Kathleen Logan provided daily guidance in the lab on all things molecular. Her patience and life-is-good demeanor made coming to work a joy. I owe a great deal of thanks to Joe Gillespie who was the wizard behind the phylogenetic analyses and to his wife Annika for sharing his time amidst all the activity surrounding the arrival of Griffin. His humor and enthusiasm kept my sanity intact during the final months of my research. He is on a trajectory for greatness, no doubt. Thanks also to Ed Riley and Roy Vogtsberger for access to the Triatominae collections at TAMU and Midwestern State University, respectively, and for backyard bug specimens from Ed. I've had many great instructors and advisors at TAMU including Bob Wharton who supported me financially for a year and always showed an interest in my project, Bob Coulson who provided printing resources and access to Maria Tchakerian who assisted me with ArcGIS and FRAGSTATS issues, Sorin Popescu who provided helpful feedback on the GIS/RS modeling chapter, and Joe Schaffner who shared his stories and expertise on reduviids. I am grateful to Leon Russell for seeing my potential as a lecturer in his epidemiology courses and giving me my first job at TAMU.

Many thanks to John Abbott for inviting me on his UT summer course field trip to West Texas and for providing access to their Triatominae collection. Thanks to

Everett Simmons for introductions to the UT folks (including Al Hook who generously provided samples and suggestions for field collection sites) and facilitating access to the Wild Basin Nature Preserve's Triatominae collection. His enthusiasm for the study of kissing bugs and Wiggelsworth was contagious. Cynthia Chappell and Steve Waring from the University of Texas School of Public Health at Houston generously provided four *T. cruzi* culture isolates which greatly enhanced the section on genetic diversity of Texas parasite isolates. A special thanks to Drs. Jon Taylor and Sherrie Hartke for supplying additional canine tissue.

In the public realm, a number of individuals at the Texas Department of State Health Services and Texas Veterinary Medical Diagnositic Laboratory were instrumental in the success of my research. Roy Burton provided a treasure trove of vintage journal articles and documents that filled in many details on the history of the disease in Texas. Jim Schuermann and Eric Fonken facilitated my designation as the entomologist responsible for identification and testing of all triatominae specimens submitted to TX DSHS. Many thanks to Laura Robinson, Greg Pye, Taffi Tull, Richard Klein, James Wright, and Max Coats for generously providing specimens and spreading the word about my research. We regretfully said goodbye to Greg Pye last year, a gentle soul with great knowledge of and respect for the flora and fauna of Texas. A special thanks to Taffi who welcomed me to her home multiple times to hunt for bugs and take in the beautiful setting. Thanks also to Glenna Teltow who provided initial training on bug processing and later provided specimens and to Robyn Seiferth for supplying data on bug testing at TX DSHS. At TVMDL, thanks to Dr. Arturo Angulo for IFA training and

to Drs. Barbara Lewis and Norman Ronald for canine data. Finally, thanks to Ellen Dotson at CDC who provided advice on molecular analysis of both *T. cruzi* and triatomine bugs.

I am grateful to a long list of Texas residents that supplied bug specimens and shared their experiences regarding bug encounters or canine Chagas disease. I am especially thankful to those who allowed me access to their property for collecting, many of whom hosted me overnight, including Rachel Allenby, Dorthea and Mick Robinson, Noel Troxclair, Mike Hassell, Forrest Mitchell, Linda and Tom Smith, the Georgacakis', Dorrie and Gil Hodge, and Melissa Priddy. Thanks to Billie Snider for securing access to Hugh Ramsey Nature Park for collecting. Many thanks to Aaron Smith for collecting specimens of the rarer species on his quest for tenebrionids.

The final acknowledgements are reserved for my family whose emotional support and encouragement made this adventure possible. Thanks to mom and dad who never doubted my choices and showed by example that it's never too late to make a career change in the pursuit of happiness. Thanks to Del and Ted for sharing my enthusiasm for the exploration of new frontiers and thereby making our individual adventures appear quite normal to our parents. Thanks to Colson for his support and understanding of his mom's crazy plan to change careers to one with a much lower earning potential. His dedication to following his dreams in music has been an inspiration to me. Finally, thanks to Steve for sharing this journey with me on a daily basis. His ability to level the great expanse of mountains that surfaced along the way was truly remarkable. It would have been a long and lonely road without him.

TABLE OF CONTENTS

CHAPTER Page

LIST OF FIGURES

FIGURE Page

LIST OF TABLES

TABLE Page

CHAPTER I

INTRODUCTION

Chagas disease, caused by the hemoflagellate protozoan parasite, *Trypanosoma cruzi*, poses a significant public health threat in the western hemisphere. The prevalence of human infection is estimated to be 12 million cases, with another 90 million people at risk of infection.[1] In addition to the morbidity and mortality suffered by the infected individuals, Chagas disease burdens the strained economies of the endemic Latin American countries, with medical costs and a loss in productivity estimated at $6.5 billion annually.[2]

Following Carlos Chagas' clarification of the epidemiology of the disease in 1909[3], researchers discovered the organism and its triatomine bug vectors in diverse ecological niches throughout the tropical and subtropical regions of North and South America, approximately between the latitudes of 42°N and 46°S.[4] *T. cruzi* has adapted to life in various mammalian tissues in an extremely wide range of hosts in multiple transmission cycles.[5] Although transmission routes of the parasite to humans include blood transfusion, organ donation, ingestion, or transplacentally, greater than 80% of all human cases are vectorborne.[6]

T. cruzi is transmitted by members of the Triatominae subfamily (Hemiptera: Reduviidae), which are obligate blood feeders in all post-egg stages. Transmission

---

This dissertation follows the style of *The American Journal of Tropical Medicine and Hygiene*.

occurs when an infected bug defecates on or near the host during or shortly after feeding; and the fecal material is subsequently rubbed into the bite wound, broken skin, or mucosal tissue.[7] Like the parasite they vector, triatomine bugs utilize a wide range of mammalian hosts. Many triatomine species also readily feed on birds and reptiles. All species of Triatominae are considered potential vectors of *T. cruzi*.[8] Due to the lack of a vaccine or highly efficacious treatment, prevention of Chagas disease is primarily dependent on the control of domiciliated triatomine vectors.[6, 9]

In 1916, shortly after Chagas' discovery, Kofoid and McCulloch initiated research efforts in the United States by their isolation of *T. cruzi* from an indigenous triatomine bug in California.[10] Of the 130 species currently recognized in the subfamily Triatominae[11], 11 have been reported in the southern half of the United States, seven in the state of Texas.[12] The data on prevalence of *T. cruzi* in U.S. vectors are primarily derived from specimens collected in Texas, California, and Arizona, with infection rates ranging from 17-48%, 14-40%, and 7.1-20.5%, respectively.[13, 14, 15, 16, 17, 18, 19, 20] *Trypanosoma cruzi*-infected vectors have also been found in Florida, Georgia, Alabama, Tennessee, and Louisiana.[21, 22, 23, 24, 25] Accounts of triatomine bugs encountered inside houses have been reported from Oklahoma, California, Texas, Florida, Tennessee, and Alabama.[21, 23, 24, 26, 27, 28]

An abundance of cross-sectional data on reservoir hosts in the United States has accumulated throughout the 20th century. In the southern United States, *T. cruzi* infections in wild populations of opossums, wood rats, raccoons, armadillos, and coyotes have been reported for the past 70 years.[15, 18, 22, 23, 29, 30, 31, 32, 33, 34, 35, 36] Acute and

chronic infections in dogs have been reported in Texas, Oklahoma, Louisiana, Virginia, South Carolina, Georgia, and Tennessee.[24, 37, 38, 39, 40, 41, 42, 43] Seroprevalence studies in domestic canines have been published from Texas (2.6-8.8%), Oklahoma (3.6%), Louisiana (2.3-4.7%), and Georgia, in combination with other southeastern states (2%).[18, 40, 43, 44, 45] Domestic canines in South and Central America are considered an important reservoir in the domestic transmission cycle,[46, 47] and serve as surveillance sentinels for human infection.[48] It has been shown that dogs have a higher capacity to infect triatomine bugs than humans due to persistent parasitemia, further supporting their reservoir role in the disease cycle in domestic settings.[49, 50] Although the importance of dogs as Chagas disease reservoirs in the U.S. has not been well characterized, there is some evidence to support their involvement in domestic transmission. Seropositive dogs were found in close proximity to two locally-acquired human cases in the U.S.[24, 28] A thorough characterization of canine Chagas disease in the U.S., including mode of transmission and demographic and clinical profiles, will greatly enhance our ability to estimate human infection risk.

Prevalence of human Chagas disease in the U.S. is substantially lower than in Latin America. Reports of five U.S. cases have been published since 1955, three being from Texas.[24, 27, 51, 52] Two additional cases were identified in 2006, one in Louisiana[53] and one in Texas.[54] There have been few human seroprevalence surveys for *T. cruzi* in the U.S, and their rates (0 to 2.4%) are difficult to interpret due to the possible inclusion of infected immigrants from endemic countries.[18, 55, 56, 57, 58, 59] A 1965 serologic study of 132 residents of Corpus Christi, Texas, with a known history of bites produced three

positive results[58], and a 1974 study of a tribe of Native Americans residing in Arizona produced 19 positives out of 452 individuals tested for *T. cruzi* antibodies.[60]

Theories for the low incidence of vectorborne human Chagas disease cases in the U.S. compared to Latin America include low virulence of native strains, less efficient bug vectors, and reduced contact with vectors due to better housing construction.[61] However, U.S. strains of *T. cruzi* have proven to be virulent as confirmed by clinical disease and death in dogs, primates, and humans.[37, 38, 52, 62, 63, 64] There is also evidence that close association between humans and triatomine bugs in the U.S. does occur. A study among California residents of a rural community revealed that 20% of participants had anti-*Triatoma protracta* saliva antibodies, an indigenous triatomine species of the western U.S.[65] Incidence of human triatomine bites are frequently reported, including severe hypersensitivity reactions.[23, 66, 67, 68]

Regardless of the low number of recognized human cases, the Chagas disease cycle is well-established in the U.S., and, like all ecological systems, is subject to change whether caused by manmade or natural forces. In this regard, human encroachment of the enzootic life cycle of *T. cruzi* in the U.S. should be a concern, as exemplified by the relatively recent emergence of Lyme disease in the northeast and upper Midwest due to human-driven changes including reforestation and construction of residences in and near vector habitats.[69, 70] As residential areas continue to expand into wildlife habitats, humans and their pets will be at increased risk for exposure. The adaptability of sylvatic triatomine species to human dwellings has been demonstrated in the Amazon basin area of Brazil where there has been a surge of new construction in previously undeveloped

areas. Although spillover from the sylvatic cycle has been the primary cause of human cases in these areas, a trend towards increased risk of transmission due to permanent human invasion and destruction of wildlife habitats has been observed.[71, 72] The popularity of sport hunting in the U.S. may also pose increased transmission hazards through exposure to infected mammalian tissues and relocation of wildlife reservoirs to replenish game preserves.[30, 44]

The influence of landscape characteristics on vectorborne disease cycles has long been recognized. The melding of landscape ecology and epidemiology was forged in the mid-1900s by Europeans such as Pavlovsky who developed the concept that natural disease foci are small scale regions driven by the entire ecosystem on a larger scale.[73] The introduction of geospatial methods utilizing remote sensing and geographic information systems (GIS) technology has greatly enhanced the study of spatial and temporal aspects of infectious disease in relation to landscape ecology.[74, 75, 76, 77] Application of statistical methods provides a basis for evaluating spatial relationships, the outcome of which could lead to development of disease transmission risk maps and predictive models. Within the past decade, the use of geospatial methods has greatly enhanced our understanding of and control efforts for vectorborne diseases including malaria[78], onchocerciasis[79], Rift Valley Fever[80], and Lyme disease[81] among many others in an expanding list. The application of geospatial methods to the study of Chagas disease is also beginning to emerge. Computerized vector distribution maps, vector ecological niche modeling, and disease transmission risk modeling have been applied to

several regions in Latin America to aid in Chagas disease vector control and disease prevention efforts.[82, 83, 84, 85]

In the U.S., little work has been done to thoroughly characterize the geospatial attributes of triatomine species and *T. cruzi* isolates. Usinger (1944)[86] and Lent and Wygodzinsky (1979)[12] rarely provide species distribution data below the state level in their widely-cited works on Triatominae. Prior to 1970, several notations on the collection sites of U.S. triatomine species and *T. cruzi* infection rates were published[16, 19, 61, 87, 88, 89, 90], but these surveys were primarily focused in small regions of the southwestern U.S. Recently, an ecological niche-modeling approach was used to predict the distribution of *Triatoma gerstaeckeri*, a vector species implicated in Chagas disease transmission in both the U.S. and Mexico.[85] However, due to the small number of field collection sites used to create the model, the resulting prediction map inadequately reflected other known collection sites for this species.[91] The application of sophisticated analyses to inadequate data sets will not advance the study of Chagas disease. There is a need for a contemporary, comprehensive analysis of the geospatial characteristics of the U.S. Chagas disease cycle, starting with a thorough compilation of distribution records.

The recent introduction of West Nile Virus into the U.S. is a reminder that the proliferation of new pathogens through indigenous vector species is possible.[92, 93] The successful infection and passage of a foreign strain of *T. cruzi* in a U.S. triatomine species provides evidence that the introduction of new *T. cruzi* strains in the U.S. is plausible.[94, 95] An estimated 25,000-75,000 Latin American immigrants infected with *T. cruzi* residing in the U.S. represent a potential source of infection to both indigenous

vectors and blood transfusion/organ transplant recipients.[96] With four published cases of blood transfusion-transmitted Chagas disease[97, 98, 99] and five organ transplant cases[100, 101] in the U.S., the American Red Cross resolved to implement a *T. cruzi* screening test for all donated blood at a cost of $50-100 million per year.[102] A *T. cruzi* diagnostic test was recently approved by the FDA for this purpose.[103, 104]

In addition to human transport of virulent *T. cruzi* strains into the U.S., movement of triatomine species and vertebrate reservoirs provides a viable route for introduction of exotic strains. Unlike humans, most free-living systems are not restricted by manmade geographic boundaries. Mexico and the U.S. share the distributions of at least eight triatomine species.[12] Chagas disease is a public health issue in Mexico, with an estimated 1.6 million infected people.[72] A recent study among U.S. blood donors living in two Texas cities located near the Mexican border (McAllen and El Paso), revealed a 1.3% *T. cruzi* seroprevalence rate.[105] The contiguous land mass and bi-directional flow of human and animal traffic between the U.S. and Mexico presents an opportunity for exchange of parasites, vectors, and reservoirs.

A multi-faceted approach to the characterization of Chagas disease in the U.S. is required to understand the complex dynamics of its transmission cycle. Analysis of the spatial distribution of triatomine species and *T. cruzi*-infected vectors and vertebrate hosts should be approached from a molecular perspective as well. Data on the genetic variation of both the vector species and pathogen may provide clues to behavior, population structure and movement, and virulence. The use of molecular methods to explore the genetic variation in triatomine bugs lags behind similar studies in mosquitoes

and other disease vectors.[106] The impetus for the use of molecular methods to study genetic variation in triatomine species is the need for improved vector surveillance of treated areas to maintain effective disease control programs.[107] It is critical to determine if triatomine bugs detected in follow-up surveys are new invaders or residual survivors. New invaders are usually species that are sylvatic in colonization behavior. Discovery of new invaders is an indication that insecticidal spraying will have to be broadened to include surrounding sylvatic areas to prevent continued reinfestation.

Identification of triatomine species and distinction of subgroups within species is critical to the control effort and can be complicated by similarities in morphology.[108] Molecular studies of distinct populations of Andean *Triatoma infestans*, the primary vector in the Southern Cone countries of South America, provided evidence that very little gene flow occurs between populations, implying a low risk of reinfestation in treated areas from migrating subgroups of *T. infestans.*[109] The origin of *Rhodnius prolixus* in Central America was inferred from comparative molecular studies between specimens collected in various parts of Central and South America. Researchers discovered a founder effect, indicating there was a single introduction of the species into Central America, likely due to an accidental release from a laboratory in El Salvador in 1915.[110] This conclusion greatly influences the methods used to regionally-control *R. prolixus*, the main Chagas disease vector north of the Amazon basin.

The initial application of non-morphologic methods to explore taxonomic and phylogenetic relationships of triatomine bugs involved protein electrophoresis, particularly isoenzyme analysis.[111, 112, 113, 114] Although isoenzyme analysis has provided

some insight into the population genetics of triatomine species, its is limited by the small number of polymorphic loci suitable to analysis by this method and the rigid requirements for specimen preparation.[108] Since 1998, molecular methods based on DNA have been applied to population-based studies of triatomine bugs, with elucidating outcomes.[106] Random amplified polymorphic DNA (RAPD) analysis using PCR amplification has been used extensively to make inferences regarding triatomine taxonomy and gene flow between populations.[115, 116, 117, 118, 119] While considered a relatively inexpensive method to survey genetic variation in populations without the requirement of extensive knowledge of the target genome, it suffers from the inability to detect non-dominant markers and limited reproducibility due to extensive standardization requirements.[120]

DNA sequencing of target genes has proved to be the most informative method for spatial population genetics and systematics (considered together as "phylogeography") and has successfully resolved taxonomic debates of crucial importance to Chagas disease vector control efforts.[121, 122, 123] Mitochondrial DNA (mtDNA) as a target of DNA analysis for population genetic studies is particularly attractive due to its simple structure, lack of recombination, maternal inheritance, and relatively rapid rate of evolutionary change.[124] Recently, mtDNA has been used to explore triatomine phylogeography, including that of a limited number of laboratory-reared U.S. species.[125, 126] Researchers utilizing mtDNA report success with the cytochrome *b*, and 12S and 16S ribosomal RNA gene fragments as markers for both inter- and intraspecific triatomine phylogeographic studies.[121, 122, 123, 125, 126, 127, 128, 129, 130,

[131] These particular genetic markers are conserved across taxonomic groups, facilitating the use of universal primers for amplifying gene homologs from most branches of the animal kingdom. To date, only four studies (involving ten specimens: one *T. recurva*, four *T. rubida*, two *T. protracta*, two *T. lecticularia*, and one *T. rubrofasciata* specimens collected from Georgia, Arizona, Oklahoma, and other undisclosed locations) have been published on genetic studies of wild U.S. triatomine species.[122, 125, 126, 131] Data are needed to establish a baseline for triatomine survelliance in the U.S. and for comparative studies with Latin American vectors.

Impressive genetic diversity within the *T. cruzi* species has been recognized since the late 1970's when analysis by protein electrophoresis divided South American strains into 3 distinct divisions, zymodemes 1-3 (Z1, Z2, Z3).[132, 133] Z1 and Z3 were originally associated with sylvatic transmission, and Z2 with domestic transmission.[134] Isoenzyme analysis proved valuable initially in monitoring vector control efforts. Acute cases of Chagas disease caused by Z1 and Z3 strains were reported in areas of Brazil where the vast majority of human cases had been due to Z2 strains prior to chemical vector contol.[133, 135] This suggested that sylvatic species or subgroups of triatomine bugs known to carry the Z1 or Z3 strains may be replacing the domestic triatomine bugs eradicated through spraying. Further study of these sylvatic vectors showed that they were able to adapt to human habitation.[136, 137]

The advent of polymerase chain reaction (PCR) technology in 1993 led to definitive proof that parasites remained in vertebrate tissues at low levels, causing continual pathogenesis in some individuals.[138] Prior to this discovery, little

consideration was given to parasite strain differences over nutritional, immunological, and environmental factors as an explanation for variation in clinical presentation. Since that time, researchers have struggled to incorporate *T. cruzi* heterogeneity into the epidemiology of the disease.[139, 140] A variety of molecular DNA analysis methodologies have been used to refine the classification scheme of *T. cruzi*, including schizodemes, RAPD-PCR, mini-exon polymorphisms, rDNA polymorphisms, and microsatellite analysis.[141] Most DNA studies have revealed the existence of two primary groups within *T. cruzi*; and, in 1999, an international committee recommended the universal acceptance of these two divisions designated as *T. cruzi* I (corresponding to zymodeme type Z1) and II (corresponding to Z2).[142] A third group was also proposed, *T. cruzi* (without a number designation), to correspond to zymodeme type Z3 and all other uncharacterized strains. Subsequent studies using RAPD, multi-locus enzyme electrophoresis, large and small subunit rRNA, and mini-exon markers further characterized *T. cruzi II* into five subgroups, collectively referring to all six divisions as discrete typing units (DTUs).[143, 144] In this classification, Z3 is equivalent to *T. cruzi* IIa and IIc. Progress towards meaningful characterization of *T. cruzi* isolates continues as researchers explore the use of additional nucleotide sequences, particularly within the small subunit ribosomal RNA (18S rRNA in eukaryotes). This gene has been especially useful for phylogenetic studies of the Kinetoplastida, the order to which *T. cruzi* belongs.[140, 145, 146] It has also proven to be informative for intraspecific studies of *T. cruzi* isolates, rendering results in line with the recognized dichotomous classification of strains.[140, 145, 147, 148, 149, 150, 151, 152]

A small collection of *T. cruzi* isolates from the U.S. (California, 2; Florida, 1; Georgia, 18; Louisiana, 7; and Texas, 3) has been analyzed by either protein electrophoresis, RAPD-PCR, or rDNA polymorphism.[21, 22, 153, 154, 155, 156] A single study examined a cross-section of isolates from five different U.S. states, and through RAPD-PCR analysis, provided evidence that U.S. strains are genetically diverse and probably indigenous to the North American continent.[153] Isolates examined in previous U.S. studies were primarily from mammals and only three from triatomine bugs. As with U.S. triatomine phylogeographic studies, a much larger sample size of *T. cruzi* isolates is required to assess diversity and spatial patterns. Analysis of isolates collected from indigenous U.S. vectors in conjunction with studies of the vector itself should begin to clarify the transmission cycle in the U.S. as it has in Latin America.

In this dissertation, the most comprehensive characterization of the components of the Chagas disease transmission cycle in the U.S. to date is provided. Using the state of Texas as the study area, the project described in the following pages combines new field studies with data abstracted from published and unpublished records. A new geographic distribution is presented for triatomine species. Distribution of the triatomine species is also described by natural ecological regions and *T. cruzi* infectious status. A habitat suitability model for *T. gerstaeckeri*, the most commonly-encountered triatomine species in Texas and important human vector in northeast Mexico, is developed using GIS and remote sensing applications. Genetic variation of triatomine species and *T. cruzi* isolates is described using PCR and DNA sequencing methods coupled with phylogenetic analyses, representing the first large scale study of this kind

using U.S. field collected samples. Additionally, the extent of Chagas disease in domestic canines of Texas is illustrated using serologic and histopathologic data accumulated from several sources. Geographic distribution, breed and age characteristics, and clinical presentation are described. The research presented in this dissertation will provide a baseline for Chagas disease surveillance in North America and will increase awareness among clinicians and public health practitioners regarding the geographic extent and infection potential of the Chagas disease transmission cycle in Texas and neighboring regions.

CHAPTER II

GEOSPATIAL ANALYSIS OF CHAGAS DISEASE VECTORS IN TEXAS

Introduction

Chagas disease, caused by the hemoflagellate protozoan parasite, *Trypanosoma cruzi*, continues to be an important public health threat in the western hemisphere with a prevalence of 12 million human cases and 21,000 deaths annually.[1] Although transmission of the parasite to humans can occur by blood transfusion, organ donation, ingestion, or transplacentally, greater than 80% of all human cases are vectorborne.[6] Members of the Triatominae (Hemiptera: Reduviidae) subfamily, which are obligate blood feeders in all post-egg stages, are the biological arthropod vectors of *T. cruzi*. Transmission occurs when the infected bug defecates on or near the host during or shortly after feeding and the fecal material is subsequently rubbed into the bite wound, broken skin, or mucosal tissue.[7] Like the parasite they vector, triatomine bugs utilize a broad range of vertebrate hosts, including mammals, birds and reptiles. All triatomine species are considered potential vectors of *T. cruzi*.[8] Due to the lack of a satisfactory treatment or vaccine, Chagas disease prevention is primarily dependent on the control of domiciliated triatomine insects.[6, 9]

T. cruzi and its triatomine bug vectors have been discovered in diverse ecological niches throughout the tropical and subtropical regions of North and South America, approximately between the latitudes of 42°N and 46°S.[4]. Of the 130 species currently recognized in the subfamily Triatominae[11], 11 have been reported in the southern half of the United States, seven in the state of Texas.[12]

Molecular and morphologic data suggest that the *T. cruzi* disease cycle, including the parasite, bug vectors, and susceptible mammalian hosts, became established in the U.S. long before the arrival of humans.[148, 157] The data on prevalence of *T. cruzi* in U.S. vectors are primarily derived from specimens collected in Texas, California, and Arizona with rates ranging from 17-48%, 14-40%, and 7.1-20.5%, respectively.[13, 14, 15, 16, 17, 18, 19, 20] *T. cruzi*- infected vectors have also been found in Florida, Georgia, Alabama, Tennessee, and Louisiana.[21, 22, 23, 24, 25] Although the reported incidence of human Chagas disease in the U.S. is low, U.S. strains of *T. cruzi* have proven to be virulent, as confirmed by clinical disease and death in a wide range of mammalian species including domestic dogs, primates, and humans.[18, 37, 38, 52, 62, 63, 64]

In an effort to enhance understanding of the Chagas disease transmission cycle to more efficiently design vector control programs, the application of geospatial methods to the study of the individual components is beginning to emerge. Computerized vector distribution maps, vector ecological niche modeling, and disease transmission risk modeling have been applied to several regions in Latin America to aid in Chagas disease vector control and disease prevention efforts.[82, 83, 84, 85] In the U.S., little work has been done to thoroughly characterize the geospatial attributes of triatomine species. Usinger (1944)[86] and Lent and Wygodzinsky (1979)[12] rarely provide species distribution data below the state level in their widely cited works on Triatominae. Prior to 1970, several notations on the collection sites of U.S. triatomine species and *T. cruzi* infection rates were published[16, 19, 61, 87, 88, 89, 90], but these surveys were primarily focused in small regions of the southwestern states. The goal of the present study was to combine U.S.

triatomine bug locality and *T. cruzi* infection status data from diverse sources to produce a comprehensive distribution map that will provide the basis for characterization of the Chagas disease transmission cycle using spatial attributes. The state of Texas was selected as the study area due to its large size (678,054 sq km)[158], diversity of ecological regions, and geographic location at the intersection of eastern and western triatomine species. In the U.S., Texas is the site of the highest triatomine species diversity.[12, 86]

Materials and Methods

Collection of triatomine specimens. Field specimens were collected from June 2005 to October 2006 from various sites within the state of Texas by the author, employees of the Texas Department of State Health Services (TX DSHS), and Texas residents. Sites sampled by the author were selected based on previous reports of triatomine bug sightings or canine Chagas disease cases. Specimens collected by health department employees and residents were primarily taken from in and around houses and dog kennels as prompted by concerns of disease transmission risk. All adult specimens were identified to the species level using the key of Lent & Wygodzinsky.[12]

In addition to field collections, preserved museum specimens from four Texas institutions (Midwestern State University, Wichita Falls; Texas A&M University, College Station; University of Texas Brackenridge Field Laboratory, Austin; and Wild Basin Wilderness Preserve, Austin) were reviewed for species identification and locality information. Species determinations were provided by the author for all preserved specimens. Finally, records of previously collected, identified, and tested specimens

were abstracted from internal TX DSHS reports from 2002-2004 and from published peer-reviewed journal articles for the period 1941 to 2003.

Detection of T. cruzi *infection in field collected specimens*. The hindgut from each field-collected bug was dissected following the procedure of Garcia and De Azambuja[159] using sterile, disposable scalpels, and forceps disinfected with a 10% bleach solution and ultrapure water rinse between samples. The excised hindgut was placed in 50 µl of molecular grade water and homogenized using a motorized sterile, disposable pestle. A 5 µl aliquot of homogenate was examined by phase contrast microscopy at 400x for the presence of trypanosomes. The remaining sample was stored at -70°C until further processing.

DNA was extracted from all hindgut samples using the PUREGENE® DNA Purification Kit (Gentra, Minneapolis, MN), body fluids protocol and used as template for PCR amplification. Briefly, 550 µl of cell lysis solution plus 3 µl of proteinase k (20 mg/ml) was added to the homogenized hindgut. The sample was inverted 25 times and incubated at 55°C overnight. 3 µl of RNase A solution was added to the cell lysate, inverted 25 times, and incubated at 37°C for 30 minutes. After cooling to room temperature, 200 µl of protein precipitation solution was added to the lysate and vortexed on high speed for 20 seconds. The sample was cooled in an ice bath for 15 minutes and then centrifuged at 14,000 x g for 10 minutes. The supernatant containing the DNA was decanted into a 1.5 ml microfuge tube containing 600 µl 100% isopropanol (2-propanol) plus 1 µl of glycogen (20 mg/ml). The sample was inverted 50 times, incubated at room temperature for 5 minutes, and then centrifuged at 14,000 x g

for 5 minutes. The supernatant was poured off and the tube drained on absorbent paper. 600 µl of 70% ethanol was added to the tube and the tube was inverted several times to wash the DNA pellet. The sample was centrifuged at 14,000 x g for 5 minutes and the ethanol decanted. The tube was drained on absorbent paper and air dried for 15 minutes. The DNA was rehydrated by adding 20 µl of DNA hydration solution and incubated at 65°C for 1 hour and several hours at room temperature. The DNA was stored at -28°C until further processing.

One of two primer sets was used for detection of *T. cruzi* in all samples: Tc24T1F-Tc24T2R[160] that target a ~550 bp segment of a *T. cruzi*-specific flagellar protein gene (Tc24T1 5'-GAC GGC AAG AAC GCC AAG GAC-3', Tc24T2 5'-TCA CGC GCT CTC CGG CAC GTT GTC-3'; and, Tc609F[149] and TcV5R (newly designed) that target a ~900 bp segment of non-specific trypanosome SSU rRNA (609F 5'-CAC CCG CGG TAA TTC CAG C-3', TcV5R 5'-ACT CTT GCG AAC GTA CTC CCC-3'). Amplifications were done in 25 µl reactions containing 1 µl of DNA template, 1x GoTaq Green Master Mix (Promega, Madison, WI), $MgCl_2$ final concentration adjusted to 2.5 mM, and 10 pM of primers. After an initial denaturation at 95°C for 1 minute, the reactions were cycled 35 times for 45 seconds at 95°C (denaturation), 45 seconds at 58°C (annealing), and 90 seconds at 72°C (extension), followed by a final extension for 7 minutes at 72°C. The amplified products were analyzed on 1.5% agarose gels with ethidium bromide. Amplified SSU rRNA gene products positive for a band at ~900 bp were extracted from a low melt 1.5% agarose gel, purified using the Wizard® SV Gel and PCR Clean-Up System (Promega, Madison, WI). Briefly, membrane binding

solution was added at a ratio of 10 µl of solution per 10 mg of agarose gel slice and incubated at 65°C for 10 minutes or until the gel slice was completely dissolved. The dissolved gel mixture was added to a minicolumn inserted into a microfuge tube, incubated for 1 minute at room temperature, and centrifuged 16,000 × g for 1 minute. The liquid was discarded. The minicolumn was washed twice with membrane wash solution (700 µl for 1 minute at 16,000 × g and 500 µl at 5 minutes), discarding the liquid after each wash. The empty minicolumn assembly was centrifuged for 1 minute at 16,000 x g to allow evaporation of any residual ethanol. The minicolumn was transferred to a new 1.5ml microcentrifuge tube. 50µl of nuclease-free water was added to the column, incubated at room temperature for 1 minute, and centrifuged for 1 minute at 16,000 × g. The minicolumn was discarded and the sample concentrated in a speed vacuum for 10 minutes. The sample was visualized on an agarose gel with ethidium bromide and the DNA was quantified using a low mass ladder. The sample was stored at -28°C until sequencing.

Double-stranded DNA amplification products were sequenced using 2.5 µl of Perkin Elmer ABI Big Dye Reaction Mix plus 10 pM of primer in a PCR. The reactions were cycled 45 times for 10 seconds at 95°C, 5 seconds at 50°C, and 4 minutes at 60C, followed by a holding temperature of 4°C. The products were analyzed on an ABI PRISM® 3100 Genetic Analyzer (Applied Biosystems, Foster City, CA) by the Gene Technologies Laboratory at Texas A&M University. Consensus sequences were constructed and edited using Sequencher software (Gene Codes Corp., Ann Arbor, MI)

and compared to sequences in GenBank using the BLASTN algorithm[161] for trypanosome species identification.

Geospatial analysis. The geographic location for all field-collected specimens was obtained by a mobile GPS unit. Geographic locations for all other specimens were abstracted from locality labels (preserved specimens) or specimen records (TX DSHS and published articles). County level location data for all specimens and decimal degree locations for specimens with point data were mapped using ArcGIS 9.1 software (ESRI, Redlands, CA). Triatomine species frequency by natural region was obtained using the zonal sum function in ArcGIS 9.1, combining specimen point data records and the Texas natural regions shape file layer.[162]

Results

Geographic distribution of triatomine bugs. The distribution of triatomine bugs in Texas was derived from 2,449 records. This number includes multiple specimens collected from the same location in some cases. Table 1 provides the distribution of triatomine specimen records by source. At least one specimen of each of the seven *Triatoma* species previously reported from Texas was collected: *T. gerstaeckeri* (Stål); *T. indictiva* Neiva; *T. lecticularia* (Stål); *T. neotomae* Neiva; *T. protracta* (Uhler); *T. rubida* (Uhler); and, *T. sanguisuga* (Leconte).

Table 1

Specimen sources used in a geospatial study of *Triatoma* spp. in Texas, 2005-2006

Source	No.
Field	233
Institution	371
TX DSHS	123
Publication	1722
Total	2449

The triatomine bug distribution in Texas covers 97 of 254 counties. Table 2 provides a summary of *Triatoma* spp. by county and source. Of the 67 counties with data on *T. cruzi* testing in bug specimens, 48 had at least one positive result. Figure 1 is a map of all triatomine specimens by county and counties with *T. cruzi*-positive specimens. The distribution of triatomine bugs in Texas is widespread, encompassing every major geographic region. The distribution of *T. cruzi*-infected bugs includes most geographic regions with the exception of the northern third of the state.

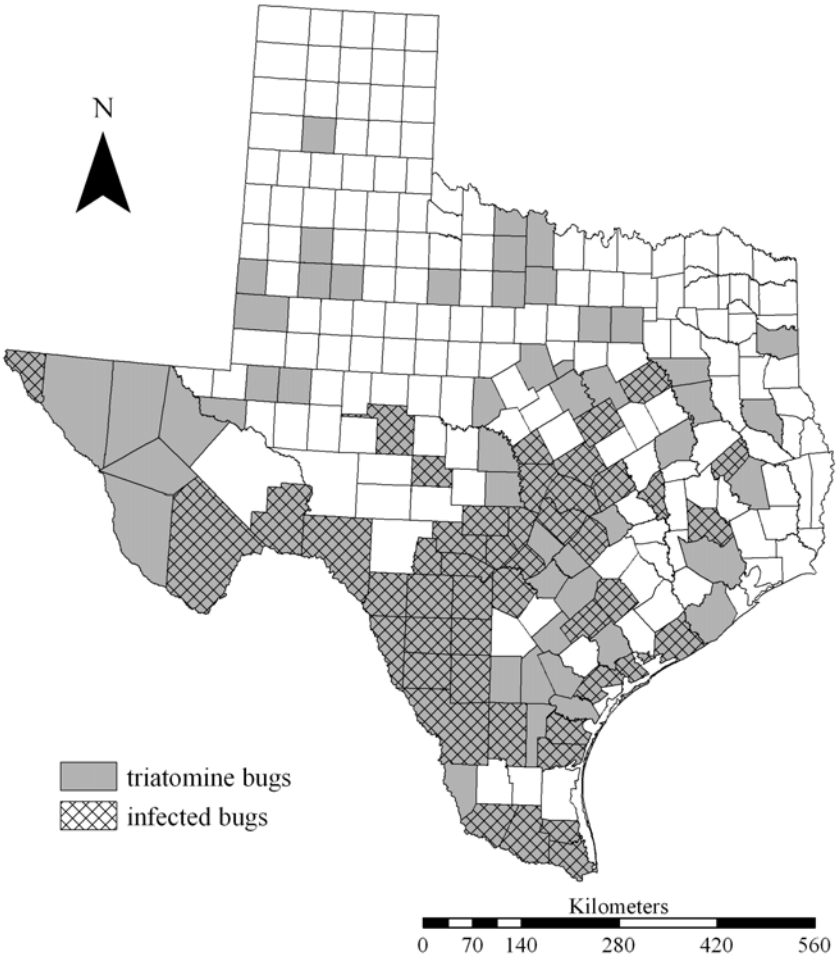

Figure 1. Distribution of *Triatoma* spp. and *T. cruzi*-infected bugs in Texas by county 1928-2006.

Table 2

Summary of *Triatoma* spp. distribution in Texas by county and source, 1928-2006

County	*T. cruzi* Reported[1]	*Triatoma* species							Source			
		gerstaeckeri	*indictiva*	*lecticularia*	*neotomae*	*protracta*	*rubida*	*sanguisuga*	Field[2]	Institution[3]	TX DSHS[4]	Publication[5]
Anderson	NT	—	—	—	—	—	—	X	—	T	—	—
Archer	NT	—	—	—	—	—	—	X	—	M	—	—
Bandera	Y	X	—	—	X	—	—	—	—	T	—	A
Bastrop	Y	X	—	—	—	—	—	—	—	—	X	—
Bee	N	—	—	—	—	—	—	X	—	—	X	—
Bell	Y	X	—	X	—	—	—	X	—	T,W	X	A
Bexar	Y	X	—	—	—	—	—	X	X	T	—	A,B
Blanco	Y	X	X	—	—	—	—	X	X	T,U	—	—
Bosque	NT	—	—	—	—	—	—	X	—	T	—	—
Brazoria	NT	—	—	—	—	—	—	X	—	T,U	—	—
Brazos	Y	X	—	X	—	—	—	X	X	T,W	—	A
Brewster	Y	X	—	—	—	X	X	—	X	T,W	—	A,C
Brown	NT	—	—	—	—	—	—	X	—	T	—	—
Burnet	Y	X	—	—	—	—	—	X	X	W	—	—
Caldwell	N	X	—	—	—	—	—	—	—	—	—	A
Calhoun	Y	X	—	—	—	—	—	X	—	T,W	—	A
Cameron	Y	X	—	X	X	—	—	X	X	T,W	X	A,D,E
Clay	NT	—	—	—	—	—	—	X	—	M	—	—
Comal	Y	X	X	—	—	—	—	—	X	—	—	—
Culberson	N	X	—	—	—	—	—	—	X	—	—	—
Dallas	N	—	—	—	—	—	—	X	—	T,W	—	A
DeWitt	Y	X	—	X	—	—	—	X	—	W	X	A
Dimmit	Y	X	—	X	—	X	—	X	X	T,U,W	—	A,C
Duval	Y	X	X	X	—	—	—	X	X	—	—	A,C
Ector	NT	—	—	—	—	—	X	—	—	W	—	—
El Paso	Y	—	—	—	—	—	X	—	X	T,W	—	A
Erath	N	—	—	X	—	—	—	X	X	T	—	—
Frio	Y	X	—	—	—	—	—	—	—	W	—	A

Table 2 Continued

County	*T. cruzi* Reported[1]	*Triatoma* species							Source			
		gerstaeckeri	*indictiva*	*lecticularia*	*neotomae*	*protracta*	*rubida*	*sanguisuga*	Field[2]	Institution[3]	TX DSHS[4]	Publication[5]
Gaines	NT	—	—	—	—	X	—	—	—	W	—	—
Garza	NT	—	—	—	—	X	—	—	—	T	—	—
Gillespie	Y	X	X	—	—	—	—	—	X	—	—	—
Gonzales	NT	—	—	—	—	—	—	X	—	U	—	—
Guadalupe	N	X	—	—	—	—	—	—	—	T	—	A
Harris	NT	—	—	—	—	—	—	X	—	M	—	—
Harrison	N	X	—	—	—	—	—	—	—	—	—	A
Haskell	NT	—	—	—	—	X	—	X	—	M	—	—
Hays	N	X	—	—	—	—	—	X	—	—	X	A
Henderson	NT	X	—	—	—	—	—	—	—	T	—	—
Hildalgo	Y	X	—	X	X	—	—	X	X	T,U	X	A,C
Hill	N	X	—	—	—	—	—	X	—	—	—	A
Hudspeth	N	—	—	—	—	X	—	—	—	—	—	C
Jack	NT	—	—	—	—	X	—	—	—	T	—	—
Jeff Davis	NT	X	—	—	—	X	—	—	—	T	—	—
Jim Wells	N	X	—	—	—	—	—	X	X	—	X	—
Karnes	Y	X	—	—	—	—	—	—	X	—	—	—
Kendall	Y	X	X	—	—	—	—	—	X	T	—	—
Kerr	Y	X	X	—	—	—	—	X	X	T	—	—
Kinney	Y	X	—	—	—	—	—	—	—	—	—	A
Kleberg	Y	X	—	—	—	—	—	—	X	—	—	—
Lampasas	Y	X	—	—	—	—	—	—	X	—	—	—
LaSalle	Y	X	—	—	—	—	—	X	X	T,U	—	—
Lavaca	Y	X	—	—	—	—	—	X	—	—	—	A
Lee	NT	X	—	—	—	—	—	X	—	T	—	—
Leon	NT	—	—	X	—	—	—	—	—	T	—	—
Live Oak	NT	X	—	—	—	—	—	—	—	W	—	—
Llano	NT	—	X	—	—	—	—	—	—	T	—	—
Lubbock	NT	—	X	—	—	X	—	—	—	T	—	—
Lynn	NT	—	—	—	—	X	—	—	—	T	—	—

Table 2 Continued

County	*T. cruzi* Reported[1]	*Triatoma* species							Source			
		gerstaeckeri	*indictiva*	*lecticularia*	*neotomae*	*protracta*	*rubida*	*sanguisuga*	Field[2]	Institution[3]	TX DSHS[4]	Publication[5]
McLennan	Y	X	—	X	—	—	—	X	X	T,W	X	A
McMullen	NT	X	—	—	—	—	—	—	X	—	—	—
Matagorda	Y	—	—	—	—	—	—	X	—	W	—	A
Maverick	Y	X	—	—	—	X	—	—	—	—	—	C
Medina	Y	X	—	X	—	X	—	—	—	—	—	C,F
Menard	Y	X	—	—	—	X	—	—	—	—	—	A
Midland	N	—	—	—	—	X	X	X	—	T,W	X	—
Milam	Y	X	—	X	—	—	—	X	X	T,W	—	A
Montgomery	Y	—	—	X	—	—	—	—	X	—	—	—
Nacogdoches	N	—	—	—	—	—	—	X	X	T	—	—
Navarro	Y	—	—	X	—	—	—	—	—	—	—	G
Nueces	Y	X	—	—	—	—	—	—	X	T	X	A
Polk	N	—	—	X	—	—	—	—	—	—	—	A
Presidio	NT	X	—	—	—	X	X	—	—	T	—	—
Randall	NT	—	—	—	—	X	—	—	—	T	—	—
Real	Y	X	—	—	—	—	—	—	X	T	—	—
Reeves	N	X	—	—	—	X	—	—	—	T	—	C
Refugio	Y	X	—	—	—	—	—	—	—	—	—	A
San Patricio	N	X	—	—	—	—	—	—	—	T,U	—	A
San Saba	NT	—	—	X	—	—	—	—	—	T,U	—	—
Somervell	N	—	—	X	—	—	—	—	—	—	—	A
Starr	Y	X	—	—	—	—	—	—	X	—	—	C
Tarrant	N	—	—	X	—	—	—	X	—	W	X	—
Terrell	Y	X	X	—	—	—	X	—	—	U	—	C
Tom Green	Y	X	X	—	—	—	—	X	X	T	X	—
Travis	Y	X	X	X	—	—	—	X	—	T,U,W	X	A
Trinity	Y	—	—	X	—	—	—	X	—	T	—	A
Uvalde	Y	X	—	X	—	X	—	X	X	T,W	X	A
Val Verde	Y	X	—	—	—	X	—	—	—	U,M	—	A
Victoria	NT	—	—	—	—	—	—	X	—	T	—	—

Table 2 Continued

County	*T. cruzi* Reported[1]	*Triatoma* species							Source			
		gerstaeckeri	*indictiva*	*lecticularia*	*neotomae*	*protracta*	*rubida*	*sanguisuga*	Field[2]	Institution[3]	TX DSHS[4]	Publication[5]
Ward	NT	—	—	—	—	—	X	—	—	T	—	—
Webb	Y	X	—	X	—	X	—	X	X	—	—	A,C
Wichita	NT	—	—	X	—	—	—	X	—	M	—	—
Willacy	Y	X	—	—	X	—	—	—	—	—	—	A
Williamson	Y	X	—	X	—	—	—	X	X	T,W	X	A
Yoakum	NT	—	—	—	—	X	—	—	—	W	—	—
Young	NT	—	—	—	—	—	—	X	—	M	—	—
Zapata	N	—	—	—	—	X	—	—	—	—	—	C
Zavala	Y	X	—	X	—	—	—	X	X	—	—	A
Total counties	48	58	11	25	4	22	7	48	34	66	16	46

[1]Y = ≥1 specimen tested and found positive for *T. cruzi* ; N = ≥1 specimen tested and none found positive; NT = no specimens tested. Sources include field[2], TX DSHS4, and/or publication[5].

[2]Specimens submitted to or collected by the author (SAK).

[3]Preserved specimens from institutional collections; species determinations provided by author (SAK). M = Midwestern State University, Wichita Falls, Texas; T = Texas A&M University, College Station, Texas; U = University of Texas Brackenridge Field Laboratory, Austin, Texas; W = Wildbasin Nature Preserve, Austin, Texas.

[4]Unpublished records of *Triatoma* specimens submitted to and processed by the Texas Department of State Health Services for the time period 2002-2004.

[5]Published records of *Triatoma* specimens. A = Sullivan (1949)[90]; B = Pippin (1970)[14]; C = Wood (1941)[87]; D = Eads (1963)[61]; E = Beard (2003)[85]; F = Ryckman (1967)[19]; G = Williams (1977)[37].

Figures 2-8 are maps of triatomine species distributions in Texas by county and field collection sites. *T. rubida* has been found exclusively in the far west region of the state. *T. protracta* and *T. indictiva* locations extended from west to the north and south central regions. *T. sanguisuga* and *T. lecticularia* were sympatric in their distributions, covering all but the far west and pan handle regions. *T. neotomae* appeared to be restricted to the mid to deep south central regions. *T. gerstaeckeri* had the broadest distribution, covering all but the northern expanse of Texas. The greatest species diversity was found primarily in the mid to south central portion of the state. Seven counties (Cameron, Dimmit, Duval, Hidalgo, Travis, Uvalde, and Webb) accounted for the highest number of species with four each. Figure 9 is a map of triatomine species diversity by county.

Distribution by natural region was determined for all triatomine bug records from Texas using point location data (623 records). Triatomine species were found in all 12 natural regions of Texas. The number of unique point locations for each of the species was as follows: *T. gerstaeckeri*, 114; *T. indictiva*, 11; *T. lecticularia*, 25; *T. neotomae*, 2; *T. protracta*, 24; *T. rubida*, 9; and, *T. sanguisuga*, 51. Figure 10 is a map of the triatomine bug records with point locations overlaid on the natural regions of Texas.

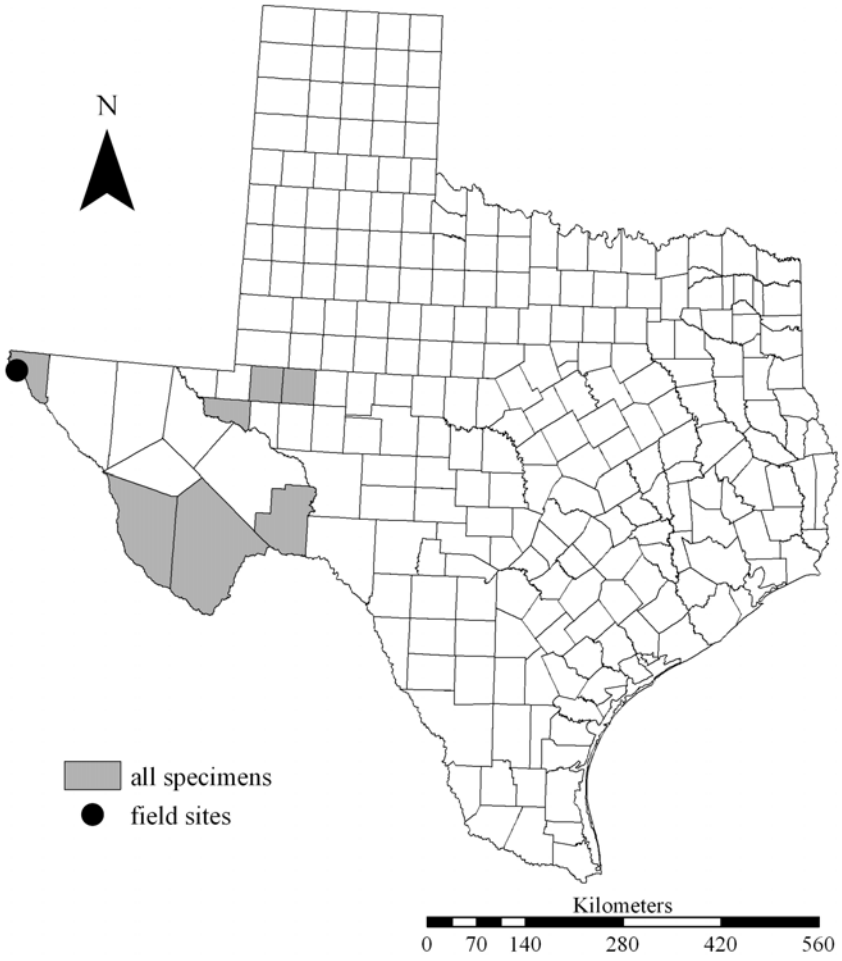

Figure 2. Distribution of *T. rubida* in Texas by county and field collection site, 1928-2006.

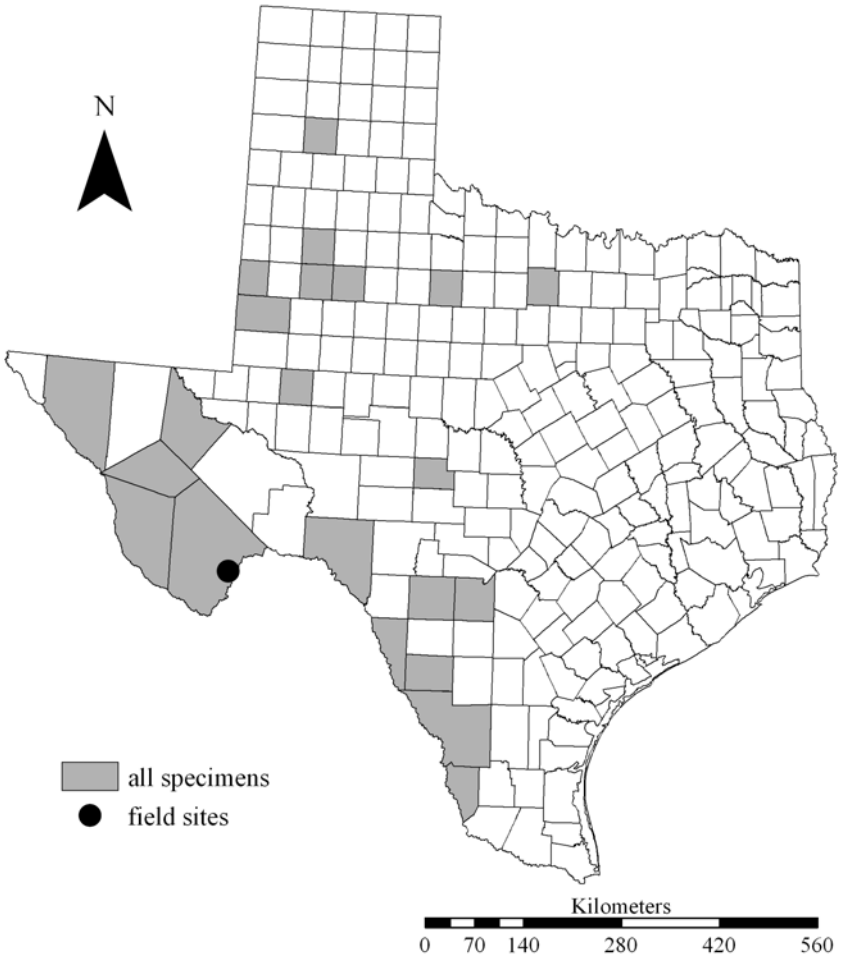

Figure 3. Distribution of *T. protracta* in Texas by county and field collection site, 1928-2006.

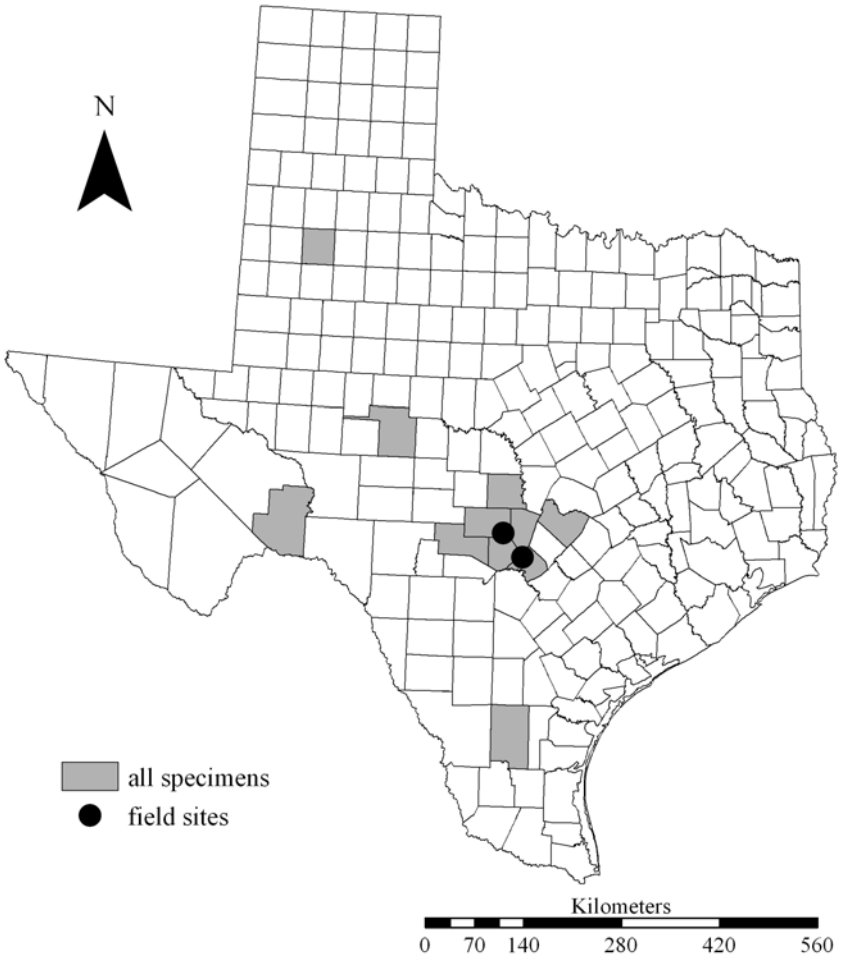

Figure 4. Distribution of *T. indictiva* in Texas by county and field collection site, 1928-2006.

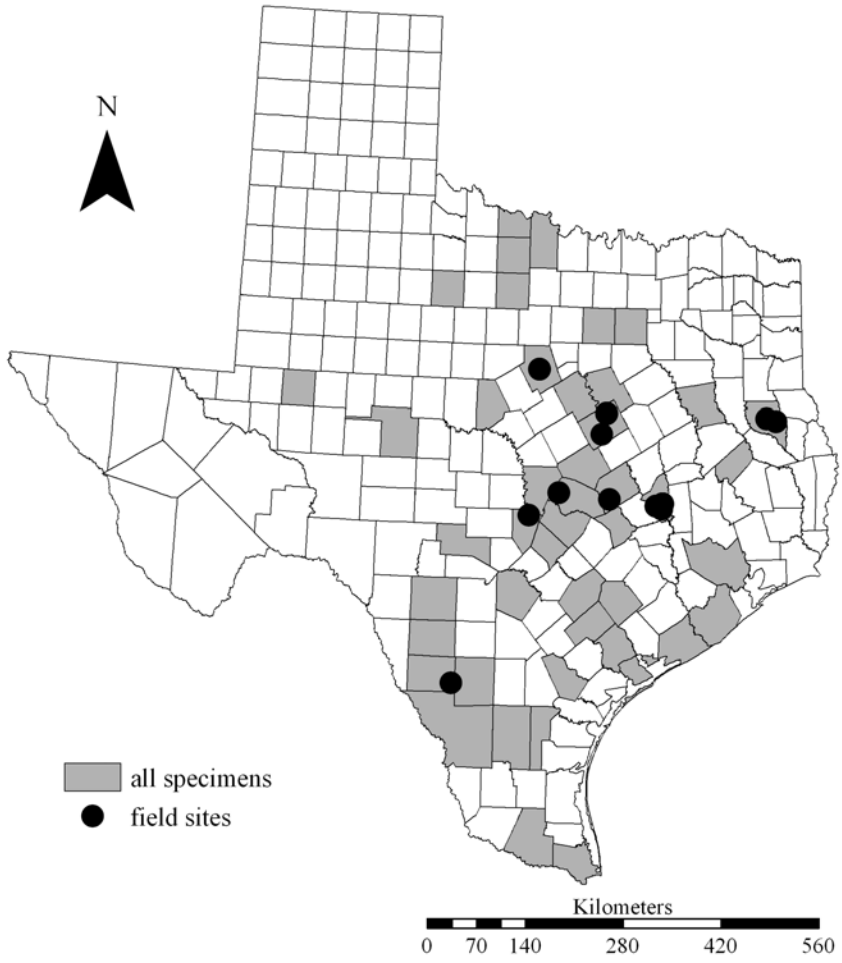

Figure 5. Distribution of *T. sanguisuga* in Texas by county and field collection site, 1928-2006.

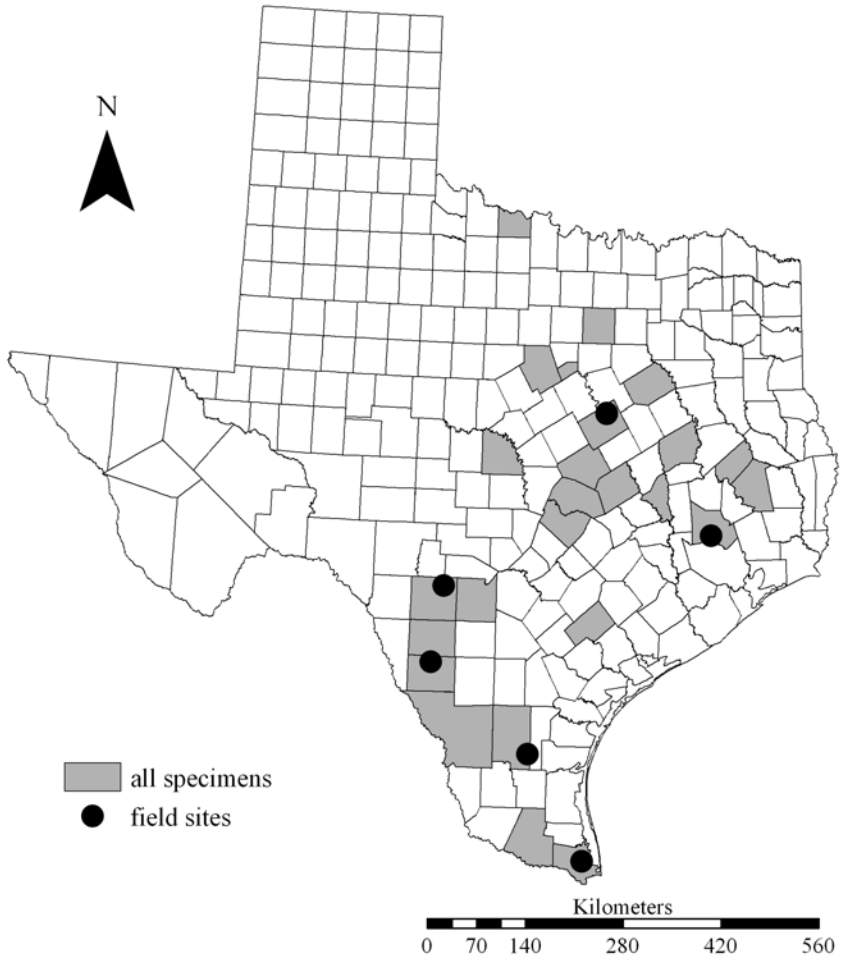

Figure 6. Distribution of *T. lecticularia* in Texas by county and field collection site, 1928-2006.

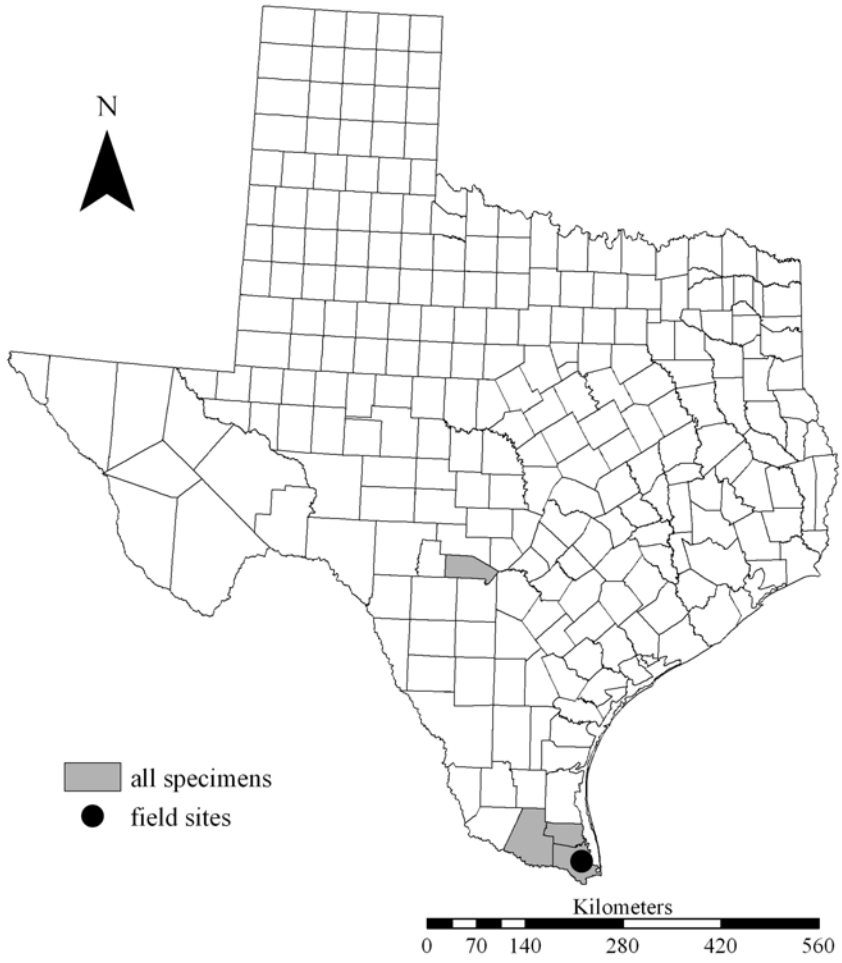

Figure 7. Distribution of *T. neotomae* in Texas by county and field collection site, 1928-2006.

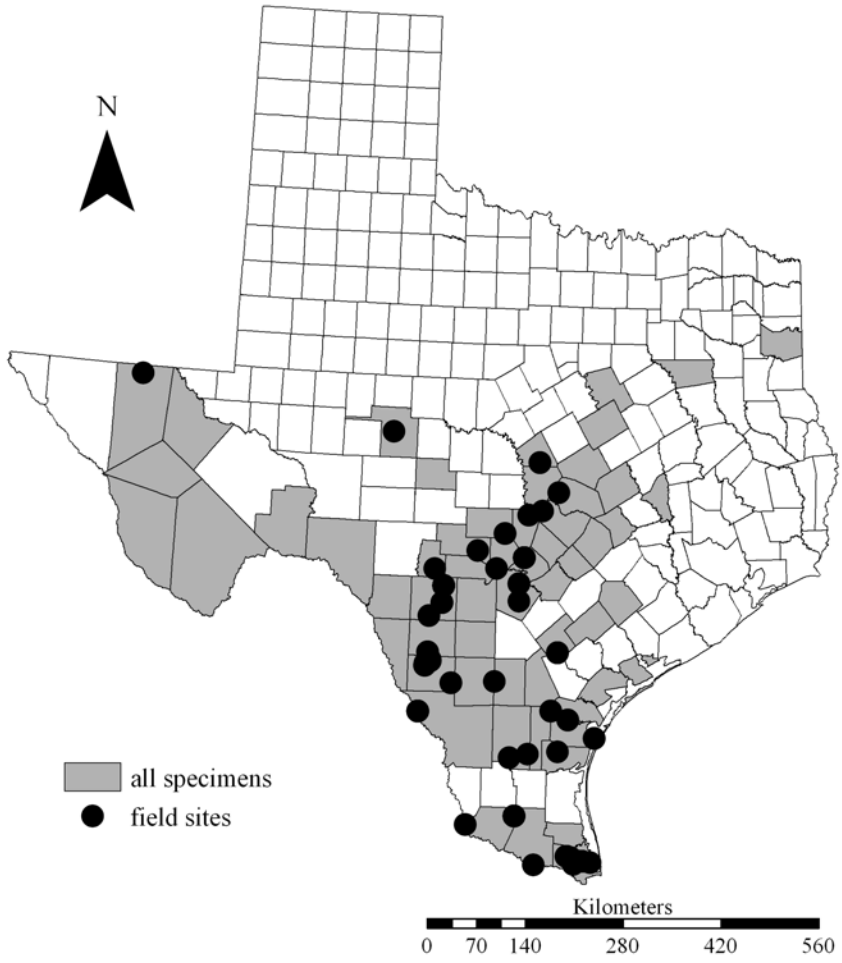

Figure 8. Distribution of *T. gerstaeckeri* in Texas by county and field collection site, 1928-2006.

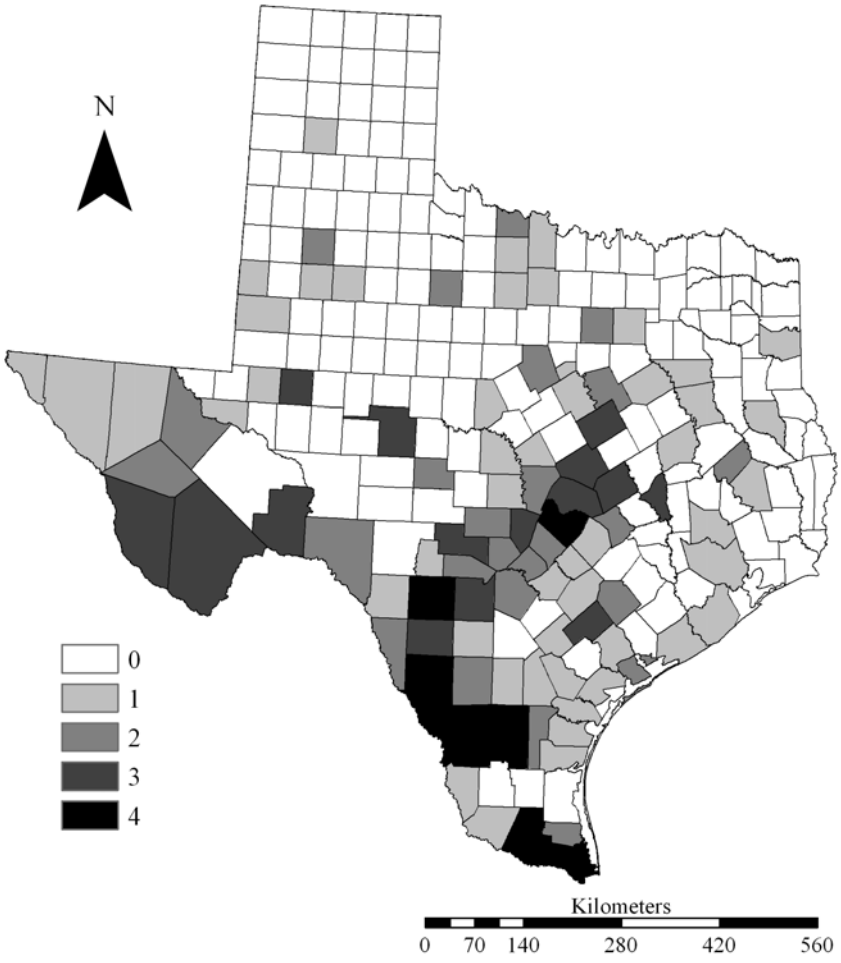

Figure 9. Triatomine bug species diversity in Texas by county, 1928-2006.

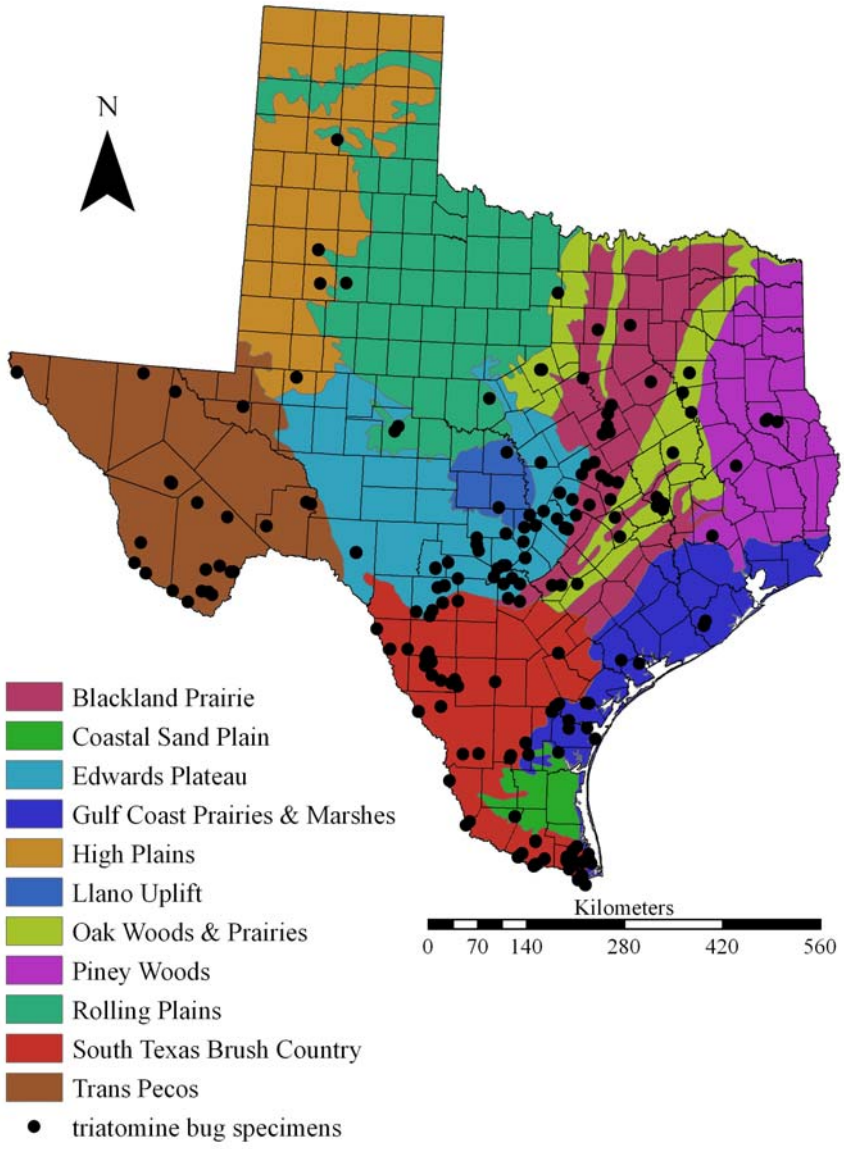

Figure 10. Distribution of triatomine bug specimens in Texas by natural region, as of 2006.

The greatest species diversity was found in the South Texas Brush Country with five species and the Oakwoods & Prairies, Gulf Coast Prairies & Marshes, Edwards Plateau, Rolling Pains, and the Trans Pecos each with four species. Most species occurred in more than one natural region with the exception of *T. neotomae* which was

found solely in the South Texas Brush Country region. *T. gerstaeckeri* was found in the greatest number of natural regions with eight, followed by *T. lecticularia* and *T. sanguisuga* with seven each. Table 3 provides a list of triatomine species by natural region.

Table 3

Triatoma spp. distribution in Texas by natural region (percent)

	Triatoma spp.						
Natural Regions	*gerstaeckeri*	*indictiva*	*lecticularia*	*neotomae*	*protracta*	*rubida*	*sanguisuga*
Piney Woods			4.0				7.8
Oakwoods & Prairies	1.8		12.0		4.2		27.5
Blackland Prairies	3.5		36.0				15.7
Gulf Coast Prairies & Marshes	13.2	9.1	4.0				11.8
Coastal Sand Plains	0.9						
South Texas Brush Country	45.6		28.0	100.0	29.2		17.6
Edwards Plateau	25.4	54.5	12.0				17.6
Llano Uplift		9.1	4.0				
Rolling Plains	1.8	9.1			8.3		2.0
High Plains		9.1			12.5	11.1	
Trans Pecos	7.9	9.1			45.8	88.9	
Total	100	100	100	100	100	100	100

Characterization of field-collected specimens. Field-collected triatomine specimens for this study were collected from 34 counties and included at least one specimen from all seven triatomine species previously reported in Texas. Of the 233 adult specimens collected, *T. gerstaeckeri* had the highest frequency with 180 specimens followed by *T. sanguisuga* with 38. At least one specimen from five of the seven species collected tested positive for *T. cruzi* (*T. gerstaeckeri, T. indictiva, T. lecticularia,*

T. protracta, and T. sanguisuga). Field collected triatomine specimens categorized by species and *T. cruzi* infection status are shown in Table 4.

Table 4

Field-collected triatomine specimens in Texas, 2005-2006, by species and *T. cruzi* infection status

Triatoma spp.	*T. cruzi* positive	*T. cruzi* negative	Not tested	Total
gerstaeckeri	86	70	24	180
indictiva	1	1	0	2
lecticularia	3	2	3	8
protracta	2	0	0	2
neotomae	0	2	0	2
rubida	0	1	0	1
sanguisuga	10	19	9	38
Total	102	95	36	233

Of the 233 specimens collected, 197 were tested for *T. cruzi* infection. The infection rate for tested specimens was 51.78% (102/197). With the exception of one specimen, all bugs that tested positive for trypanosomes by microscopy also tested positive by PCR. It is likely that the DNA from the one microscopy-positive/PCR-negative sample was lost or degraded during the extraction process, or below detection sensitivity. For the purposes of the current study, this specimen was treated as negative for *T. cruzi* because the species of trypanosome observed by microscopy could not be

determined. Of the 102 PCR-positive specimens, 21 were negative by microscopy. All but one of the 21 specimens were dead prior to dissection. Samples from 30 bug specimens were not tested by microscopy due to prior storage by freezing or alcohol, rendering phase contrast microscopy ineffective for trypanosome detection. Of the 197 specimens analyzed by PCR amplification, 141 were tested using the trypanosome SSU rRNA primer set and 56 were tested using the *T. cruzi*-specific flagellar protein primer set. All but two specimens testing positive for the SSU rRNA segment (61 specimens) had their amplification products sequenced and were found to be highly similar (99-100%) to *T. cruzi* entries in GenBank. DNA amplification sequences from the other two specimens were 99% similar to a *Blastocrithidia triatomae* SSU rRNA sequence in GenBank (accession number AF153037). The *B. triatomae*-positive specimens were extracted from a *T. neotomae* found in a dog kennel in Cameron County and a *T. gerstaeckeri* found inside an office building in Zavala County.

The majority of field-collected specimens were found inside or near houses (68%), followed by dog kennels (18%), and sylvatic settings (14%) which were primarily woodrat (*Neotoma micropus*) nests. Of bug specimens tested for *T. cruzi* infection, 55% were positive among those collected from dog kennels and inside or near houses, and 31% were positive among those found in sylvatic settings. Multiple *Triatoma* species were collected from the same location at eight sites: six were inside or near houses (Blanco, Comal, Gillespie, McLennan, Uvalde, and Williamson counties), a dog kennel (Cameron County), and a state park camp site (LaSalle County). Table 5 lists field-collected triatomine specimens by site and infection status.

Table 5

Field-collected triatomine specimens in Texas, 2005-2006, by site and *T. cruzi* infection status

	Inside House	Human Bite	Near House	Dog Kennel	Sylvatic	Total
T. cruzi positive	15	6	52	21	8	102
T. cruzi negative	17	1	42	17	18	95
Not tested	4	0	22	4	6	36
Total	36	7	116	42	32	233

Discussion

Visualization of the spatial attributes of vector-borne disease data has often been the starting point in epidemiologic studies, and the advent of computer-based geographic information systems (GIS) has greatly increased the capability of investigators to explore this type of data for patterns in both place and time.[163] Determination of triatomine species geographic distribution has been essential to Chagas disease prevention programs in Latin America. This study provides new information on the distribution and infection status of triatomine species in the U.S., where little work has been done to characterize the bug vectors. The last extensive survey of Texas triatomine species was published in 1949 and included distribution information for 40 counties.[90] Distribution data for 97 counties was achieved in this study as well as additional characteristics for individual specimens collected at 225 unique point locations. Similar to the 1949

survey, *T. gerstaeckeri* was the most commonly-collected species followed by *T. sanguisuga*.

There is considerable overlap in species distribution. No single species appears to occupy an exclusive geographic region within Texas. *T. gerstaeckeri, T. sanguisuga, T. indictiva, T. lecticularia,* and *T. protracta* all share a large area encompassing the north, mid, and south central regions. Not surprisingly, these same species are spread across diverse ecological areas within Texas, with each species occupying a minimum of 5 natural regions. *T. rubida* and *T. neotomae* appear to be more restricted in habitat type, occupying only one and two natural regions, respectively. However, the small number of collections site for these two species may impact the ability of this study to accurately estimate their distribution. Distribution of triatomine species may be a reflection of their low host specificity. With the exception of *T. neotomae* which is almost exclusively known from woodrat nests, all Texas species have been reported to associate with a wide range of vertebrate hosts with diverse habitats.[12] Distributions of some triatomine species have been predicted fairly accurately using vertebrate host habitat characteristics.[82]

The overall *T. cruzi* infection rate for field collected triatomine specimens in this study (51.78%) was higher than previous reports of 17-48%.[13, 14, 18, 90] The seven species collected in this study have previously been found to be naturally infected with *T. cruzi* in Texas.[90, 164] This research supports a single earlier account of *T. indictiva* field specimens found naturally infected with *T. cruzi*.[164] PCR analysis of hindgut samples proved to be more sensitive than direct microscopy in the field portion of this study. Of

the 21 samples that were microscopy-negative/PCR-positive, 20 were extracted from dead bug specimens, suggesting that direct microscopy may be more sensitive when using live specimens.

Primer sets for two different gene targets were used to confirm *T. cruzi* infection in field collected specimens. The Tc24T1/Tc24T2 primers were previously proven to be specific for *T. cruzi*[160]; and therefore, DNA sequencing was not performed for confirmatory species identification on specimens that tested positive using this primer set. The majority of specimens (72%) were tested with the Tc609F/TcV5R primer set targeting the SSU rRNA to accommodate future phylogenetic studies. Because the segment amplified by the Tc609F/TcV5R primer set is not *T. cruzi*-specific, sequencing and comparative analyses were performed on all positive specimens. The use of the nonspecific primers allowed for the discovery of additional hindgut organisms, including *B. triatomae* found in two bug species (*T. gerstaeckeri* and *T. neotomae*) collected in different counties. *B. triatomae* is a single host, flagellate parasite pathogenic for triatomine bugs. Both *T.cruzi* and *B. triatomae* have morphologically similar epimastigote and trypomastigote forms that colonize the small intestine and rectum, but unlike *T. cruzi*, *B. triatomae* has the ability to develop a drought-resistant cyst form.[165] *B. triatomae* has been documented in several *Triatoma* spp. in South America[166, 167] and in *T. gerstaeckeri* collected in Texas.[18] Because mixed infections of *T. cruzi* and *B. triatomae* have been reported[168], both *B. triatomae*-positive specimens identified in this study were analyzed with the *T. cruzi*-specific Tc24T1/Tc24T2 primers and found to be

negative. The two trypanosomes appear similar morphologically when viewed by direct microscopy, making *T. cruzi* identification difficult with this diagnostic method.

A high percentage of triatomine specimens found in close association with humans in this study were infected with *T. cruzi*. Of bugs collected inside or near houses, 55% were infected, including six of seven that were found feeding on the human occupants. Of the 180 *T. gerstaeckeri* specimens collected, 113 (63%) were found inside or near houses, as compared to a survey in Mexico where 181 of 192 (94%) *T. gerstaeckeri* were found in similar settings.[169] Accounts of triatomine bugs encountered inside houses in the U.S. have been sporadically reported for the past 60 years,[21, 24, 26, 27, 28] but few human Chagas disease cases due to local vector exposure have been reported. Reports of five U.S. cases have been published since 1955,[24, 27, 51, 52] three from Texas. Two additional cases were identified in 2006, one in Louisiana[53] and one in Texas.[54] TX DSHS personnel collected 12 triatomine bug specimens from the residence of the most recent Texas case and submitted them to the author for identification and testing. All were adult *T. gerstaeckeri* and one of the two specimens tested was positive for *T. cruzi*. The remaining specimens were not tested due to their deteriorated state.

Theories for the low prevalence of vectorborne human Chagas disease cases in the U.S. compared to Latin America include low virulence of native strains, less efficient bug vectors, and reduced contact with vectors due to better housing construction.[61] Another possible explanation for the low number of reported human cases is that, due to the nonspecific, infrequent presentation of acute symptoms and long latent period of the chronic form of the disease, U.S. physicians rarely consider Chagas disease in a

differential diagnosis. Data from this study support previously published reports on prevalence of human exposure to triatomine bites[66, 67, 68, 170] that close association between humans and triatomine bugs in the U.S. continues to occur. The opportunity for introduction of additional virulent strains of *T. cruzi* has also been recognized. An estimated 25,000-75,000 Latin American immigrants infected with *T. cruzi* residing in the U.S. represent a potential source of infection to both indigenous vectors and blood transfusion/organ transplant recipients.[96] A *T. cruzi* diagnostic test was recently approved by the FDA in response to the 2003 American Red Cross announcement to implement *T. cruzi* screening of all donated blood.[102, 103] The current study provides additional evidence that the Chagas disease transmission cycle is well-established in the U.S. Both the bug vectors and parasite are widely distributed throughout Texas and able to occupy varied ecological regions. This triatomine bug distribution and infection rate data can serve as a baseline for future surveillance efforts.

CHAPTER III

MODELING HABITAT SUITABILITY FOR *Triatoma gerstaeckeri* in TEXAS USING GIS AND REMOTE SENSING APPLICATIONS

Introduction

The influence of landscape characteristics on vectorborne disease cycles has long been recognized. The melding of landscape ecology and epidemiology was forged in the mid-1900s by Europeans such as Pavlovsky who developed the concept that natural disease foci are small scale regions driven by the entire ecosystem on a larger scale.[73] Vectorborne disease transmission cycles are typically restricted to areas that contain overlapping spatial distributions of arthropod vectors, hosts, and pathogens. Disease cycles, like landscapes, are never in a steady state of equilibrium but rather are dynamic systems subject to fluctuating internal and external forces, which is the nature of spatial heterogeneity. Lyme disease in the United States provides a good illustration of the link between vector-borne disease transmission cycles and landscape characteristics. Its emergence has been linked with specific land cover types and patch fragmentation based on analysis of landscape patterns using satellite imagery.[171, 172, 173]

The introduction of geospatial methods utilizing remote sensing and geographic information systems (GIS) technology has significantly enhanced the study of spatial and temporal aspects of infectious disease in relation to landscape ecology.[74, 75, 76, 77] Application of statistical methods provides a basis for evaluating spatial relationships, the outcome of which could lead to development of disease transmission risk maps and

predictive models. Within the past decade, the use of geospatial methods has greatly improved our understanding of and control efforts for vectorborne diseases including malaria[78], onchocerciasis[79], Rift Valley Fever[80], and Lyme disease[81] among many others in an expanding list.

The application of geospatial methods to the study of Chagas disease is also beginning to emerge. Chagas disease, caused by the hemoflagellate protozoan parasite, *Trypanosoma cruzi*, continues to be an important public health threat on the American continents, with a prevalence of 12 million cases and another 90 million people at risk of infection.[1] The pathogen and its triatomine insect vectors have been discovered in diverse ecological niches throughout North and South America.[4] Computerized vector distribution maps, vector ecological niche modeling, and disease transmission risk modeling have been applied to several regions in Latin America to aid in Chagas disease vector control and disease prevention efforts.[82, 83, 84, 85]

In the U.S., little work has been done to thoroughly characterize the geospatial attributes of triatomine species and *T. cruzi* isolates. Usinger (1944)[86] and Lent and Wygodzinsky (1979)[12] rarely provide species distribution data below the state level in their widely-cited works on Triatominae. Prior to 1970, several notations on the collection sites of U.S. triatomine species and *T. cruzi* infection rates were published[16, 19, 61, 87, 88, 89, 90], but these surveys were primarily focused in small regions of the southwestern U.S. Eleven species of triatomine bugs have been reported in the United States, seven in Texas.[12] Reported prevalence of *T. cruzi* infection in Texas species ranges from 17-48%.[13, 14, 16, 174] *Triatoma gerstaeckeri* (Stål), a commonly encountered

insect species in Texas, has a geographic distribution that extends into Mexico where it is considered an important vector species for transmission of Chagas disease to humans.[72] It is widely distributed across Texas[90] and has been frequently reported in close association with humans[175,85, 87, 89, 169, 176]

The goal of the present study was to describe landscape features associated with *T. gerstaeckeri* in the state of Texas using remote sensing and GIS methods. The specific aims included: 1.) Determining land cover classes associated with *T. gerstaeckeri* field sites using land use/land cover information; 2.) Determining area ranges of each land cover class based on landscape metrics calculated from habitat buffer zones around field collection points; and, 3.) Modeling suitable habitat for *T. gerstaeckeri* based on the area ranges of land cover classes.

Materials and Methods

Determination of land cover classes. Classification of remotely sensed images was used to delineate land cover classes in Texas. Field collections of *T. gerstaeckeri* specimens were made by the author during the time period 2005-2006 in 19 counties spanning from central to southern Texas. Geographic coordinates were recorded with a handheld GPS unit for each of the 33 sites used in the current study. Six Landsat ETM+ satellite images, encompassing the field collection sites, were used as the base layers for land cover classification. All satellite-derived scenes were acquired in the year 2003 at a 30 meter resolution. Aerial photographs, in the form of digital orthophoto quadrangles (DOQs), were used in the classification process for selecting regions of interest (ROIs)

in the training and accuracy assessment procedures. Each DOQ covered a subset of the land area included in the remotely sensed scene. A description of the data used for land cover classification is provided in Table 6.

Table 6

Data sources for land cover classification of 2003 satellite imagery in selected areas of Texas

Landsat ETM+ scenes[1]		DOQ[2]	
ID	Acquistion date	Classification (ROI selection)	Accuracy assessment
2641/y2003/d089/nlaps	3/30/2003	2797131/Corpus Christi NW/1m	2797011/Orange Grove NW/1m
2642/y2003/d089/nlaps	3/30/2003	2697612/Los Fresnos NE/1m	2697512/Harlingen NE/1m
2739/y2003/d016/nlaps	1/16/2003	3098391/Spicewood NW/1m	2998051a/Spring Branch NW/1m
2740/y2003/d080/nlaps	3/21/2003	2897101/Kenedy NW/1m	2897104/Kenedy SE/1m
2839/y2003/d151/nlaps	5/31/2003	2999502/Uvalde NE/1m	2999503/Uvalde SW/1m
2840/y2003/d151/nlaps	5/31/2003	2899262/Carrizo Springs East NE/1m	2899263/Carrizo Springs East SW/1m

DOQ = digital orthophoto quadrangle; ROI = region of interest

[1]Landsat ETM+ scene source: http://www.fri.sfasu.edu/pages/archives/rs/html/landsat.html

[2]DOQ source: http://www.tnris.state.tx.us/DigitalData/doqs.htm

Classification of satellite imagery by land cover classes was performed using ENVI 4.2 software (Research Systems, Inc., Boulder, CO). Selection of land classes was based on the USGS Land-use/Land-cover Classification System for Use with Remote Sensor Data[177], Level I, which includes the following classes: urban or built-up land; agricultural land; rangeland; forestland; and water.

Mahalanobis distance, a supervised, parametric classification algorithm, was used to classify all scenes. Four of the seven Landsat ETM+ spectral bands (2, 3, 4, and 5) were used in the classification process. Regions of interest were selected for each land class using the author's experience with ground features at the field sites and the

designated DOQ, which provided a view of the study site on a finer scale. Only homogeneous (unimodal) ROIs, as determined by spectral histograms, were used for training the classification algorithm to the user-specified land classes. A minimum of 400 pixels for each ROI was selected following the >10*n pixels rule of thumb, where n represents the number of spectral bands used for classification.[178] The ROI separability function was used to assess the land class discriminatory power of the training ROIs.

The classification function converted each satellite scene to a grid file containing seven land classes (forest, water-shallow, water-deep, urban, rangeland, agriculture-type A, and agriculture-type B). An additional class for water and agriculture was used to accommodate the wide range of spectral values for these two land types found in the Landsat ETM+ scenes. After classification, the two water and two agriculture classes were combined in each scene to create a total of five land classes. Each pixel in a scene was assigned a numeric value based on its land class.

After classification, an accuracy assessment of each classified scene was conducted. ROI point features were selected using the designated DOQ for each scene. The number of ROI points required for accuracy assessment was determined using the binomial probability theory for a 95%, two-sided confidence interval, where the expected percent accuracy of the entire map was set at 90% and allowable error at 7.5%.[179] For this project, 64 ROI points were required. Once the ROI points were selected for each land class, the confusion matrix function was run to determine the accuracy of the classified scenes.

Calculation of landscape metrices. Each *T. gerstaeckeri* field collection site used to create the model was characterized using landscape metrics. Of the 33 total *T. gerstaeckeri* collection sites available for analysis, 18 sites from 17 counties were used to develop the model and 15 sites from five counties were used to test the accuracy of the model. Figure 11 shows the locations of the model and test field collection sites.

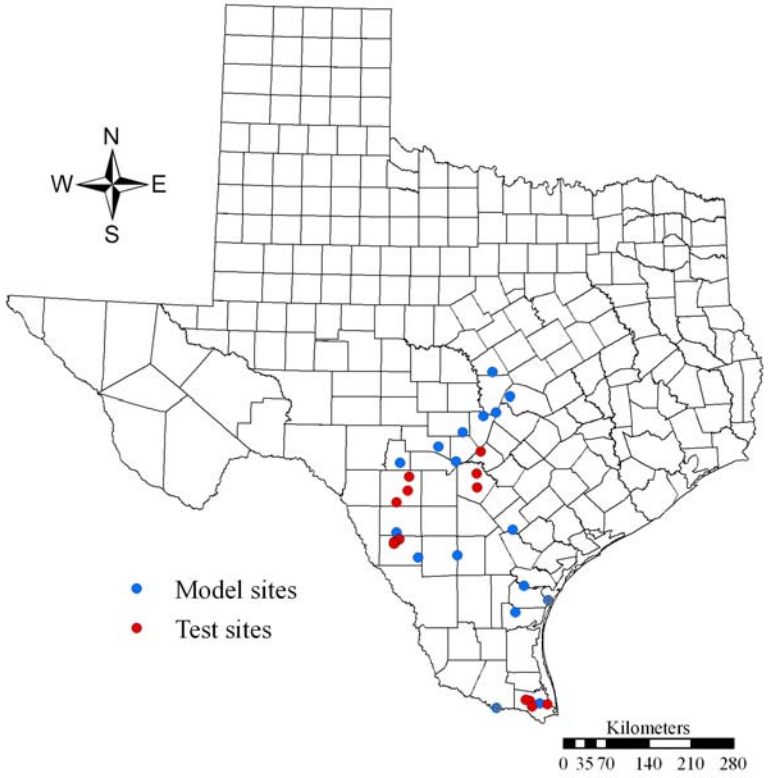

Figure 11. Location of *T. gerstaeckeri* collection sites in Texas 2005-2006 used for creation and accuracy assessment of a suitable habitat model.

The determination of the extent of habitat surrounding each *T. gerstaeckeri* field collection site was based on an estimated flight distance for the bug. Although there was no available data on flight distances achievable by *T. gerstaeckeri* specifically, maximum flight distances for other triatomine bug species have been projected to be up to several kilometers.[180, 181] Based on this estimate, a three kilometer radius boundary around the field collection site was chosen to delineate the insect habitat area of interest.

Habitat buffer zones around each of the 18 field sites selected for model development were created using ArcGIS 9.1 software (ESRI, Redlands, CA). A three and five kilometer circular section around each field site was extracted from classified scenes using the SelectMask command in the raster calculator function. The land class values in the five kilometer section were converted to negative numbers using raster calculator and then, joined to the three-kilometer section using the grid mosaic function. The resulting habitat buffer zone was composed of a three kilometer-radius circular area of positive land class values surrounded by a ring of negative values that extended outward two kilometers. Figure 12 shows an example of a habit buffer zone derived from one of the classified scenes.

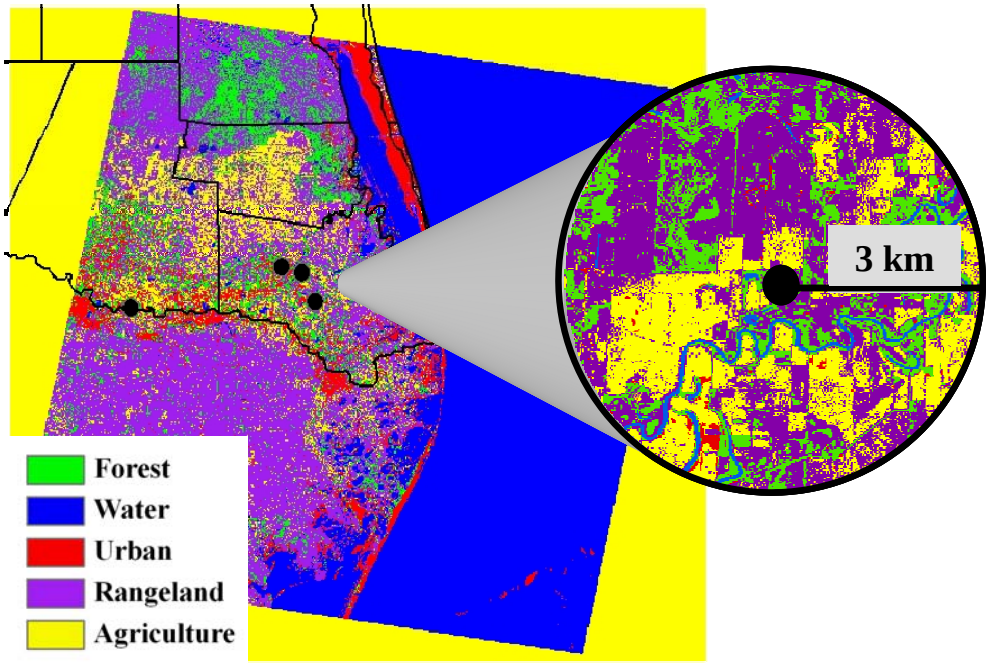

Figure 12. A *T. gerstaeckeri* habitat buffer zone created around a field collection site in Cameron County, Texas.

Landscape metrices for each habitat buffer zone were calculated using FRAGSTATS 3.3.[182] The ring of negative values surrounding the positive values in each habitat buffer zone was treated by FRAGSTATS as a border region, with the division between the negative and positive values defined as the landscape boundary. Only the positive values within the three kilometer section were included in land class area calculations. The negative values in the contiguous outer ring were incorporated into the calculation of edge length metrics of patches. A patch was defined as a region of neighboring pixels having the same land class values. If a patch extended beyond the three kilometer landscape boundary into the border area, the edge between the negative

and positive portions of the patch was not considered a true edge and, therefore, not included in the calculation of total edge length. The 8-cell patch neighbor rule was used for determining patch membership. Using the 8-cell rule, the four adjacent pixels sharing a side with the center pixel, plus the four diagonal pixels, were all evaluated for membership in the same patch. If these neighboring pixels had the same land class value, they were considered members of the same patch.

After landscape metrices were calculated for each habitat buffer zone, the data were combined by land class. An area range for each land class was determined by selecting the lowest and highest values across the habitat buffer zones.

Development of a suitable habitat model. The area ranges for each land class were used to predict suitable habitat for *T. gerstaeckeri*. Sections of the classified scenes surrounding the field sites designated for model testing were delineated using ArcGIS 9.1 software. Each section was separated into five layers, one for each land class. For each layer, pixels that contained a land class value that corresponded to the layer class value were assigned a value of one, and all other pixels were assigned a value of zero using the reclassify operation. Using the focal sum function, the values within a 2.825 km radius of the central pixel (optimized from the original 3 km radius) were summed to define the area covered by the land class in that zone. The resulting value was assigned to the central (or focal) pixel and the operation was repeated for all pixels in the layer.

The summed area value of each pixel was evaluated using the conditional command in the raster calculator function. Pixels with values that fell within the designated area range, as determined in FRAGSTATS, were assigned a value of one.

All other pixels were assigned a zero value. Finally, the values were summed on a pixel-by-pixel basis across all land class layers using the local sum function.

Results

Classification of satellite scenes into specified land classes. Before proceeding with the satellite scene classification process, the input parameters were optimized. All satellite scenes and DOQs had been radiometrically corrected and georeferenced by the provider, and no further processing was required to meet the objectives of the current study. Prior to classification of the scenes, bands 1-5 and 7 from Landsat ETM+ scene 2839 were analyzed using the 2D scatter plot function to determine individual band utility in discriminating between land cover classes. Bands 2, 3, 4, and 5 provided significant information and were selected for use in classification of all six Landsat ETM+ scenes.

Analysis of the training ROIs yielded good results. The selection of ROIs is critical because they are used to train the software to identify characteristics associated with each user-defined land cover class. Ideally, each ROI defines a unique land class with little overlap in spectral features as interpreted by the classification algorithm. The separability report in ENVI provides an estimate of the ROI overlap. A score of 2.0 indicates complete separation, the desired outcome. For each scene, 21 ROI comparisons were made. All scores were between 1.9 and 2.0, with the exception of one comparison between urban and rangeland from scene 2739, which was 1.81. All scenes were classified without further adjustment to the ROIs.

The classification process yielded six grid files, with all pixels in each file assigned one of five land class values: forest, 1; water, 2; urban, 3; rangeland, 4; agriculture, 5. To assess the accuracy of the classification, additional ROI points were selected for each land class and used in the generation of an error matrix. Errors of omission (pixels not assigned to the correct land class) and errors of commission (pixels assigned incorrectly to a land class) for each land class were calculated from the error matrix generated for each classified scene. Overall, the forest and water classes had consistently low error rates. The urban and agriculture classes had variable results across the classified scenes and the rangeland class registered a low level of error in every category. The classification of scene 2641 suffered from a fairly significant misclassification of true urban pixels as rangeland. The error rates by land class for each scene are summarized in Table 7.

Overall accuracy of each classified scenes was also derived from the error matrices. The results are summarized in Table 8. The kappa coefficient is an estimate of the agreement between the classified scene and reference data (ROIs). Values greater than 80% generally represent strong agreement, which is the desired outcome.[183] The minimum kappa value was well above the 80% level at 0.8813. The overall accuracy goal of 90% set for this project was exceeded or satisfactorily achieved for all scenes. No further adjustments were made to the classified Landsat ETM+ scenes.

Table 7

Errors of omission and commission by land class for Landsat ETM+ scenes used in a study of *T. gerstaeckeri* distribution in Texas, 2005-2006

Land class	Scene					
	2641	2642	2739	2740	2839	2840
Forest						
O	0.0	4.7	1.6	0.0	0.0	0.0
C	3.0	20.8	1.6	12.3	13.5	0.0
Water						
O	0.0	0.0	0.0	0.0	0.0	0.0
C	0.0	9.5	2.3	0.0	3.2	0.0
Urban						
O	43.7	14.1	21.9	6.3	23.1	0.0
C	0.0	0.0	0.0	0.0	0.0	0.0
Rangeland						
O	1.5	52.3	4.7	10.9	18.8	0.0
C	31.6	3.1	16.4	32.9	23.5	1.5
Agriculture						
O	3.9	0.0	2.3	21.1	12.5	0.8
C	0.8	10.4	3.7	1.3	8.6	0.0

O = errors of omission (%); C = errors of commission (%)

Table 8

Accuracy assessment of classified Landsat ETM+ scenes used in a study of *T. gerstaeckeri* distribution in Texas, 2005-2006

Scene	Overall accuracy (%)	Kappa coefficient
2641	92.48	0.9122
2642	89.82	0.8813
2739	95.31	0.9453
2740	91.52	0.9010
2839	90.67	0.8911
2840	99.74	0.9969

Landscape metrices. The following landscape metrices were calculated by land class for each habitat buffer zone: total area, number of patches, and large patch index. All habitat buffer zones contained all five land class types. Table 9 provides a summary of the landscape metrices averaged across all habitat buffer zones.

Table 9

Landscape metrices for designated *T. gerstaeckeri* habitat buffer zones in Texas, 2005-2006, by land class

Land Class	CA*	PLAND*	NP*	LPI*
Forest	827.0	33.4	352.8	17.7
Water	108.2	4.4	51.7	3.6
Urban	68.9	2.8	81.7	0.7
Rangeland	862.1	35.0	336.8	19.7
Agriculture	603.2	24.4	461.5	7.3

*The average of the 18 habitat buffer zone values

CA = Total class area (hectares); PLAND = Percentage of landscape

NP = number of patches; LPI = large patch index (%)

On average, the rangeland and forest classes occupied the largest area in the classified scenes (862 ha and 827 ha, respectively) followed by agriculture (603 ha). The urban and water classes accounted for a much smaller area in the habitat buffer zones. The water class had the fewest number of patches (52) and agriculture the most (462). The large patch index, which is the percentage of total landscape area occupied by the largest patch in the class, was highest on average for rangeland (20%) and forest

(18%), with much lower values for the other land classes. The landscape metrices results for individual habitat buffer zones are provided in Appendices A-E.

S*uitable habitat model*. Minimum and maximum area limits for each land class across all habitat buffer zones were determined from the class area results. These ranges were used to define suitable habitat in Texas for *T. gerstaeckeri* in the model. A list of the land class ranges used in the model is provided in Table 10.

Table 10

Land class area ranges (hectares) for *T. gerstaeckeri* habitat suitability model in Texas

Land class	Minimum	Maximum
Forest	280.2	1,265.4
Water	0.2	1,208.4
Urban	2.3	204.8
Rangeland	13.6	2,121.1
Agriculture	23.9	1,403.3

The forest land class had the highest minimum area requirement (280 ha) and water the lowest (0.2 ha). The urban land class had the most narrowly-defined area range (203 ha) and rangeland had the broadest area range (2,108 ha). These minimum and maximum limits were applied on a pixel-by-pixel basis, using the focal sum function in ArcGIS 9.1. Calibration of the focal sum function was required in order to match the catchment of the original habitat buffer zones used to calculate the land class ranges.

The circular radius was adjusted down to 2.825 meters from the original three kilometers to attain equivalent results.

After execution of the focal sum function, each pixel was tested to see if its value fell within the set range. A large portion of pixels in each land class layer were within the set limits, which was not surprising due to the broad area ranges for most land classes. However, it was evident after combining the land class layers, that there were clearly defined areas of optimal habitat (the intersection of suitable areas in all five land classes). The habitat suitability index reflects the intersection of land class layers. Areas of least suitable habitat, indicated by yellow, occurred at the intersection of unsuitable regions in all five land class layers. Areas of most suitable habitat, indicated by dark blue, occurred at the intersection of suitable regions in all five land class layers. The intermediate index values represent various combinations of suitable and unsuitable regions at the intersection of the land class layers. The individual steps of the model are illustrated in Figure 13.

1. Separate classified Landsat ETM+ scene into layers by land class. *Colored areas indicate presence of land class.*

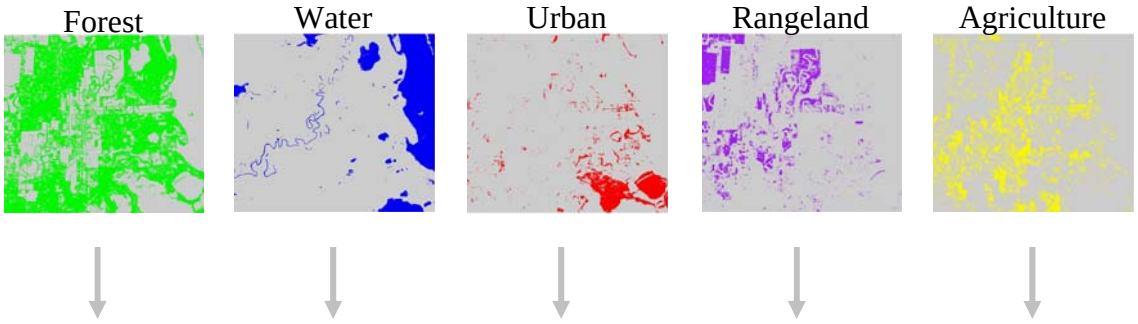

2. Calculate land class area for each pixel within a specified radius. *Stronger color intensity indicates high area values.*

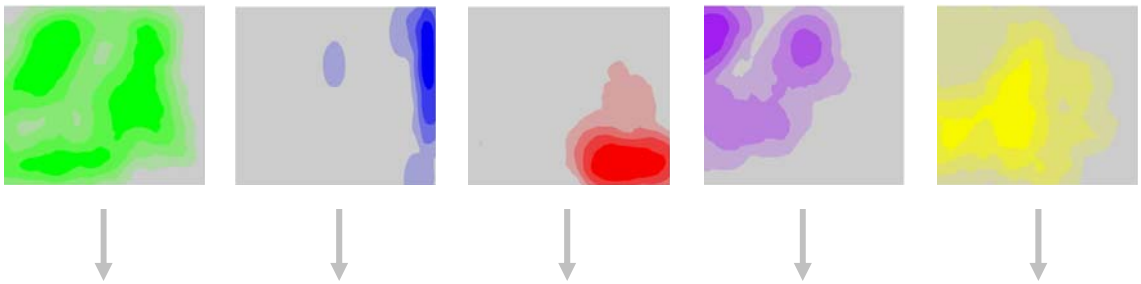

3. Designate pixels as suitable or unsuitable based on minimum and maximum land class values. *Blue indicates suitable areas.*

4. Combine land class layers to determine suitable habitat for *T. gerstaeckeri.*

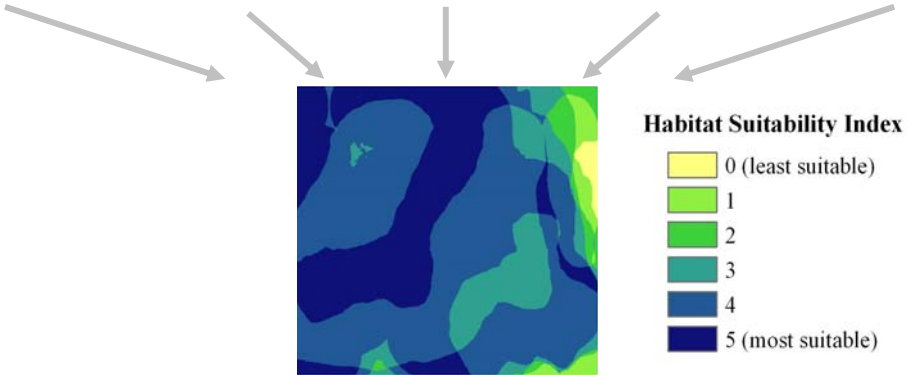

Figure 13. Steps in *T. gerstaeckeri* suitable habitat model developed for Texas.

To assess the validity of the model, 15 *T. gerstaeckeri* field collection sites were overlaid on the final habitat suitability maps. Sixty percent of the sites fell within the highest suitable regions, and 20%, 13%, and 6% fell within the second, third, and fourth highest suitable regions, respectively. None of the sites fell within the two most unsuitable regions. Of sites that did not fall within the highest suitable regions, most had values for the forest and urban land classes that exceeded the maximum limits for those classes. A small number of those sites had values that were less than the minimum limit for the agriculture class. Table 11 shows the results of the model validity testing. Figure 14 displays the 15 field collection sites used for validity testing overlaid on the modeled habitat areas.

Table 11

Validity of *T. gerstaeckeri* habitat suitability model developed for Texas

Habitat suitability index*	No. of Sites	Land class discordance
0	0	---
1	0	---
2	1	F, U, A
3	2	U, A, F
4	3	F, U
5	9	---

F = forest; U = urban; A = agriculture

*0 indicates the lowest level of suitability and 5 the highest

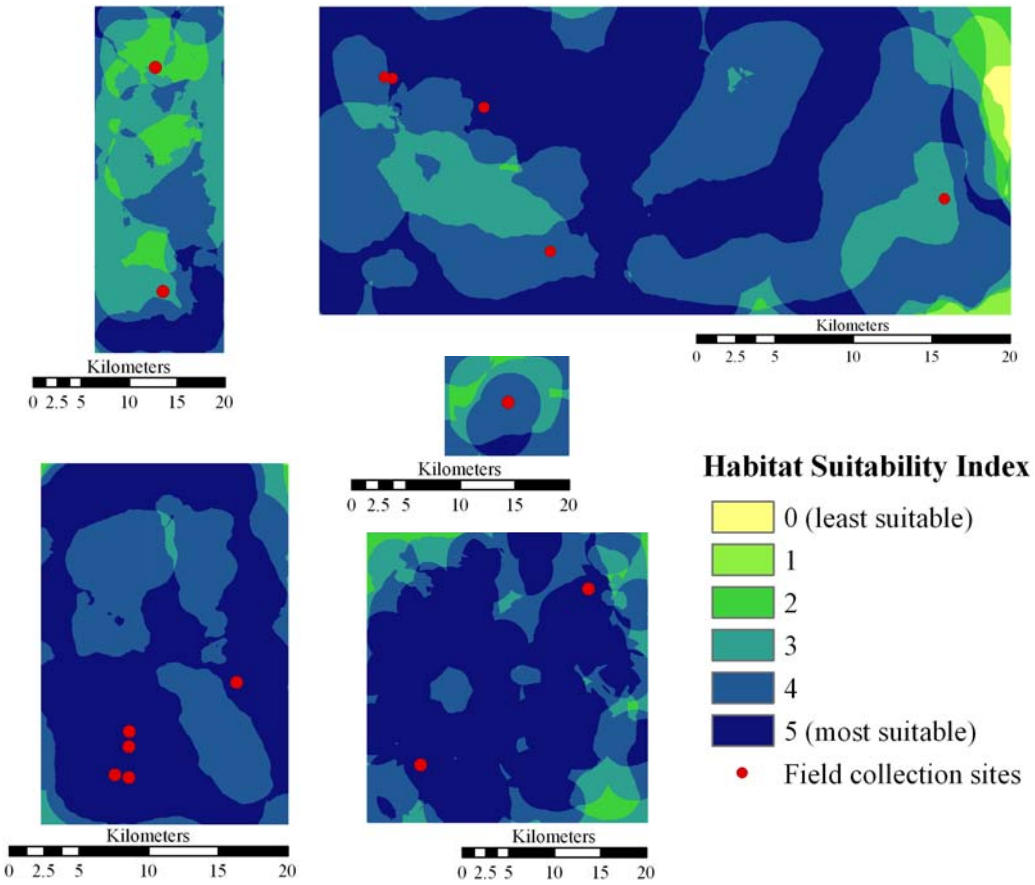

Figure 14. Suitable *T. gerstaeckeri* habitat modeled in selected areas of Texas with actual field collections sites overlaid.

Discussion

The Mahalanobis distance algorithm generally yielded good results for classification of the six Landsat ETM+ scenes. The correct classification of the rangeland, agriculture, and urban classes appeared to be the most problematic. A difficulty encountered during the selection of training ROIs for these classes was

achieving unimodality in the spectral histograms. Supervised classification methods, such as Mahalanobis distance, are parametric algorithms that require spectral unimodality for ROIs. The rangeland and agriculture classes exhibited large variation in their spectral characteristics. This was especially true for the agriculture class where areas indicative of crops (circular irrigation plots and rectangular fields) exhibited distinct differences in reflectance, creating bimodal spectral histograms. Some plots displayed bright red in a false color composite of bands 4, 3, and 2, while others displayed green. This discrepancy in reflectance could be due to a variation in the state of the crops at different sites. Bright red areas indicate high reflectance in band 4 (near-infrared), which is sensitive to vegetation biomass. Green areas indicate high reflectance in band 3, which is useful for detecting healthy vegetation. The disparity in reflectance uniformity may be due to the fact that the green areas had recently been harvested, and, therefore contained less vegetation biomass, while the red areas indicate unharvested crops. To correct for this disparity, two agricultural land classes (one for the bright red reflectance and one for the bright green reflectance) were created from separate ROIs. After classification, the two classes were combined to form a single agriculture class.

The same approach was used for the water class where two classes (one for deep water and one for shallow water) were used for classification and later combined. This technique proved to be more successful for the water class, which had little classification error, than for the agriculture class. The variation in rangeland spectral characteristics can be attributed to the mix of landscape features that comprise this class including sparse vegetation, grassland, scrub brush, and intermittent trees.

Some misclassification occurred between the urban and rangeland classes where true urban pixels were classified as rangeland by the algorithm. For this project, the urban class was intended to include areas of bare earth, which can have similar reflectance values in satellite imagery as sparsely-vegetated rangeland. The algorithm was programmed to assign every pixel to one of the five land classes, so it is not unexpected that a portion of pixels with values bordering between two classes were misclassified.

The consistency of classification across the six landscape scenes is not known. Each scene was processed separately using ROIs selected from within the respective scene. The year of acquisition was the same for all scenes, but the month varied. One scene was acquired in January, three in March, and two in May. Although seasonal changes are not as significant in Texas as regions located in more northern latitudes, vegetation cover does vary to some degree. The seasonal differences did not appear to have an impact on the determination of the minimum and maximum land class area limits. All values derived from the field collection sites located in the scene acquired in January, fell within the range of values derived from all other sites located in scenes acquired in months of presumably higher vegetation cover.

Temporality of field collection sites and acquisition of satellite scenes should also be considered. Field collections were conducted during 2005 and 2006 and the satellite images were all acquired in 2003, the most recent year available. Land cover changes that occurred between 2003 and the time of field collection could introduce error into the land class area ranges used to build the habitat suitability model. At a

higher resolution (e.g., 1 m x 1 m), the error rate would be more significant than at the 30 m x 30 m resolution used in this study.

Calculation of landscape metrices revealed that *T. gerstaeckeri* has been able to adapt to a broad range of area sizes within the specified land cover classes. This was expected based on the wide distribution of field collection locations across ecological zones. Forest and rangeland are the predominant land cover classes found within *T. gerstaeckeri* habitat buffer zones. In addition to accounting for the largest percentage of area within the zones, these two class types had the highest large patch index score, an estimate of class type dominance. However, the minimum rangeland area tolerated by *T. gerstaeckeri* in this study was low (13.6 hectares), suggesting that rangeland may not have much influence on habitat choice. After analyzing the values for the individual habitat buffer zones a pattern emerged, i.e., when rangeland is relatively low, forest area is much higher; and, when forest area is low, rangeland area is much higher. It appears these two land classes compensate for each other to maintain a dominate presence in the habitat buffer zones. Forest area may be the most important land cover for *T. gerstaeckeri* as indicated by significantly higher minimum area limit than the other four classes. Also, the maximum limit for forest area is likely much higher than derived in this study, or perhaps, unlimited. Of the field collection sites used to validate the model, four had forest values that exceeded the maximum limit, suggesting a high tolerance for forest land cover. Other triatomine species from the U.S. and Latin America have been found in densely forested-areas.[23, 71, 184]

The water and agriculture land classes had little influence on habitat choice in this study. The ranges of minimum to maximum area values for these two classes were extremely wide. Of the field collection sites used to validate the model, two had agriculture values that were lower than the minimum limit, suggesting that agriculture may not be a necessary component for presence of *T. gerstaeckeri*. Finally, the urban land class may be more tolerated by this bug species than suggested by this model. Like the forest class, four field collection sites used to validate the model had values that exceeded the maximum limit set for this class. As stated previously, *T. gerstaeckeri* has been frequently reported invading houses in Texas, so it is possible that this species has adapted to living in semi-urban or urban environments. Including additional levels of land cover classification such as type of forest or agriculture may also improve the precision of the model, but at the risk of increasing classification error.

The habitat suitability model in this study was based on the proportion of land class types found in the habitat buffer zone. Proportion of land class alone has been used successfully to predict distribution of wildlife species such as wild turkey in the Midwest.[185] A study of *Triatoma dimidiata*, the main Chagas disease vector in the Yucatan peninsula of Mexico, found a significant association between vector presence and particular vegetation cover.[186] However, the influence of landscape structure on complex disease transmission cycles may not be this simplistic. Land patch characteristics such as size, distribution, and shape may have an important influence on both vector habitat and disease transmission cycles. In a recent study on Lyme disease in Connecticut, the emergence of the disease in that area was linked to effects of forest

fragmentation rather than to change in the proportion of forest land cover.[171] The authors provide evidence that increased tick-infection prevalence was associated with a decrease in forest patch size, and suggest that human risk in the study area was driven by the proximity of these patches to other forested patches rather than size alone.

Habitat characteristics of nonhuman, vertebrate hosts may also increase the predictive power of triatomine habitat suitability models. The distributions of certain woodrat species were included in ecological niche models used to predict the distribution of two different *Triatoma* spp. in Mexico and southwest Texas.[82, 85] Host species distributions may be important components of a habitat suitability model, but their inclusion may present some difficulties for vector species such as *T. gerstaeckeri* that exploit a wide range of vertebrate hosts. The results of the current study provide information on the land cover composition associated with *T. gerstaeckeri* in Texas. Additional characterization of land cover, using a smaller spatial scale and higher resolution imagery, may provide further insights to the ecological dynamics influencing the presence and abundance of *T. gerstaeckeri*.

CHAPTER IV

GENETIC CHARACTERIZATION OF CHAGAS DISEASE VECTORS IN TEXAS BASED ON MITOCHONDRIAL DNA SEQUENCES

Introduction

Members of the Triatominae subfamily of insects (Hemiptera: Reduviidae) are vectors of *Trypanosoma cruzi*, the causative agent of Chagas disease. Chagas disease continues to be an important public health threat in the western hemisphere with a prevalence of 12 million human cases and 21,000 deaths annually.[1] Although transmission of the parasite to humans can occur by blood transfusion, organ donation, ingestion, or transplacentally, greater than 80% of all human cases are vectorborne.[6] Due to the lack of a vaccine or highly efficacious treatment, prevention of Chagas disease is primarily dependent on the control of triatomine vectors.[6, 9]

The organism and its triatomine bug vectors have been found in diverse ecological niches throughout the tropical and subtropical regions of North and South America, approximately between the latitudes of 42°N and 46°S.[4] Triatomine bugs are obligate blood feeders in all post-egg stages and are susceptible to infection with *T. cruzi* from the first blood meal forward. Transmission occurs when an infected bug defecates on or near the host during or shortly after feeding and the fecal material is subsequently rubbed into the bite wound, broken skin, or mucosal tissue.[7] Like the parasite they vector, triatomine bugs utilize a wide range of mammalian hosts. Many triatomine

species also readily feed on birds and reptiles. All species of Triatominae are considered potential vectors of *T. cruzi*.[8]

Identification of triatomine species and distinction of subgroups within species is critical to the control efforts mounted against these bugs and can be complicated by similarities in morphology.[108] The evolutionary processes involved in speciation are being explored with much interest. As control efforts successfully eliminate domesticated species, the adaptation of sylvatic species to this vacant ecological niche has become a concern. Many of the sylvatic species exhibit nonspecificity in host and habitat preference and presumably have the potential for adaptation to more specific settings.[11]

Molecular-based studies of triatomine species are beginning to clarify phylogenetic relationships between species, resolving taxonomic debates of crucial importance to Chagas disease vector control efforts.[121, 122, 123] Mitochondrial DNA (mtDNA) as a target of DNA analysis for population genetic studies is particularly attractive due to its simple structure, lack of recombination, maternal inheritance, and relatively rapid rate of evolutionary change.[124] Researchers utilizing mtDNA report success with fragments from the cytochrome oxidase I gene and the 12S and 16S ribosomal RNA genes as markers for interspecific triatomine phylogeographic studies.[121, 122, 123, 125, 126, 127, 128, 129, 130, 131] The cytochrome *b* (*cytB*) gene has been useful for detecting variation between closely related triatomine species[122, 129, 130, 131] and at the intraspecific level[127, 187, 188].

Of the 130 species currently recognized in the subfamily Triatominae[11], 11 have been reported in the southern half of the United States with seven in the state of Texas, to include *Triatoma gerstaeckeri* (Stål), *T. indictiva* Neiva, *T. lecticularia* (Stål), *T. neotomae* Neiva, *T. protracta* (Uhler), *T. rubida* (Uhler), and *T. sanguisuga* (Leconte).[12] Six of the recognized Texas species have distributions that extend into Mexico where there are an estimated 1.6 million human cases of Chagas disease.[72] At least two species, *T. gerstaeckeri* and *T. rubida*, have become closely associated with human habitats and transmission of *T. cruzi* in certain areas of Mexico.[72, 189] Although colonization of domestic habitats are rare in the U.S., accounts of triatomine bugs frequently encountered inside houses have been reported from Oklahoma, California, Texas, Florida, Tennessee, and Alabama.[21, 23, 24, 26, 27, 28]

Little work has been done to characterize the genetic variation in U.S. triatomine species or to determine their phylogenetic placement among Latin American species. To date, only four studies involving ten specimens (one *T. recurva*, four *T. rubida*, two *T. protracta*, two *T. lecticularia*, and one *T. rubrofasciata* specimens collected from Georgia, Arizona, Oklahoma, and other undisclosed U.S. locations) have been published on phylogenetic characteristics of U.S. triatomine species.[122, 125, 126, 131] The purpose of this study is to provide additional information on the genetic variation of U.S. triatomine species, particularly *T. sanguisuga* and *T. gerstaeckeri*, which have been frequently reported in close association with humans in the U.S.[23, 24, 53, 85, 87, 89, 175, 176] The state of Texas was selected as the study area due to its large size (678,054 sq km)[158], diversity of ecological regions, and geographic location at the intersection of eastern and western

triatomine species. In the U.S., Texas is the site of the highest triatomine species diversity.[12, 86, 190] In this study, the mitochondrial gene, *cytB*, was chosen to explore the genetic variation within and between triatomine species found in Texas and to determine their phylogenetic position among Latin American species.

Materials and Methods

Collection of triatomine specimens. Field specimens were collected from June 2005 to October 2006 from various sites within the state of Texas by the author, employees of the Texas Department of State Health Services (TX DSHS), and Texas residents. All adult specimens were identified to the species level using the key of Lent & Wygodzinsky.[12]

DNA extraction, amplification, and sequencing. Genomic DNA was extracted from legs using the PUREGENE® DNA Purification Kit (Gentra, Minneapolis, MN) for solid tissue with proteinase K digestion. Prior to the cell lysis incubation step, 4 legs were added to 900 µl cell lysis solution and ~1.2 g of 2.4 mm zirconia beads (Biospec Products, Inc., Bartlesville, OK) and pulverized using the Mini-Beadbeater-1 (Biospec Products, Inc., Bartlesville, OK). After pulverizing, 4.5 µl of proteinase K (20 mg/ml) was added to the sample. The sample was inverted 25 times and incubated at 55°C overnight. 4.5 µl of RNase A solution was added to the cell lysate, inverted 25 times, and incubated at 37°C for 30 minutes. The sample was transferred to a new 2 ml tube, leaving behind the beads. After cooling to room temperature, 300 µl of protein precipitation solution was added to the lysate and vortexed on high speed for 20 seconds.

The sample was cooled in an ice bath for 15 minutes and then centrifuged at 14,000 x g for 10 minutes. The supernatant containing the DNA was decanted into a 2 ml microfuge tube containing 900 µl 100% isopropanol (2-propanol) plus 1.5 µl of glycogen (20 mg/ml). The sample was inverted 50 times, incubated at room temperature for 5 minutes, and then centrifuged at 14,000 x g for 5 minutes. The supernatant was poured off and the tube drained on absorbent paper. 600 µl of 70% ethanol was added to the tube and the tube was inverted several times to wash the DNA pellet. The sample was centrifuged at 14,000 x g for 5 minutes and the ethanol decanted. The tube was drained on absorbent paper and air dried for 15 minutes. The DNA was rehydrated by adding 20 µl of DNA hydration solution and incubated at 65°C for 1 hour and several hours at room temperature. The DNA was stored at -28°C until further processing.

Standard polymerase chain reaction (PCR) techniques were used to amplify an ~700 bp fragment of c*ytB* using primers CYTB7432F, 5'-GGA CG(AT) GG(AT) ATT TAT TAT GGA TC -3', and CYTB7433R, 5'-GC(AT) CCA ATT CA(AG) GTT A(AG)T AA - 3'.[188] Amplifications were done in 25 µl reactions containing 1 µl of DNA template, 1x GoTaq Green Master Mix (Promega, Madison, WI), $MgCl_2$ final concentration adjusted to 2 mM, and 25 pM of primers. After an initial denaturation at 95°C for 1 minute, the reactions were cycled 35 times for 45 seconds at 95°C (denaturation), 45 seconds at 55°C (annealing), and 90 seconds at 72°C (extension), followed by a final extension for 7 minutes at 72°C. A dilution of 1:10 for *T. gerstaeckeri* DNA template was required before amplification was successful. The amplified products were visualized on 1.5% agarose gels with ethidium bromide. Bands

were extracted from low melt 1.5% agarose gels, purified using the Wizard SV Gel and PCR Clean-up System (Promega, Madison, WI). Details on gel purification are provided in Chapter II. Double-stranded DNA amplification products were sequenced using 2.5 μl of Perkin Elmer ABI Big Dye Reaction Mix plus 10 pM of primer in a PCR. The reactions were cycled 45 times for 10 seconds at 95°C, 5 seconds at 50°C, and 4 minutes at 60C, followed by a holding temperature of 4°C. The products were analyzed on an ABI PRISM® 3100 Genetic Analyzer (Applied Biosystems, Foster City, CA) by the Gene Technologies Laboratory at Texas A&M University. Consensus sequences were constructed and edited using Sequencher software (Gene Codes Corp., Ann Arbor, MI).

Sequence alignment and phylogenetic analysis. Edited *cytB* sequences were combined with other published triatomine *cytB* sequences into a Fasta formatted file and aligned locally using default parameters in the command-line version of the program MUSCLE.[191, 192] The aligned dataset was converted to Nexus format using the program seqConverter.pl, version 1.1.[193] MacClade v. 4.0[194] was used to color-code the *cytB* sequences by translated amino acid state (using the mold-protozoan mtDNA genetic code) to check for stop codons and gap-induced shifts to the reading frame. This Nexus file was analyzed under parsimony in a heuristic search in the program PAUP* version 4.10 (Altivec).[195] Five hundred random sequence additions were performed saving the 100 best trees from each generation. Branch support was assessed using the bootstrap[196] with default settings in PAUP*. One million bootstrap replications were performed in this study. Resultant equally-parsimonious trees were used to construct a strict

consensus tree. Tree images were exported from PAUP* and manually adjusted in Adobe® Illustrator® CS2 v.12.0.1.

Bayesian analysis under maximum likelihood was performed using the program MRBAYES 3.[197] Three analyses from different starting seeds were run for both 3 and 5 million generations, resulting in six total analyses. Sampling of the posterior distribution of trees was done every 1000 generations throughout each analysis using six Markov chains, keeping all chains at the same temperature and saving all branch lengths throughout. Flat priors were used for all analyses. Initial analyses were performed to determine the burn-in, or time until an acceptable plateau is reached in the sampling of likelihoods, trees and parameters in the posterior probability distribution. These burn-in values were determined by plotting log likelihoods (-ln *L*) and tree lengths (TL) over generation number in the program Tracer ver. 1.2.1.[198] Ultimately, a highly conservative value of 1,000,000 generations was selected for the burn-in prior to each of the three analyses. All resultant trees were combined in a majority rule consensus (50%) tree generated in PAUP*. Both parsimony and Bayesian tree images were exported from PAUP* and manually adjusted in Adobe® Illustrator® CS2 v.12.0.1.

Results

A total of 61 field specimens were included in the study: *T. sanguisuga*, 38 from 13 sites; *T. gerstaeckeri*, 10 from 7 sites; *T. lecticularia*, 7 from 5 sites; *T. indictiva*, 2 from 2 sites; *T. neotomae*, 2 from 1 site; *T. protracta*, 1; and *T. rubida*, 1. Figure 15 is a map of the field collection sites. All specimens were adults with the exception of one *T.*

gerstaeckeri fifth instar nymph (specimen SK TG 2). Thirteen additional sequences available in GenBank were used in the phylogenetic analyses. A description of all triatomine specimens used in the study including location, collection site, and *T. cruzi* infection status is provided in Table 12.

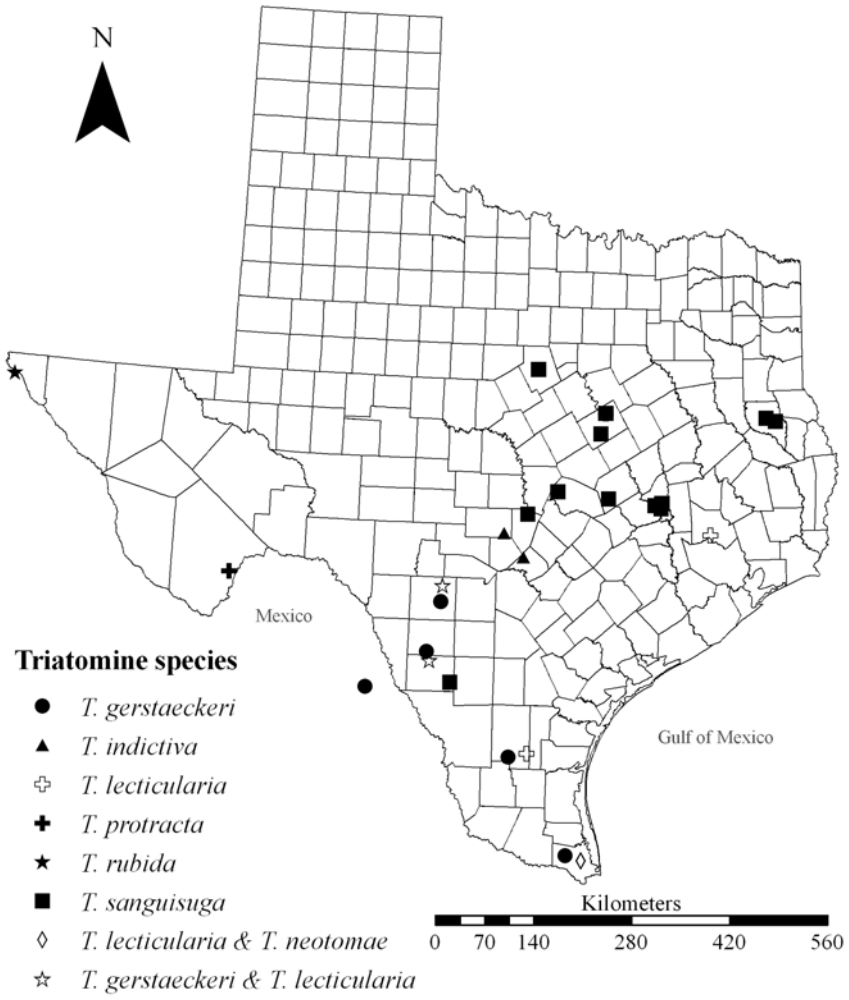

Figure 15. Location of triatomine field collection sites in Texas and Mexico, 2005-2006.

Table 12

Triatomine samples used in a study of the genetic variation of *Triatoma* spp. in Texas, 2005-2006

Taxon	Locality	Habitat[1]	*T. cruzi*[2]	Label	Reference[3]
Triatoma rubida cochimiensis	La Paz, BCS, Mexico			DQ198811	A
Triatoma rubida sonoriana	Sonora, Mexico			DQ198810	A
Triatoma rubida uhleri	Arizona, USA			DQ198809	A
Triatoma recurva	Arizona, USA			DQ198813	A
Triatoma phyllosoma	Oaxaca, Mexico			DQ198818	A
Triatoma mazzottii	Oaxaca, Mexico			DQ198816	A
Triatoma picturata	Jalisco, Mexico			DQ198817	A
Triatoma pallidipennis	colony			AF045724	B
Triatoma dimidiata	colony			AF045726	B
Triatoma protracta	colony			AF045727	B
Triatoma infestans	colony			AF045721	B
Rhodnius prolixus	colony			AF045718	B
Triatoma sanguisuga	Georgia, USA			AF045725	B
Triatoma protracta woodi	Brewster Co., Texas, USA	S	+	SK TP 2	this study
Triatoma lecticularia	McLennan Co., Texas, USA	D	+	SK TL 7	this study
Triatoma lecticularia	Montgomery Co., Texas, USA	S	+	SK TL 8	this study
Triatoma lecticularia	Cameron Co., Texas	K	NT	SK TL 3	this study
Triatoma lecticularia	Cameron Co., Texas	P	+	SK TL 4	this study
Triatoma lecticularia	McLennan Co., Texas, USA	P	NT	SK TL 2	this study
Triatoma lecticularia	Dimmit Co., Texas, USA	N	-	SK TL 1	this study
Triatoma lecticularia	Uvalde Co., Texas, USA	P	-	SK TL 5	this study
Triatoma neotomae	Cameron Co., Texas	K	-	SK TN 1	this study
Triatoma neotomae	Cameron Co., Texas	K	-	SK TN 3	this study
Triatoma rubida	El Paso Co., Texas, USA	P	-	SK TR 1	this study
Triatoma gerstaeckeri	Dimmit Co., Texas, USA	K	+	SK TG 7	this study
Triatoma gerstaeckeri	Uvalde Co., Texas, USA	P	+	SK TG 117	this study
Triatoma gerstaeckeri	Zavala Co., Texas, USA	D	-	SK TG 56	this study
Triatoma gerstaeckeri	Uvalde Co., Texas, USA	P	+	SK TG 61	this study
Triatoma gerstaeckeri	Uvalde Co., Texas, USA	P	+	SK TG 116	this study
Triatoma gerstaeckeri	Uvalde Co., Texas, USA	P	-	SK TG 10	this study
Triatoma gerstaeckeri	Villa Union, Mexico	P	+	SK TG 210	this study
Triatoma gerstaeckeri	Duval Co., Texas, USA	N	-	SK TG 12	this study
Triatoma gerstaeckeri	Cameron Co., Texas	N	NT	SK TG 2	this study
Triatoma gerstaeckeri	Uvalde Co., Texas, USA	P	-	SK TG 120	this study
Triatoma indictiva	Gillespie Co., Texas, USA	S	+	SK TI 2	this study
Triatoma sanguisuga	Blanco Co., Texas, USA	D	+	SK TS 32	this study
Triatoma sanguisuga	Brazos Co., Texas, USA	D	-	SK TS 27	this study
Triatoma indictiva	Comal Co., Texas, USA	P	-	SK TI 1	this study
Triatoma sanguisuga	Brazos Co., Texas, USA	P	NT	SK TS 14	this study
Triatoma sanguisuga	Brazos Co., Texas, USA	D	-	SK TS 7	this study
Triatoma sanguisuga	Williamson Co., Texas, USA	D	-	SK TS 1	this study
Triatoma sanguisuga	Brazos Co., Texas, USA	S	-	SK TS 39	this study
Triatoma sanguisuga	McLennan Co., Texas, USA	P	-	SK TS 20	this study
Triatoma sanguisuga	Williamson Co., Texas, USA	K	-	SK TS 33	this study
Triatoma sanguisuga	Brazos Co., Texas, USA	P	-	SK TS 29	this study
Triatoma sanguisuga	Brazos Co., Texas, USA	D	+	SK TS 35	this study
Triatoma sanguisuga	Williamson Co., Texas, USA	K	-	SK TS 34	this study
Triatoma sanguisuga	Milam Co., Texas, USA	D	+	SK TS 38	this study
Triatoma sanguisuga	Brazos Co., Texas, USA	D	NT	SK TS 6	this study

Table 12 Continued

Taxon	Locality	Habitat[1]	*T. cruzi*[2]	Label	Reference[3]
Triatoma sanguisuga	Brazos Co., Texas, USA	D	+	SK TS 26	this study
Triatoma sanguisuga	McLennan Co., Texas, USA	P	NT	SK TS 25	this study
Triatoma sanguisuga	McLennan Co., Texas, USA	P	+	SK TS 18	this study
Triatoma sanguisuga	Brazos Co., Texas, USA	D	+	SK TS 31	this study
Triatoma sanguisuga	Nacogdoches Co., Texas, USA	P	-	SK TS 16	this study
Triatoma sanguisuga	Nacogdoches Co., Texas, USA	P	NT	SK TS 15	this study
Triatoma sanguisuga	Nacogdoches Co., Texas, USA	P	-	SK TS 17	this study
Triatoma sanguisuga	Brazos Co., Texas, USA	P	-	SK TS 28	this study
Triatoma sanguisuga	Brazos Co., Texas, USA	P	NT	SK TS 13	this study
Triatoma sanguisuga	Brazos Co., Texas, USA	P	-	SK TS 37	this study
Triatoma sanguisuga	Brazos Co., Texas, USA	P	+	SK TS 22	this study
Triatoma sanguisuga	Brazos Co., Texas, USA	P	+	SK TS 23	this study
Triatoma sanguisuga	Brazos Co., Texas, USA	P	-	SK TS 8	this study
Triatoma sanguisuga	Brazos Co., Texas, USA	P	-	SK TS 9	this study
Triatoma sanguisuga	Brazos Co., Texas, USA	P	-	SK TS 10	this study
Triatoma sanguisuga	Brazos Co., Texas, USA	P	-	SK TS 11	this study
Triatoma sanguisuga	McLennan Co., Texas, USA	P	+	SK TS 21	this study
Triatoma sanguisuga	McLennan Co., Texas, USA	P	-	SK TS 24	this study
Triatoma sanguisuga	Erath Co., Texas, USA	D	-	SK TS 2	this study
Triatoma sanguisuga	Erath Co., Texas, USA	D	NT	SK TS 4	this study
Triatoma sanguisuga	McLennan Co., Texas, USA	D	+	SK TS 36	this study
Triatoma sanguisuga	McLennan Co., Texas, USA	P	-	SK TS 19	this study
Triatoma sanguisuga	Erath Co., Texas, USA	D	NT	SK TS 3	this study
Triatoma sanguisuga	Erath Co., Texas, USA	D	NT	SK TS 5	this study

[1]D = "Domestic" found inside house; K = "Kennel" found inside dog kennel; N = "*Neotoma*" found in wood rat nest; P = "Peridomestic" found on or near house; S= "Sylvatic" found in other sylvatic setting

[2]*T. cruzi* infection determined by PCR; NT = "not tested"

[3]A = Pfeiler (2006)[130]; B = Lyman (1999)[121]

The average length of new sequences was 698 bp, with 90% of sequences falling within 10 bp of the average length. Analysis of *cytB* sequences was based on 856 characters including gaps. The nucleotide composition of the 61 sequences was approximately 30% A, 21% C, 14% G, and 35%T. The high A-T composition (65%) is commonly found in insect mitochondrial genomes.[199] The sequence from *T. protracta* (SK TP 2) was significantly longer than all others with 789 bp, but with minimal differences in the nucleotide composition compared to the other sequences with the

common 698 bp length. Evaluation of the sequence revealed an insertion of non-coding and coding regions flanking the 3' end of the reverse primer. This same insertion was found in a *T. dimidiata cytB* sequence available in GenBank (accession number AF301594).

Analysis of the nucleotide variation across the sequences detected 271 variable sites with informative characters. The distribution of informative characters across codon positions was codon 1 with 62 (23%), codon 2 with 15 (5%), and codon 3 with 194 (72%). Results of the Bayesian analysis are shown in Figure 16. The examined species split into two main groups based on geographic location in South America (*T. infestans* and *Rhodnius prolixus*) and North and Central America (all others). Within the North and Central American clade, species divided into two groups: a *T. protracta* + *T. lecticularia* clade and a clade containing all other species in the study. Within the latter clade, the species divided into two groups: *T. neotomae* + *T. rubida* and a clade containing the *phyllosoma* complex species + *T. recurva* + *T. gerstaeckeri* and *T. sanguisuga* + *T. indictiva*. Within the *phyllosoma* complex + *T. recurva* + *T. gerstaeckeri* clade, members of the *phyllosoma* complex (*T. phyllosoma*, *T. mazzottii*, *T. pallidipennis*, and *T. picturata*) + *T. recurva* formed a clade and *T. dimidiata* + *T. gerstaeckeri* formed another clade. Sequences from the 61 new specimens separated into species groups based on morphologic characters with the exception of *T. indictiva*, which was contained within the *T. sanguisuga* clade. Bootstrap support was high for all clades described above (minimum of 81). Results from the parsimony analysis were similar to the Bayesian, but with less resolution within the primary clades (Fig. 17).

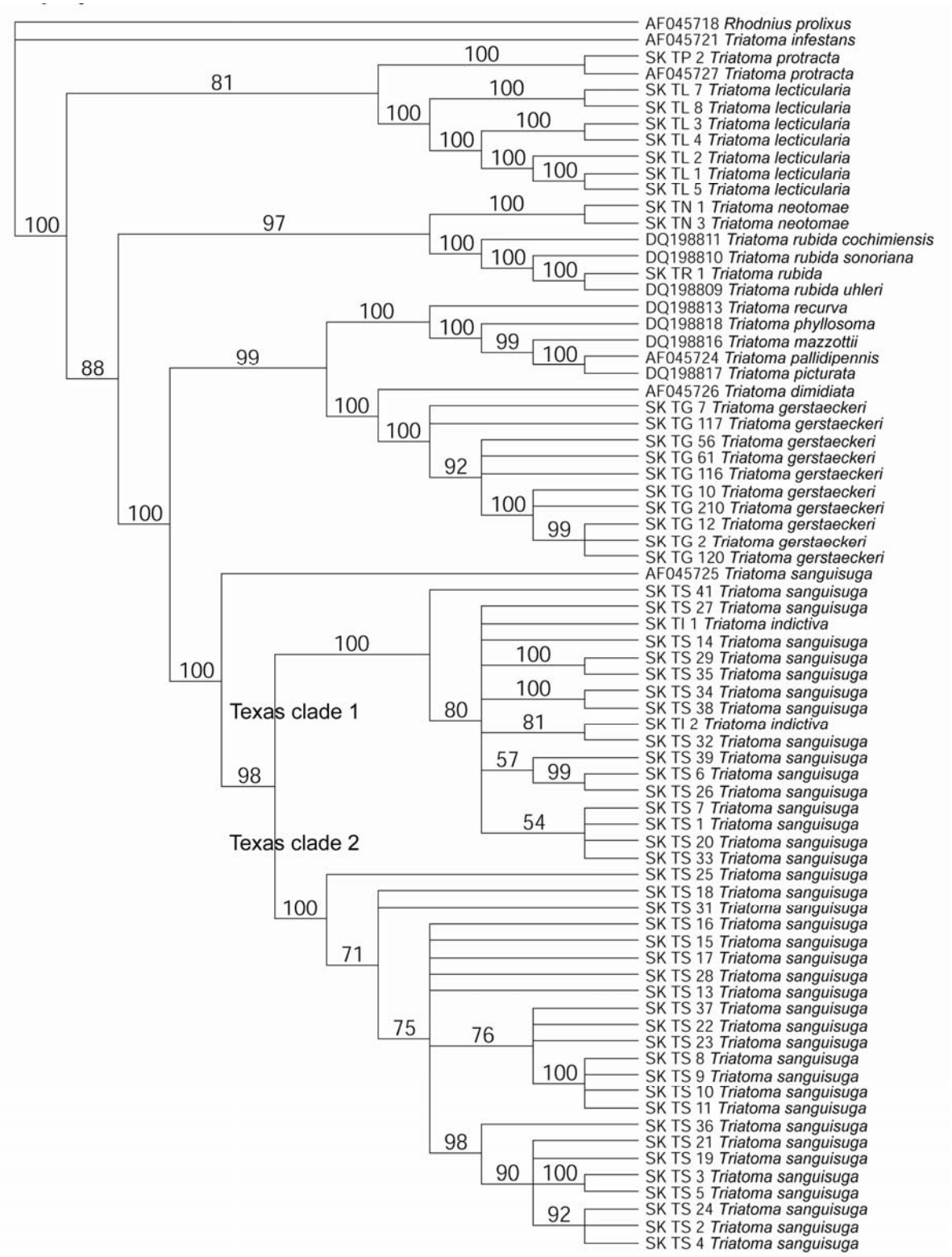

Figure 16. Bayesian estimated phylogeny based on *cytB* mtDNA data set for triatomine species. All members with the "SK" prefix were sequenced in the current study of *Triatoma* spp. species collected in Texas during 2005-2006. All others were obtained from GenBank and are labeled with the accession number and species name.

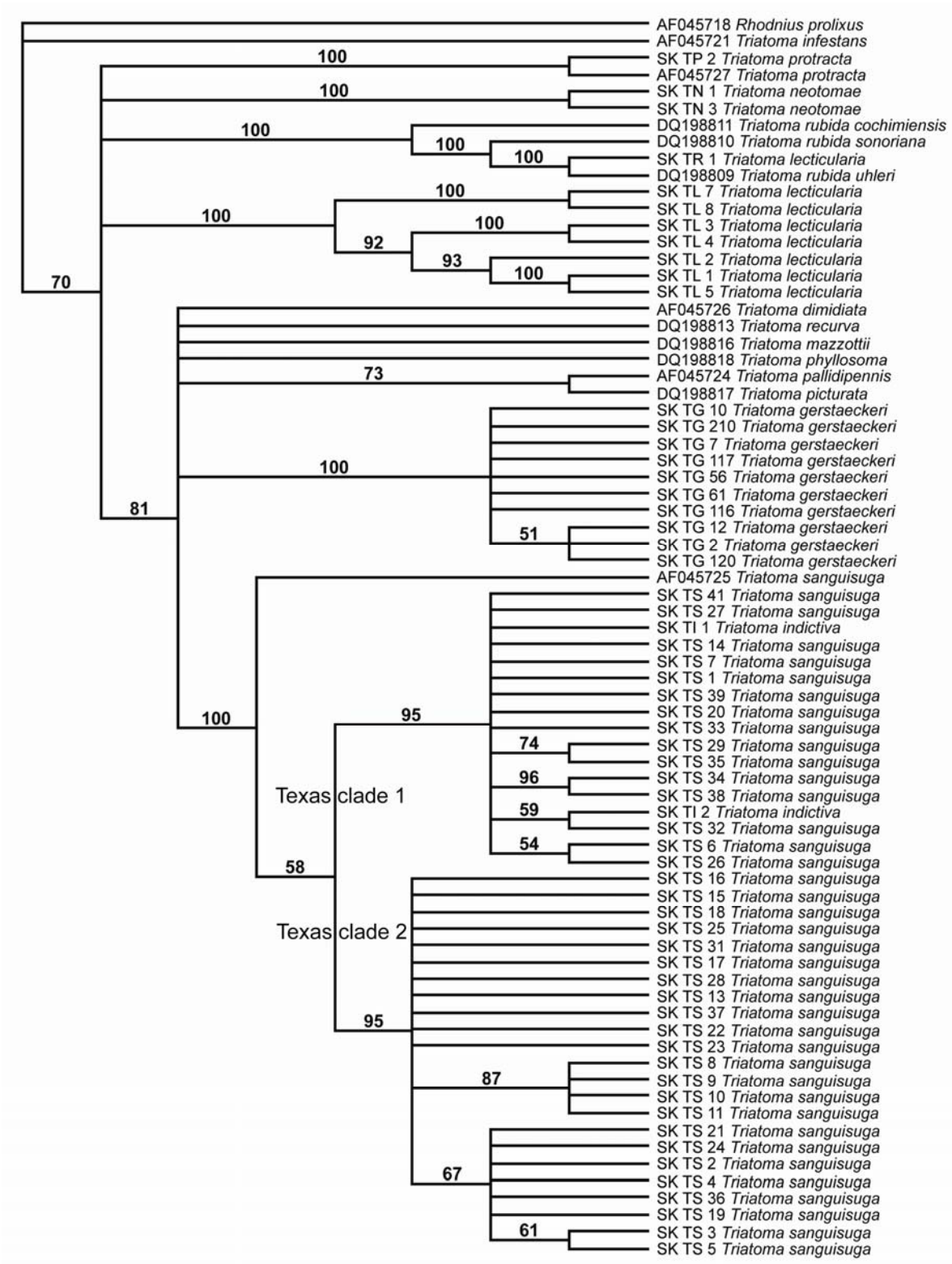

Figure 17. Parsimony tree based on *cytB* mtDNA data set for triatomine species. All members with the "SK" prefix were sequenced in the current study of *Triatoma* spp. species collected in Texas during 2005-2006. All others were obtained from GenBank and are labeled with the accession number and species name.

Discussion

The placement of the U.S. triatomine species analyzed in this study within the in the nine recognized *Triatoma* complexes by morphologic characters has been largely tentative.[157] Table 13 provides the list of *Triatoma* species used in the current study by complex based on morphologic characters.

Table 13

Species complexes[1] within the genus *Triatoma* and species used in the study of genetic variation of Texas specimens, 2005-2006

Complex	Species[2]
infestans	*infestans*
lecticularia	*(indictiva), lecticularia, sanguisuga*
phyllosoma	*(dimidiata), mazzottii, pallidipennis, picturata, phyllosoma*
protracta	*(neotomae), protracta*
rubrofasciata	*(rubida)*

[1]based on morphologic characters after Lent and Wygodzinsky, 1979, and Schofield, 1988

[2]placement of species in parenthesis is uncertain

[3]*gerstaeckeri* and *recurva* have not been associated with a complex

This was the first study to analyze the taxonomic status of *T. gerstaeckeri, T. indictiva,* and *T. neotomae* using molecular markers. Although collected from a limited geographic region in the current study, *T. gerstaeckeri* is widely distributed across the state of Texas.[90] The Bayesian analysis placed this species in the same major grouping as the *phyllosoma* complex and closely aligned with *T. dimidiata*. If this taxonomic

relationship is confirmed, *T. gerstaeckeri* would represent the northern extent of the *phyllosoma* complex which stretches southward to northern Peru.

Originally classified as a subspecies of *T. sanguisuga* by Usinger (1944)[86], *indictiva* was elevated to species status by Lent & Wygodzinsky (1979)[12] and later retained by Ryckman (1984)[190]. The inclusion of *T. indictiva* within the *T. sanguisuga* clade found in the current study warrants a reconsideration of its taxonomic status. Interestingly, the two *T. indictiva* sequences did not group together in either analysis. Both specimens met the morphologic characterizations of Lent and Wygodzinsky (1979)[12] for this species with the exception of a pale yellowish rather than reddish coloring of the connexival markings on specimen SK TI 2.

T. neotomae is considered to be closely related to *T. nitida* (a tropical species found in Mexico, Guatemala, and Honduras) based on morphologic characters, and both have been assigned to the *protracta* complex.[12, 86] *T. nitida* grouped together with *T. protracta* in a poorly-supported clade in two previous studies using 12S and 16S rDNA sequences.[125, 126] However, two subsequent studies using *cytB* and *COI* sequences found *T. nitida* to be more closely related to *T. rubida* and separated from *T. protracta*, which may correlate to the grouping of *T. neotomae* with *T. rubida* but separate from *T. protracta* found in the current study.[130, 131]

The inclusion of *T. sanguisuga* (and *indictiva*) in the *lecticularia* complex may also require re-evaluation. Tree topologies from Martinez et al.[130] and the current study suggest that *T. sanguisuga* is more closely related to the *phyllosoma* complex than

lecticularia complex, and *T. lecticularia* and *T. protracta* are more closely related to each other than *T. protracta* and *T. nitida* or *T. neotomae*.

The morphologic species determinations for field collected specimens in this study were based on Lent and Wygodzinsky (1979)[12] who did not support subspecies status for variants within *T. sanguisuga* and *T. rubida*. When using the subspecies morphologic characteristics proposed by Usinger (1944)[86] for these two species, the *T. rubida* specimen in this study (SK TR 1) would be classified as *T. rubida uhleri*, and the *T. sanguisuga* specimens would all be *T. sanguisuga sanguisuga*, with the exception of one specimen (SK TS 41) which would be *T. sanguisuga texana*. The phylogenetic relationships determined by the current analyses provide strong support for these subspecies classifications.

The meaning of intraspecific groupings obtained in this study for *T. sanguisuga* and *T. gerstaeckeri* was not readily apparent. The distinct separation between the *T. sanguisuga* sequence obtained from GenBank (AF045725) and the other *sanguisuga* sequences could be due to differences in geographic location (Texas vs. Georgia) or perhaps subspecies membership. For the *T. gerstaeckeri* and *T. sanguisuga* specimens collected in Texas, segregation did not occur by geographic location, collection site, or *T. cruzi* infection status. For *T sanguisuga*, there appears to be a north-south orientation for clade 1 and an east-west orientation for clade 2, but there is a large degree of overlap for these two lineages (Fig. 18). Absence of partitioning by geographic location has been reported for other triatomine species as well, suggesting that these species may be panmitic within the respective study areas.[127, 131] Both *T. gerstaeckeri* and *T. sanguisuga*

have widespread geographic distributions and have been associated with an extensive range of hosts and habitats including humans and domestic dwellings.[14, 23, 90] Although the dispersion capabilities and flight ranges have not been explored for these two species, their low specificity regarding host and habitat may allow them to be opportunistic in their mating, leading to a high degree of gene flow across their ranges.

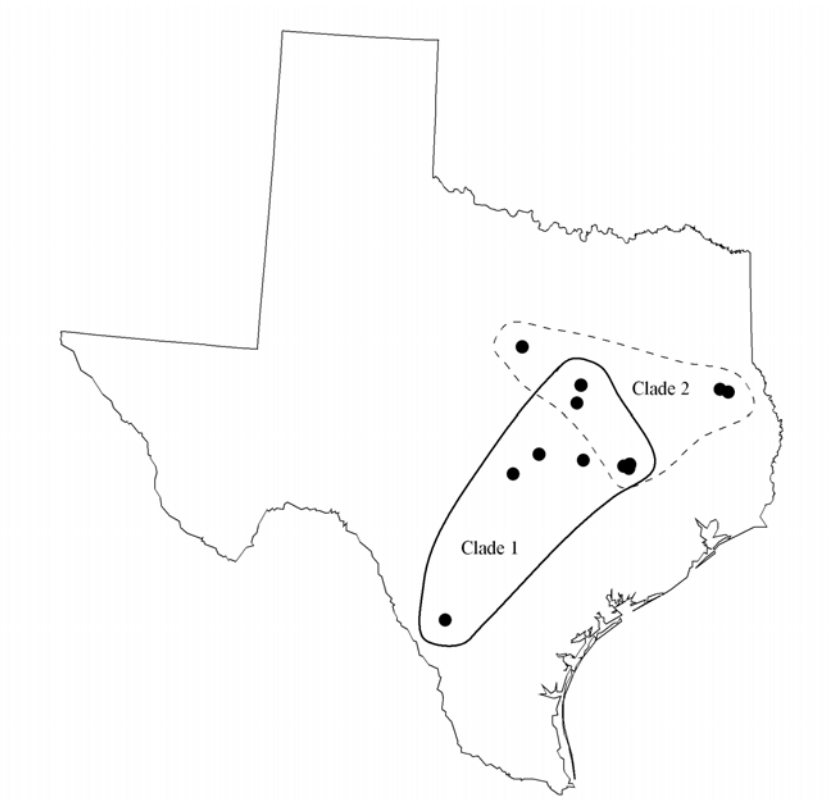

Figure 18. Geographic distribution of clades 1 and 2 for *T. sanguisuga* collected in Texas during 2005-2006.

Although the tree topology is based on a single gene segment, *cytB*, several triatomine phylogenetic studies have found similar or improved results when using *cytB* as compared to other molecular markers.[122, 123, 130, 131, 188] The application of additional molecular markers to the analysis of sequences included in the current study would be useful to establish the phylogenetic position of U.S. species with greater certainty. The results of this study suggest the following: 1) *T. sanguisuga* is more closely related to the *phyllosoma* complex than the *lecticularia* complex; 2) *T. gerstaeckeri* is closely aligned with the *phyllosoma* complex; 3) *T. indictiva* is a subspecies of *T. sanguisuga*; 4) A high degree of gene flow occurs for *T. sanguisuga* and *T. gerstaeckeri* across their ranges within the state of Texas. The results of this study will provide baseline data for more extensive evaluation of intraspecific variation within the U.S. species groups.

CHAPTER V

GENETIC CHARACTERIZATION OF *Trypanosoma cruzi* ISOLATES FROM *Triatoma* spp. IN TEXAS BASED ON SMALL SUBUNIT RIBOSOMAL RNA GENE SEQUENCES

Introduction

It is well recognized that *Trypanosoma cruzi* is endemic in the United States, as evidenced by infections reported in a wide range of mammalian wild life species, domestic dogs, and in some instances, humans. In the southern United States, *T. cruzi* infections in wild populations of opossums, wood rats, raccoons, armadillos, and coyotes have been reported for the past 70 years.[15, 18, 22, 23, 29, 30, 31, 32, 33, 34, 35, 36] Acute and chronic infections in domestic dogs have been reported in Texas, Oklahoma, Louisiana, Virginia, South Carolina, Georgia, and Tennessee.[24, 37, 38, 39, 40, 41, 42, 43] The data on prevalence of *T. cruzi* in U.S. vectors are primarily derived from specimens collected in Texas, California, and Arizona, with rates ranging from 17-48%, 14-40%, and 7.1-20.5%, respectively.[13, 14, 15, 16, 17, 18, 19, 20] *T. cruzi*- infected vectors have also been found in Florida, Georgia, Alabama, Tennessee, and Louisiana.[21, 22, 23, 24, 25] Although the reported incidence of human Chagas disease in the U.S. is low, U.S. strains of *T. cruzi* have proven to be virulent, as confirmed by clinical disease and death in a wide range of mammalian species including domestic dogs, primates, and humans.[18, 37, 38, 52, 62, 63, 64]

Impressive genetic diversity within the *T. cruzi* species has been recognized since the late 1970's when analysis by protein electrophoresis divided South American strains

into 3 distinct divisions, zymodemes 1-3 (Z1, Z2, Z3).[132, 133] Z1 and Z3 were originally associated with sylvatic transmission, and Z2 with domestic transmission.[134] Isoenzyme analysis proved valuable initially in monitoring vector control efforts. Acute cases of Chagas disease caused by Z1 and Z3 strains were reported in areas of Brazil where the vast majority of human cases had been due to Z2 strains prior to chemical vector contol.[133, 135] This suggested that sylvatic species or subgroups of triatomine bugs known to carry the Z1 or Z3 strains may be replacing the domestic triatomine bugs eradicated through spraying. Further study of these sylvatic vectors showed that they were able to adapt to human habitation.[136, 137]

The advent of polymerase chain reaction (PCR) technology in 1993 led to definitive proof that parasites remained in vertebrate tissues at low levels, causing disease progression in some individuals.[138] Prior to this discovery, little consideration was given to parasite strain differences over nutritional, immunological, and environmental factors as an explanation for variation in clinical presentation. Since that time, researchers have struggled to incorporate *T. cruzi* heterogeneity into the epidemiology of the disease.[139, 140] A variety of molecular DNA analysis methodologies have been used to refine the classification scheme of *T. cruzi*, including schizodemes, RAPD-PCR, mini-exon polymorphisms, rDNA polymorphisms, and microsatellite analysis.[141] Most DNA studies have revealed the existence of two primary groups within *T. cruzi*; and, in 1999, an international committee recommended the universal acceptance of these two divisions designated as *T. cruzi* I (corresponding to zymodeme type Z1) and II (corresponding to Z2).[142] A third group was also proposed, *T. cruzi*

(without a number designation), to correspond to zymodeme type Z3 and all other uncharacterized strains. Subsequent studies using RAPD, multi-locus enzyme electrophoresis, large and small subunit rRNA, and mini-exon markers further characterized *T. cruzi II* into five subgroups, collectively referring to all six divisions as discrete typing units (DTUs).[143, 144] In this classification, Z3 is equivalent to *T. cruzi* IIa and IIc. Progress towards meaningful characterization of *T. cruzi* isolates continues as researchers explore the use of nucleotide sequences, particularly within the small subunit ribosomal RNA (18S rRNA in eukaryotes). This gene has been especially useful for phylogenetic studies of the Kinetoplastida, the order to which *T. cruzi* belongs.[140, 145, 146] It has also proven to be informative for intraspecific studies of *T. cruzi* isolates, rendering results in line with the recognized dichotomous classification of strains.[140, 145, 147, 148, 149, 150, 151, 152].

A small collection of *T. cruzi* isolates from the U.S. (California, 2; Florida, 1; Georgia, 18; Louisiana, 7; and Texas, 3) has been analyzed by either protein electrophoresis, RAPD-PCR, or rDNA polymorphism.[21, 22, 153, 154, 155, 156] A single study examined a cross-section of isolates from five different U.S. states, and through RAPD-PCR analysis, provided evidence that U.S. strains are genetically diverse and probably indigenous to the North American continent.[153] Isolates examined in previous U.S. studies were primarily from mammals and only three from triatomine bugs. Further analysis of additional U.S. *T. cruzi* isolates is required to understand the genetic diversity and evolutionary pathway of the parasite in North America. The aim of this study was to collect and evaluate new *T. cruzi* specimens from the state of Texas using 18S rRNA as

the molecular marker for phylogenetic analyses. Texas supports the highest diversity of triatomine bug species and has been the site for five of the seven human cases of Chagas disease reported in the U.S.[27, 51, 52, 54]

Materials and Methods

Collection of T. cruzi *isolates.* Triatomine bug specimens were collected from June 2005 to October 2006 from various sites within the state of Texas by the author, employees of the Texas Department of State Health Services (TX DSHS), and Texas residents. Sites sampled by the author were selected based on previous reports of triatomine bug sightings or canine Chagas disease cases. Specimens collected by health department employees and residents were primarily taken from in and around houses and dog kennels as prompted by concerns of disease transmission risk. All adult specimens were identified to the species level using the key of Lent & Wygodzinsky.[12] *T. cruzi* isolates from 4 dogs and a baboon from Texas and a human isolate from Brazil were included. The baboon, human, and 3 dog isolates were from culture stocks, and 1 dog isolate was extracted directly from cardiac tissue.

Processing of triatomine specimens. The hindgut from each field-collected bug was dissected following the procedure of Garcia and De Azambuja[159] using sterile, disposable scalpels, and forceps disinfected with a 10% bleach solution and ultrapure water rinse between samples. The excised hindgut was placed in 50 µl of molecular grade water and homogenized using a motorized sterile, disposable pestle. A 5 µl aliquot of homogenate was examined by phase contrast microscopy at 400x for the

presence of trypanosomes. The remaining sample was stored at -70°C until further processing.

DNA extraction and PCR analysis. DNA was extracted from all bug hindgut and vertebrate samples using the PUREGENE® DNA purification Kit (Gentra, Minneapolis, MN), body fluids protocol and used as template for PCR amplification. Refer to Chapter II for details on DNA extraction. One of two primer sets was used for detection of *T. cruzi* in all samples: Tc24T1F-Tc24T2R[160] that target a ~550 bp segment of a *T. cruzi*-specific flagellar protein gene; and, Tc609F[149] and TcV5R (newly designed) that target a ~900 bp segment of non-specific trypanosome nuclear 18S rRNA. A nested primer set was created to amplify specimens with a weak response to the 18S rRNA primer set: TcV4F (newly designed) and Tc706R_mod (modified from Da Silva et al.[149]). An internal reverse primer, Tc1369, was designed to bridge the Tc609F and TcV5R SSU rRNA sequences when required. A list of all primers used in the current study is provided in Table 14.

Amplifications were done in 25 µl reactions containing 1 µl of DNA template, 1x GoTaq Green Master Mix (Promega, Madison, WI), $MgCl_2$ final concentration adjusted to 2.5 mM, and 10 pM of primers. After an initial denaturation at 95°C for 1 minute, the reactions were cycled 35 times for 45 seconds at 95°C (denaturation), 45 seconds at 58°C (annealing), and 90 seconds at 72°C (extension), followed by a final extension for 7 minutes at 72°C. The amplified products were analyzed on 1.5% agarose gels with ethidium bromide. Amplified SSU rRNA gene products positive for a band at ~900 bp were extracted from a low melt 1.5% agarose gel, purified using the Wizard SV Gel and

PCR Clean-up System (Promega, Madison, WI). Refer to Chapter II for details regarding gel purification. Double-stranded DNA amplification products were sequenced using 2.5 μl of Perkin Elmer ABI Big Dye Reaction Mix plus 10 pM of primer in a PCR. The reactions were cycled 45 times for 10 seconds at 95°C, 5 seconds at 50°C, and 4 minutes at 60C, followed by a holding temperature of 4°C. The products were analyzed on an ABI PRISM® 3100 Genetic Analyzer (Applied Biosystems, Foster City, CA) by the Gene Technologies Laboratory at Texas A&M University. Consensus sequences were constructed and edited using Sequencher software (Gene Codes Corp., Ann Arbor, MI) and compared to sequences in GenBank using the BLASTN search for trypanosome species identification.

Table 14

Primer sets used in a study of *T. cruzi* isolates from Texas, 2005-2006

Primer	Gene	Sequence
Tc609 (F)	SSU rRNA	5’-CAC CCG CGG TAA TTC CAG C-3’
TcV5 (R)	SSU rRNA	5’-ACT CTT GCG AAC GTA CTC CCC-3’
Tc1369 (R)	SSU rRNA	5'-GCC TAC GAC CAA AAA CTC CC-3'
TcV4 (F)	SSU rRNA	5'-CTC CAA AAG CGT ATA TTA ATG-3'
Tc706_mod (R)	SSU rRNA	5'-CTG AGA CTG TAA CCT CAA-3'
Tc24T1 (F)	24kDa flagellar	5’-GAC GGC AAG AAC GCC AAG GAC-3'
Tc24T2 (R)	24kDa flagellar	5’-TCA CGC GCT CTC CGG CAC GTT GTC-3’

Sequence alignment and phylogenetic analysis. The *T. cruzi* 18S rRNA sequences were combined with other published trypanosome 18S rRNA sequences and aligned manually according to secondary structure[200], with the notation following Gillespie (2004).[201] Alignment of the 18S rRNA initially followed the cytoplasmic 18S rRNA secondary structural model of *T. cruzi*[202], with refinement to the variable region 4[203] made from the double pseudoknot model of Wuyts *et al*.[204] and the tertiary interaction between V4 and V2.[205] The recent helix numbering scheme for arthropod SSU rRNA was used.[206, 207] All regions variable in sequence length and base composition, especially hairpin-stem loops, were evaluated in the program *mfold* version 3.1[208], which folds RNA based on free energy minimizations.[209, 210, 211] These free energy-based predictions were used to facilitate the search for potential base-pairing helices, which were confirmed only by the presence of compensatory base changes across a majority of taxa. Regions in which positional homology assignments were ambiguous across all taxa were defined according to structural criteria as in Kjer[212] and characterized according to Gillespie[201]. All of these unaligned regions were enclosed within brackets and not included in phylogeny estimation.

The structurally-aligned dataset was converted to a Nexus file and analyzed under parsimony in a heuristic search in the program PAUP* version 4.10 (Altivec).[195] Five hundred random sequence additions were performed saving the 100 best trees from each generation. Branch support was assessed using the bootstrap[196] with default settings in PAUP*. One million bootstrap replications were performed and resultant equally-parsimonious trees were used to construct a strict consensus tree. A tree was

also estimated under distance methods in PAUP* to provide an alternative topology to the consensus parsimony tree. Tree images were exported from PAUP* and manually adjusted in Adobe® Illustrator® CS2 v.12.0.1. Ribosomal RNA secondary structure diagrams were manually created in Adobe® Illustrator® CS2 v.12.0.1 following the convention of the Comparative RNA Web (CRW) Site.[202]

Results

T. cruzi *detection in field collected triatomine bugs*. Triatomine bugs from 31 counties in Texas and two specimens from Villa Union, Mexico, collected between June 2005 and August 2006 were included in the study. Of 178 bug specimens tested, 91 produced an 18S rRNA PCR product at the target length of ~900 bp, resulting in a 51% infection rate. Of the 91 positive amplifications, DNA sequence data were successfully obtained for 65 products. Five specimens required the use of a nested primer reaction to increase amplification, and eight required the use of an internal sequencing primer to bridge the two sequence segments and provide sufficient sequence overlap. A 1:10 dilution of DNA template was required for five specimens to obtain sufficient amplification. The PCR for all negative specimens was repeated using a 1:10 dilution of DNA template to ensure no positive samples were missed. Of the isolates sequenced, 63 were characterized as *T. cruzi* based on similarity (99-100%) to GenBank sequences. Sequences from the other two specimens were 99% similar to a *Blastocrithidia triatomae* SSU rRNA sequence in GenBank (accession number AF153037). The *B. triatomae*-positive specimens were extracted from a *T. neotomae* found in a dog kennel

in Cameron County, Texas, and a *T. gerstaeckeri* found inside an office building in Zavala County, Texas. The 26 positive samples not sequenced all appeared as double bands at the 18S rRNA target product length. These 26 samples all produced positive results when tested with *T. cruzi*-specific primers for a 24kDa flagellar protein. Figure 19 is a gel image showing a subset of the double-banded products.

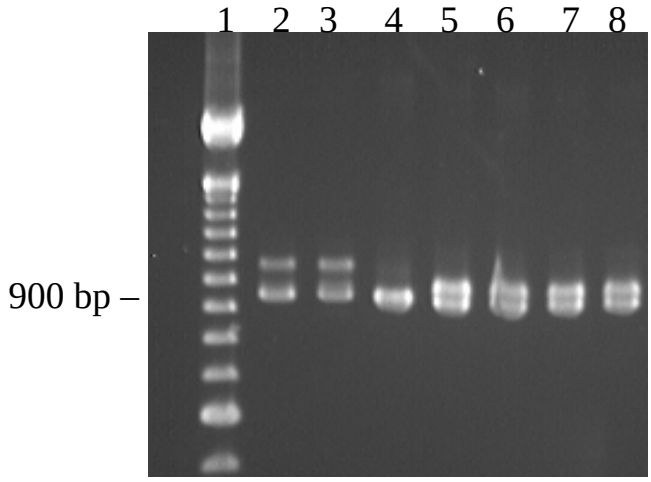

Figure 19. *T. cruzi* 18S rRNA gene PCR amplification products derived from *T. gerstaeckeri* hindgut specimens from Texas, 2005-2006. Lane 1 is a 100 bp ladder. Lanes 2, 3, and 5-8 show products with double bands.

New 18S rRNA sequences (65) were recovered from 6 triatomine bug species collected from 22 Texas counties and Mexico. A list of sequences by host and parasite species is provided in Table 15. Figure 20 shows the geographic distribution of the sequenced isolates.

Table 15

New SSU rRNA sequences analyzed in a study of *T. cruzi* isolates from Texas, 2005-2006

Host	*T. cruzi*	*B. triatomae*
Dog	4	0
Baboon	1	0
Human	1	0
Triatoma spp.		
gerstaeckeri	50	1
indictiva	1	0
lecticularia	2	0
neotomae	0	1
protracta	2	0
sanguisuga	8	0
Total	69	2

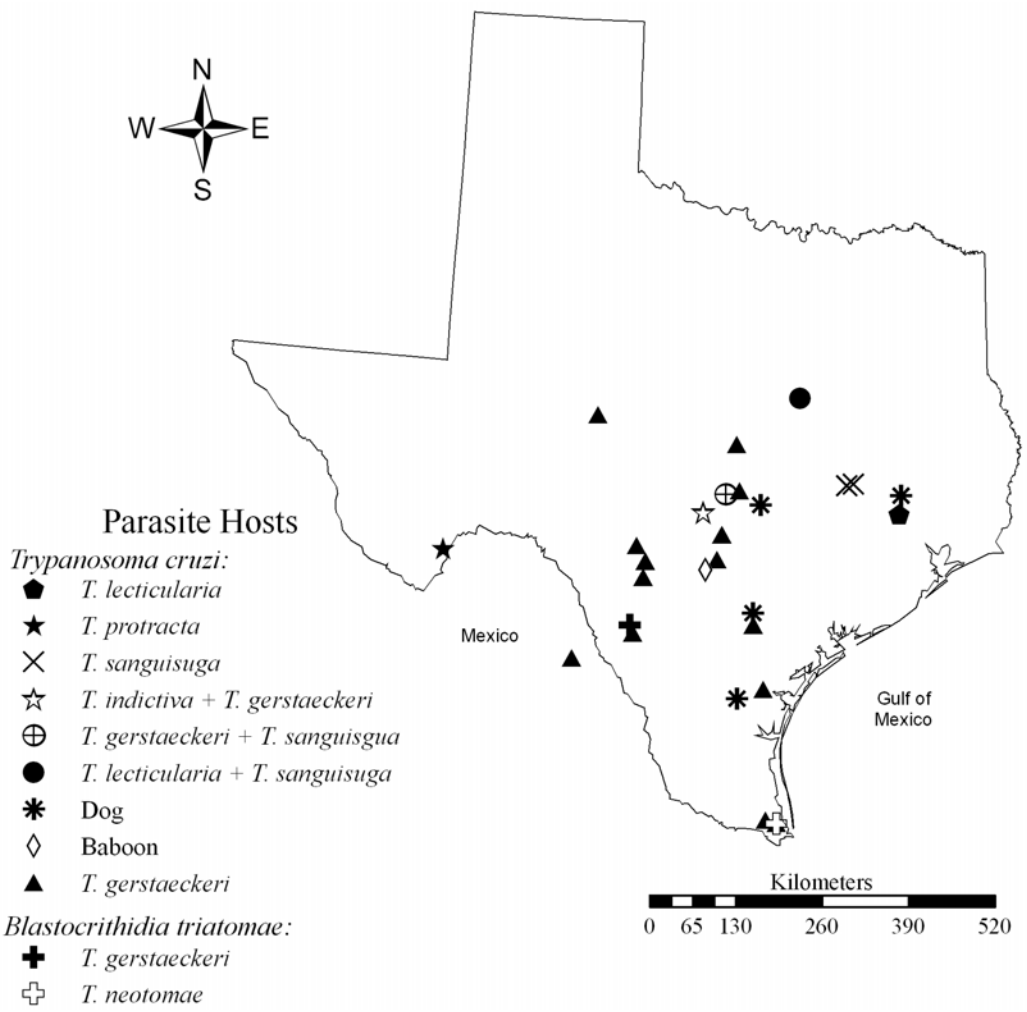

Figure 20. Distribution of sequenced SSU rRNA parasite isolates in a study of *T. cruzi* in Texas, 2005-2006.

Of the 178 hindgut specimens tested with the 18S primer set, 66 (37%) had a PCR product that displayed a prominent band at ~600 bp. Of these 66 specimens, 19 were positive for *T. cruzi* and one was positive for *B. triatomae*. For six of these

specimens, the band was excised from the gel, purified, and sequenced. Using the BLASTN algorithm[161] search to GenBank, the DNA sequences were 95-97% similar to several *Hepatozoon* spp., primarily *H. canis*, *H. felis*, *H. catesbianae*, and *H. americanum*. There are over 300 recognized *Hepatozoon* species (Apicomplexa: Adeleorina: Hepatozoidae) that are known to infect mammals and reptiles.[213] *Hepatozoon* species have been reported in dogs and wild carnivores in Texas.[214, 215] A wide variety of hematophagous invertebrates serve as definitive hosts for the parasite, including triatomine bugs.[216, 217] The species *Hepatozoon triatomae* has been reported from several species of *Triatoma* bugs, including *Triatoma rubida uhleri* collected from rodent nests in Arizona.[218] It could not be determined whether the *Hepatozoon*-like organisms were transient components of a blood meal or the result of infection in the bug.

Secondary structure of T. cruzi *SSU rRNA*. A diagram of the secondary structure of the 18S rRNA of *T. cruzi* (Fig. 21) was constructed using a previously-available GenBank sequence (accession number AF245382). The original diagram was obtained from the Comparative RNA Web Site[202] and modified to illustrate the nine variable regions of the 18S (shown in light blue) and further structure in variable regions V4 and V5 as predicted by comparative analysis and thermodynamic modeling in *mfold*. Helices within the region sequenced in this study are shaded gray, with the helix notation following the *E. coli* scheme.[202] Tertiary interactions (where there was strong comparative support) and base triples are shown connected by continuous lines. Base-pairing is indicated as follows: standard canonical pairs by lines (C-G, G-C, A-U, U-A);

wobble G•U pairs by dots (G•U); A•G pairs by open circles (A∘G); and, other non-canonical pairs by filled circles (e.g. C•A). Primers used in this study are marked on the structure diagram in red.

The predicted secondary structure of variable region V4 is shown in Figure 22. Helices are shaded gray, with helix numbering and secondary structure model following Wuyts et al. (2000)[204] and Alkemar & Nygård (2003, 2004)[205, 219]. Three regions of problematic alignment are shaded dark gray and numbered 1-3. Selected sequences from each of these regions are shown to illustrate the hypervariable regions of the alignment. Homology was not assigned between *Trypanosoma* spp. and *B. triatomae* sequences in regions 2 and 3 (separated by lines in Fig. 22). Regions of alignment ambiguity across *T. cruzi* and other *Trypanosoma* spp. are shaded dark gray in regions 2 and 3. Structural annotation for helix E23-15 follows the convention of Gillespie (2004).[201]

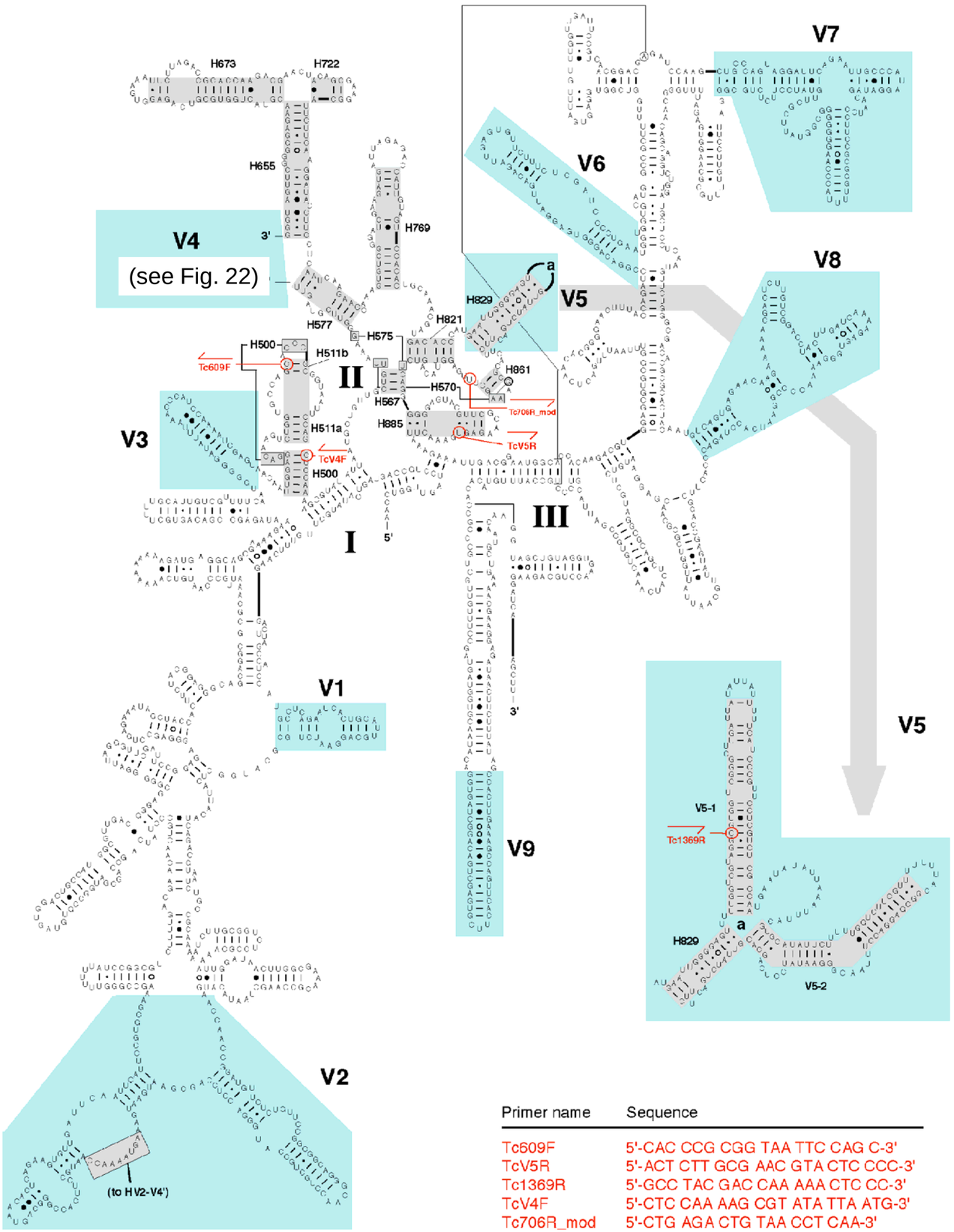

Figure 21. Secondary structure diagram of the SSU rRNA of *T. cruzi*. Variable regions are shown in light blue. Helices within the region sequenced in this study are shaded gray. Tertiary interactions and base triples are shown connected by continuous lines. Base-pairing is indicated as follows: standard canonical pairs by lines (C-G, G-C, A-U, U-A); wobble G·U pairs by dots (G·U); A·G pairs by open circles (AG); other non-canonical pairs by filled circles (e.g. CA).

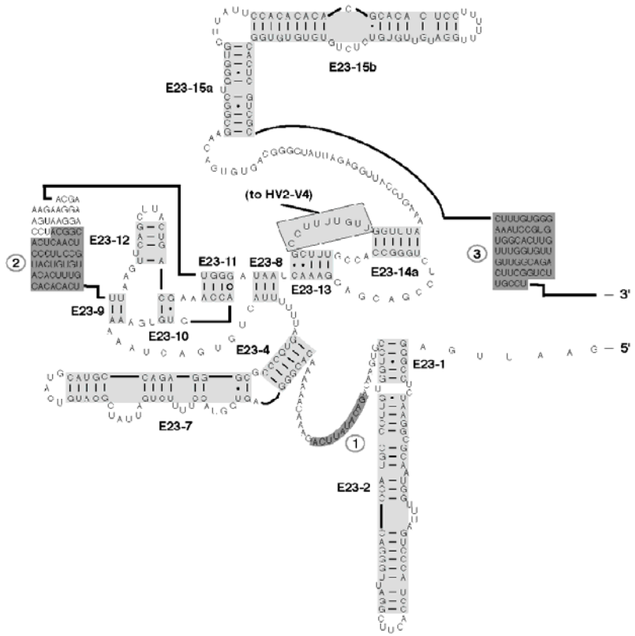

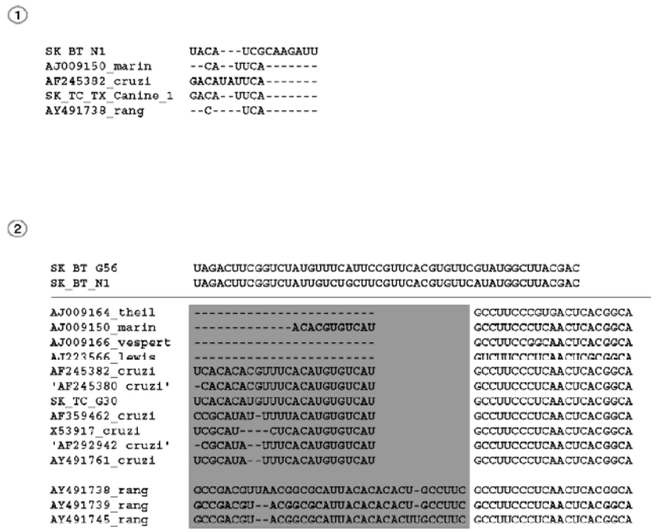

Figure 22. Predicted secondary structure of variable region V4 of the SSU rRNA from *T. cruzi*. Helices are shaded gray. Three regions of problematic alignment are shaded dark gray and numbered 1-3. Selected sequences from each of these regions are shown to illustrate the hypervariable regions of the alignment. Homology was not assigned between Trypanosoma spp. and Blastocrithidia sequences in 2 and 3 (separated by lines). Regions of alignment ambiguity across T. cruzi and other Trypanosoma spp. are shaded dark gray in 2 and 3.

Phylogenetic analysis. A total of 116 trypanosome nuclear SSU rRNA sequences were analyzed in the current study, including 71 new sequences and 45 sequences available in GenBank. The average length of the new sequences was 850 characters, ranging from 803 to 881. The average nucleotide composition was 23.6% A, 21.6% C, 25.6% T, and 29.2% G. A total of 1,294 characters (including gaps) were used for the phylogenetic analysis. Of 255 variable characters, 181 were parsimony-informative (14% of total characters). Further secondary structure predicted for the variable regions of the 18S encompassed by the primers in this study (V4, V5) revealed alignment challenges in three regions of the V4. The alignment within *T. cruzi* was evident but across *T. cruzi* and the other trypanosomes it was ambiguous. Characters from these three regions were excluded from the phylogenetic analysis. Determination of secondary structure was previously shown to be useful in nucleotide alignment of rRNA molecules, improving phylogeny estimation.[200, 220] The estimated phylogeny is provided in Figures 23-25.

The tree topology is derived from a distance analysis. The results from a separate parsimony analysis were bootstrapped and are shown superimposed over the distance tree. Nodes with an asterisk were not recovered in a constructed strict consensus of 10,000 equally-parsimonious trees. The strain, locality, host, and group are provided for *T. cruzi* sequences. The four main recovered lineages of *T. cruzi* are noted in blue and labeled I-IV. Red branches in lineage II formed a monophyletic group (bootstrap = 64) in the consensus parsimony tree. The parsimony analysis was repeated with the variable ends of the aligned sequences trimmed. The results did not change,

indicating that the phylogenetic signal is internal and not confounded by the sequencing process.

Due to the low level of branch resolution in the parsimony analysis, an additional distance analysis was performed. The major divisions between and within species was the same for both analyses. The two new *B. triatomae* sequences grouped together with one previously published *B. triatomae* sequence which was derived from a culture stock, seeded by an isolate from a *T. infestans* bug in Argentina.[221] The analysis was not able to completely resolve their positions. *B. triatomae* is a single host, flagellate parasite pathogenic for triatomine bugs. Both *T.cruzi* and *B. triatomae* have morphologically-similar epimastigote and trypomastigote forms that colonize the small intestine and rectum, but unlike *T. cruzi*, *B. triatomae* has the ability to develop a drought-resistant cyst form.[165] *B. triatomae* has been documented in several *Triatoma* spp. in South America[166, 167] and in *T. gerstaeckeri* collected in Texas.[18] Because mixed infections of *T. cruzi* and *B. triatomae* have been reported[168], both *B. triatomae*-positive specimens identified in this study were analyzed with the *T. cruzi*-specific Tc24T1/Tc24T2 primers and found to be negative.

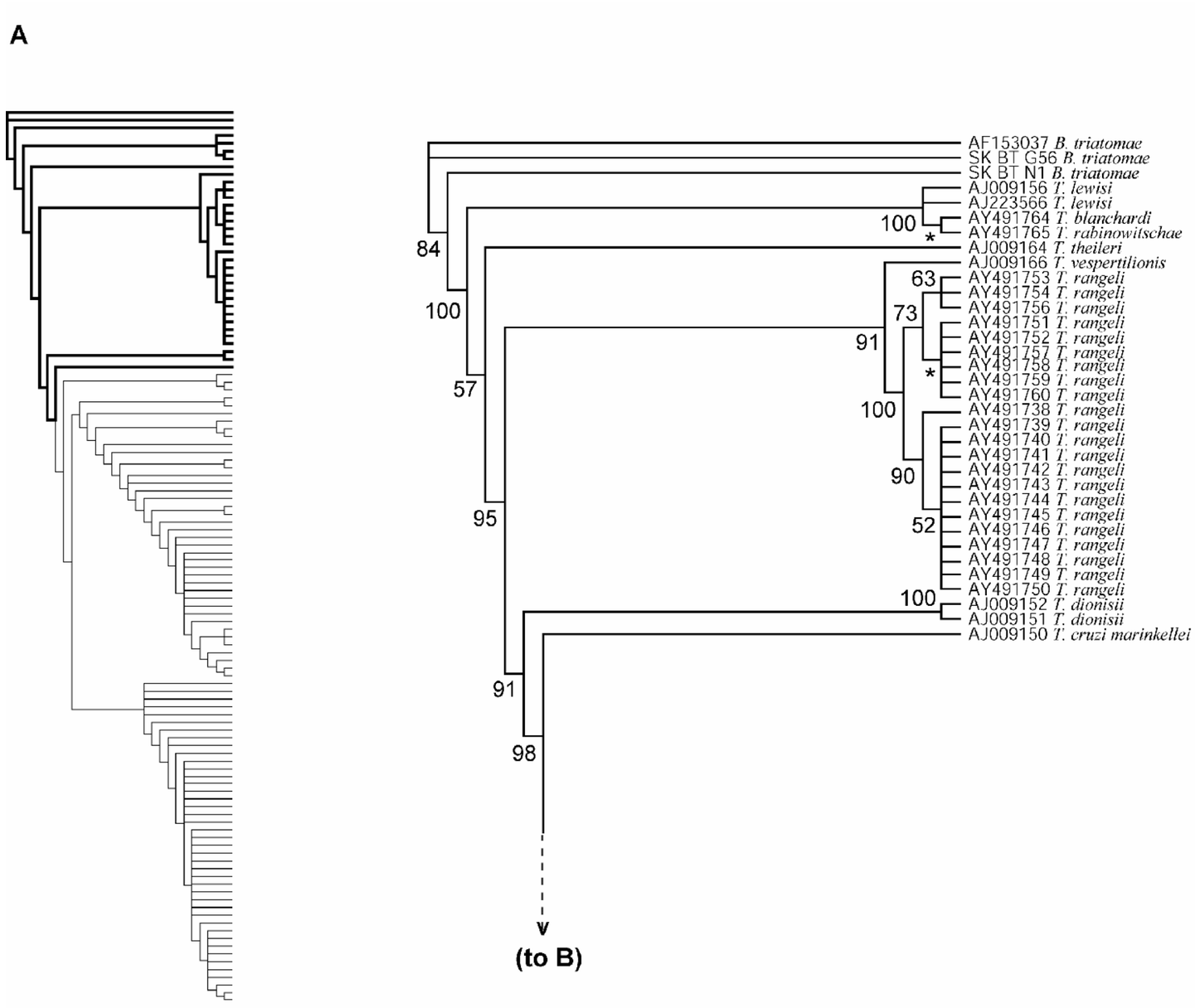

Figure 23. Estimated phylogeny for 116 SSU rRNA trypanosome sequences (Part A). The entire cladogram is presented to the left and the darkened section is shown in an enlarged format to the right. Tree topology is from a distance analysis. Results from a separate parsimony analysis were bootstrapped and are shown superimposed over the distance tree. Nodes with an asterick were not recovered in a constructed strict consensus of 10,000 equally parsimonious trees. New sequences begin with "SK". All others were available sequences in GenBank and are labeled with the accession number and species name.

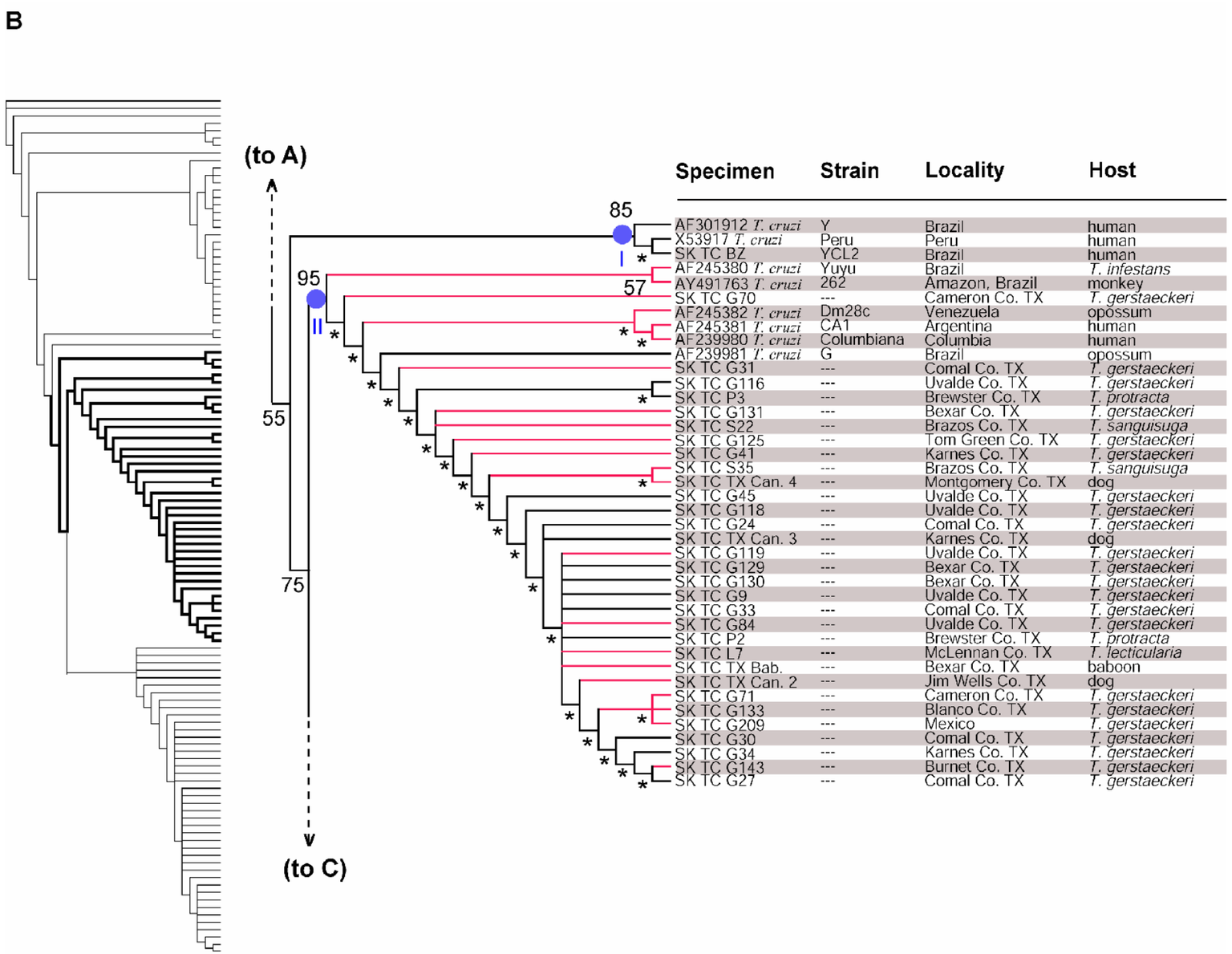

Figure 24. Estimated phylogeny for 116 SSU rRNA trypanosome sequences (Part B). The entire cladogram is presented to the left and the darkened section is shown in an enlarged format to the right. Tree topology is from a distance analysis. Results from a separate parsimony analysis were bootstrapped and are shown superimposed over the distance tree. Nodes with an asterick were not recovered in a constructed strict consensus of 10,000 equally parsimonious trees. New sequences begin with "SK". All others were available sequences in GenBank and are labeled with the accession number and species name. Strain, locality, host, and group are provided where applicable for the T. cruzi sequences. The four main recovered lineages of T. cruzi are noted in blue and labeled I-IV. Red branches in lineage II formed a monophyletic group (bootstrap=64) in the parsimony tree.

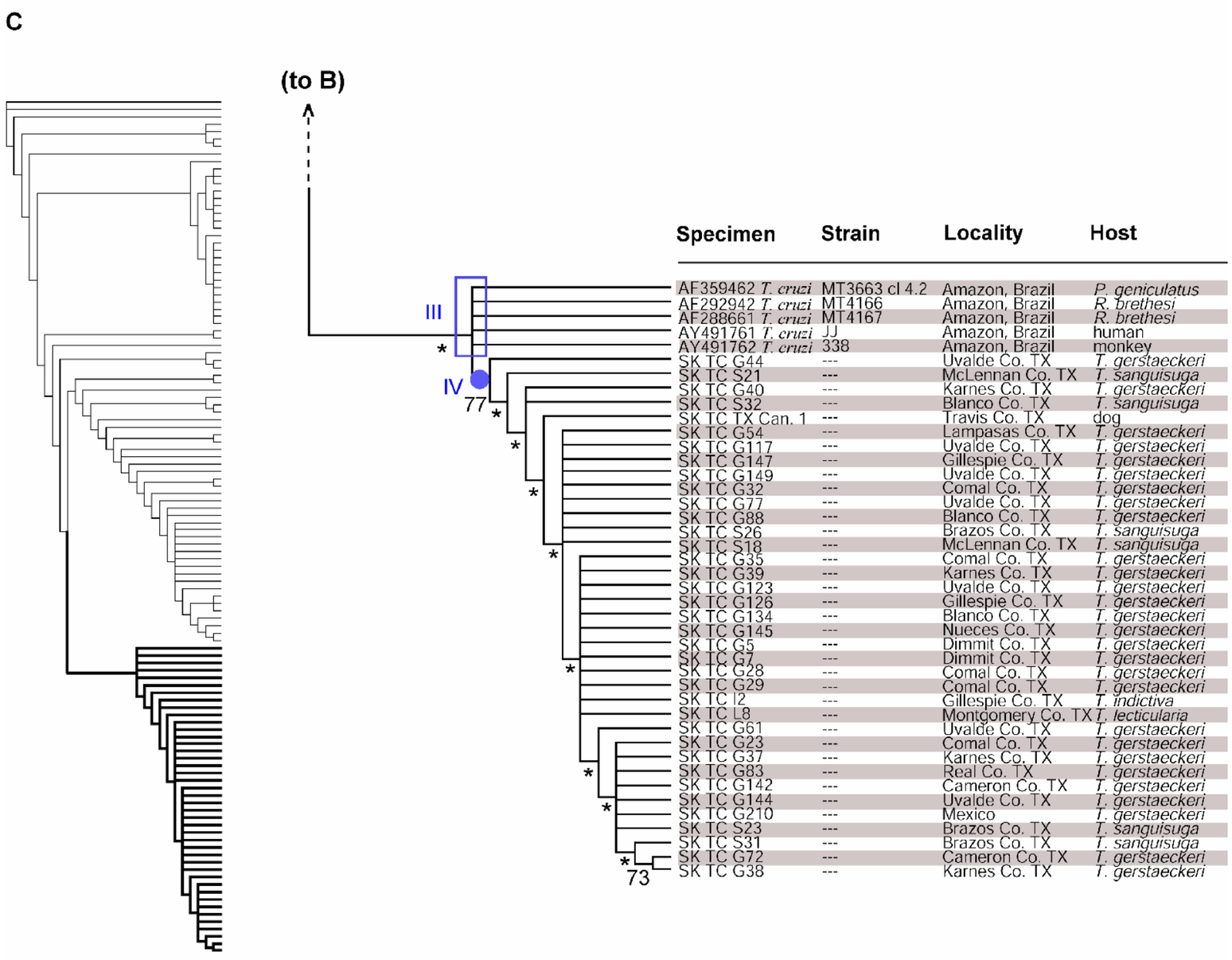

Figure 25. Estimated phylogeny for 116 SSU rRNA trypanosome sequences (Part C). The entire cladogram is presented to the left and the darkened section is shown in an enlarged format to the right. Tree topology is from a distance analysis. Results from a separate parsimony analysis were bootstrapped and are shown superimposed over the distance tree. Nodes with an asterick were not recovered in a constructed strict consensus of 10,000 equally parsimonious trees. New sequences begin with "SK". All others were available sequences in GenBank and are labeled with the accession number and species name. Strain, locality, host, and group are provided where applicable for the T. cruzi sequences. The four main recovered lineages of T. cruzi are noted in blue and labeled I-IV.

The *T. cruzi* sequences segregated from all other trypanosome species with good bootstrap support, rooted by the bat trypanosome *T. cruzi marinkellei*. Two primary *T. cruzi* clades were evident which is consistent with the results of most studies in the past decade.[142] Both the distance and parsimony trees supported further division of the second clade into two clades, with one branching into two primary divisions. Clade I consists of three sequences, two of which (Y and Peru) have been classified as *T. cruzi* II strains in previous studies using other molecular markers (Table 16). The Peru strain grouped with other Z1/*T. cruzi* I strains using the spliced leader promoter gene, but as Z2/*T. cruzi* II using zymodeme typing by the same authors.[152] The third member, the YCL2 strain sequenced in this study, is a clone of the Y strain and displayed no nucleotide differences from the original Y strain sequence. Clade II includes previously published sequences typed as equivalent Z1/*T. cruzi* I strains using other markers and 30 sequences derived from isolates from Texas (1 baboon, 3 dog, and 26 triatomine). Clade III consists of five previously published sequences derived from isolates exclusively from the Amazon region of Brazil. Four of these strains have been typed as Z3/*T cruzi* IIa,c based on zymodeme analysis. Finally, clade IV includes the remaining 37 specimens from Texas (1 dog, 36 triatomine).

Table 16

T. cruzi sequences used in a study of Texas isolates 2005-2006, categorized by typing results from other markers

Sequence[1]	Strain	18S rRNA[2] (partial)	18S rRNA[3] (whole)	D7-24Sa rRNA	rRNA promoter[6]	SL RNA promoter[6]	ME[4]	Zymodeme
AF301912	Y	1	1	1[4], 1[5]	1	1	1	Z2[6]
X53917	Peru	1	1	---	---	2	---	Z2[6]
SK TC BZ	YCL2	1	---	---	---	---	---	---
AF245380	Yuyu	2	2	2[4]	---	---	2	---
AY491763	262	2	---	---	---	---	---	---
SK TC G70	---	2	---	---	---	---	---	---
AF245382	Dm28c	2	2	2[4]	2	2	2	---
AF245381	CA1	2	2	---	---	---	---	---
AF239980	Columbiana	2	2	---	2	2	---	Z1[6]
AF239981	G	2	2	2[4], 2[5]	---	---	2	---
SK TC G31	---	2	---	---	---	---	---	---
SK TC G116	---	2	---	---	---	---	---	---
SK TC P3	---	2	---	---	---	---	---	---
SK TC G131	---	2	---	---	---	---	---	---
SK TC S22	---	2	---	---	---	---	---	---
SK TC G125	---	2	---	---	---	---	---	---
SK TC G41	---	2	---	---	---	---	---	---
SK TC S35	---	2	---	---	---	---	---	---
SC TC TX Canine 4	---	2	---	---	---	---	---	---
SK TC G45	---	2	---	---	---	---	---	---
SG TC G118	---	2	---	---	---	---	---	---
SK TC G24	---	2	---	---	---	---	---	---
SK TC TX Canine 3	---	2	---	---	---	---	---	---
SK TC G119	---	2	---	---	---	---	---	---
SK TC G129	---	2	---	---	---	---	---	---
SK TC G130	---	2	---	---	---	---	---	---
SK TC G9	---	2	---	---	---	---	---	---
SK TC G33	---	2	---	---	---	---	---	---
SK TC G84	---	2	---	---	---	---	---	---
SK TC P2	---	2	---	---	---	---	---	---
SK TC L7	---	2	---	---	---	---	---	---
SK TC TX Baboon	---	2	---	---	---	---	---	---
SK TC TX Canine 2	---	2	---	---	---	---	---	---
SK TC G71	---	2	---	---	---	---	---	---

Table 16 Continued

Sequence[1]	Strain	18S rRNA[2] (partial)	18S rRNA[3] (whole)	D7-24Sa rRNA	rRNA promoter[5]	SL RNA promoter[5]	ME[4]	Zymodeme
SK TC G133	---	2	---	---	---	---	---	---
SK TC G209	---	2	---	---	---	---	---	---
SK TC G30	---	2	---	---	---	---	---	---
SK TC G34	---	2	---	---	---	---	---	---
SK TC G143	---	2	---	---	---	---	---	---
SK TC G27	---	2	---	---	---	---	---	---
AF359462	MT3663 cl 4.2	3	3	3[5]	---	---	---	Z3[5]
AF292942	MT4166	3	3	3[5]	---	---	---	Z3[5]
AF288661	MT4167	3	3	3[5]	---	---	---	Z3[5]
AY491761	JJ	3	---	---	---	---	---	Z3[5]
AY491762	338	3	---	---	---	---	---	---
SK TC G44	---	4	---	---	---	---	---	---
SK TC S21	---	4	---	---	---	---	---	---
SK TC G40	---	4	---	---	---	---	---	---
SK TC S32	---	4	---	---	---	---	---	---
SK TC TX Canine 1	---	4	---	---	---	---	---	---
SK TC G54	---	4	---	---	---	---	---	---
SK TC G117	---	4	---	---	---	---	---	---
SK TC G147	---	4	---	---	---	---	---	---
SK TC G149	---	4	---	---	---	---	---	---
SK TC G32	---	4	---	---	---	---	---	---
SK TC G77	---	4	---	---	---	---	---	---
SK TC G88	---	4	---	---	---	---	---	---
SK TC S26	---	4	---	---	---	---	---	---
SK TC S18	---	4	---	---	---	---	---	---
SK TC G35	---	4	---	---	---	---	---	---
SK TC G39	---	4	---	---	---	---	---	---
SK TC G123	---	4	---	---	---	---	---	---
SK TC G126	---	4	---	---	---	---	---	---
SK TC G134	---	4	---	---	---	---	---	---
SK TC G145	---	4	---	---	---	---	---	---
SK TC G5	---	4	---	---	---	---	---	---
SK TC G7	---	4	---	---	---	---	---	---
SK TC G28	---	4	---	---	---	---	---	---
SK TC G29	---	4	---	---	---	---	---	---

Table 16 Continued

Sequence[1]	Strain	18S rRNA[2] (partial)	18S rRNA[3] (whole)	D7-24Sa rRNA	rRNA promoter[5]	SL RNA promoter[5]	ME[4]	Zymodeme
SK TC I2	---	4	---	---	---	---	---	---
SK TC L8	---	4	---	---	---	---	---	---
SK TC G61	---	4	---	---	---	---	---	---
SK TC G23	---	4	---	---	---	---	---	---
SK TC G37	---	4	---	---	---	---	---	---
SK TC G83	---	4	---	---	---	---	---	---
SK TC G142	---	4	---	---	---	---	---	---
SK TC G144	---	4	---	---	---	---	---	---
SK TC G210	---	4	---	---	---	---	---	---
SK TC S23	---	4	---	---	---	---	---	---
SK TC S31	---	4	---	---	---	---	---	---
SK TC G72	---	4	---	---	---	---	---	---
SK TC G38	---	4	---	---	---	---	---	---

ME = mini-exon; SL = sliced leader

[1]entries beginning with "SK" were sequenced in this study, all others were downloaded from GenBank

[2]determined in this study

[3]determined by Kawashita et al. 2001[149]

[4]determined by Souto et al. 1996[150]

[5]determined by Fernandes et al. 2001[220]

[6]determined by Nunes et al. 1997[151]

Discussion

This represents the largest phylogenetic study of U.S. *T. cruzi* isolates to date. All U.S. sequences partitioned into two groups, one (clade II) which included other sequences previously typed as Z1/*T. cruzi* I, and a second (clade IV) which included only U.S. sequences but was positioned closest to a group populated by sequences previously typed as Z3 /*T. cruzi* IIa,c. Clade IV may represent a subgroup of Z3 type strains. A dichotomy among Z3 strains has been previously recognized[222] and led to their classification as separate groups (*T. cruzi* IIa and *T. cruzi* IIc) using RAPD and multi-locus enzyme electrophoresis typing.[143] Mendonca et al. (2002) have previously characterized the strains of clade III in this study as Z3-A (MT3663) and Z3-B (MT4166, MT4167, JJ), but they did not determine whether or not these two groups correspond to the *T. cruzi* IIa and IIc classification.[223] This study was not able to detect a difference in these four strains based on the corresponding GenBank sequences analyzed. Comparison of the specimens in clade IV with currently known representatives of *T. cruzi* IIa and IIc would reveal whether or not these U.S. isolates represent a new subdivision of Z3/*T. cruzi* IIa,c strains. In general the results from the current study agree with the findings of previous studies on U.S. specimens where only Z1 and Z3 isolates have been found. [21, 22, 153, 154, 155, 156] Partitioning of the U.S. isolates did not occur according to host, geographic location, or collection site, e.g., inside or in close proximity to houses, dog kennels, or sylvatic settings (data not shown). In clade II, U.S. isolates were collected from four species of triatomine bugs (*T. gerstaeckeri, T. lecticularia*, *T. protracta*, and *T. sanguisuga*), three dogs, and a baboon. Hosts of clade

IV isolates also included four species of triatomine bugs three of which are the same as in clade II (*T. gerstaecker*i, *T. indictiva*, *T. lecticularia*, and *T. sanguisuga*) and 1 dog. In some cases, triatomine bug hosts of the same species and collected in the same location were separated into different clades. Sympatric distribution of Z1 and Z3 type *T. cruzi* strains has been reported previously in Texas and Georgia, and both types have been isolated from *T. sanguisuga* (Z1 from a specimen in Florida and Z3 from a specimen in Georgia).[21, 153, 224] If clades II and IV from this study are considered roughly equivalent to Z1 and Z3 based on membership of previously typed strains, this is the first U.S. study to find both types in the same host species within the same geographic location.

Similar to isolates derived from triatomine hosts, the separation of dog isolates from Texas into two different clades does not appear to be based on geographic location. The isolates from canines in clade II were derived from blood (canines 2 and 3) and cardiac tissue (canine 4). The isolate from the only canine in clade IV (canine 1) was derived from lymph node aspirate. Canine 4 suffered acute myocarditis and died suddenly at ~8 weeks of age, and the clinical presentation of canines 2 and 3 is unknown. Although fatal, infection in canine 1 was atypical showing no cardiac involvement. This could be a reflection of variation in host immune response or the presence of multiple strains of *T. cruzi* in Texas with varying tissue predilections.[141, 225, 226, 227] Both Z1 and Z3 type strains have been reported in dogs from the U.S.[153]

The results of this phylogenetic analysis are considered preliminary. It is not known what impact the addition of the 26 *T. cruzi*-positive specimens that were not

successfully sequenced would have on the tree topology. These specimens had PCR products that displayed double banding patterns that could not be resolved through gel slicing or amplification with nested primers. All 26 were isolated from *T. gerstaeckeri* triatomine bugs. It is possible that the double bands represent amplification products of multiple clonal strains or gene copies present in the sample with different 18S rRNA gene lengths. Length heterogeneity across closely related taxa is characteristic for 18S rRNA genes due to the occurrence of insertion and deletion events in structurally less conserved regions.[201] These specimens will be cloned, sequenced, and included in a subsequent phylogenetic analysis.

Another issue to be resolved is whether or not heterogeneity exhibited by the 18S rRNA gene fragment used in this study can be explained by the presence of multiple clonal strains or paralogous gene copies in the isolates. Sequences were derived from the product of a single PCR reaction which would not allow for the detection of other clonal strains or gene copies that may be present. Mulitple clonal strains with divergent genetic and biological properties have been documented simultaneously existing in individual vertebrate and invertebrate hosts. [228, 229, 230]

Another possible source of confounding data in the current study is the presence of paralogous or heterologous rRNA gene copies. Two hundred and fifteen copies of the SSU rRNA have been documented in the nucleus of *T. cruzi*.[231] The ribosomal RNA genes belong to a multigene family that is considered to be driven by concerted evolution through unequal crossing over, gene conversion, or other recombination events.[232] However, this assumption applied to *T. cruzi* is somewhat controversial due to

the detection of divergent paralogous 18S gene copies in other protozoa.[233, 234] It has also been suggested that the exclusion of hypervariable regions within the 18S in *T. cruzi* from phylogenetic analyses may circumvent issues with paralogous copies should they exist.[235] In the current study, areas of ambiguous alignment in the variable regions detected through analysis of secondary structure were excluded.

It has also been suggested that heterogeneity across the 18S may be due to genetic transfer through hybridization events.[236] Although *T. cruzi* has been shown to have a predominantly clonal population structure through linkage disequilibrium analysis, the occurrence of occasional horizontal genetic exchange is still compatible with this theory and could explain inconsistencies with gene sequence phylogenies.[227, 237] Results from recent studies support the occurrence of specific hybridization events within *T. cruzi* based on RFLP analysis of multiple loci and in vitro experiments.[233, 238, 239]

For specimens analyzed in the current study, sequencing and comparison of a set of cloned products from each isolate may offer a solution provided a sufficient number of clones are evaluated.[240] As an alternative, PCR amplification using primer sets specific to each *T. cruzi* clade should corroborate intra-isolate homogeneity. Each isolate would be tested against each primer set representing the four clades and amplification to more than one would suggest the presence of either divergent clonal strains or paralogous gene copies. This assay has been successfully applied in a similar study using the rRNA promoter sequence as the marker.[152]

Overall the results of this study provide support for the previous categorization of U.S. *T. cruzi* isolates into two lineages resembling the Z1/*T. cruzi* I and Z3/*T. cruzi* IIa,c classifications. Additional analysis of isolates from a diversity of hosts from other states is needed to fully characterize the heterogeneity and understand the evolution of *T. cruzi* in North America.

CHAPTER VI

DISTRIBUTION AND CHARACTERIZATION OF CANINE CHAGAS DISEASE IN TEXAS

Introduction

It is well recognized that *Trypanosoma cruzi* is endemic in the United States, as evidenced by infections reported in humans, domestic dogs, and a wide range of mammalian wild life species. In the southern United States, *T. cruzi* infections in wild populations of opossums, wood rats, raccoons, armadillos, and coyotes have been reported for the past 70 years.[15, 18, 22, 23, 29, 30, 31, 32, 33, 34, 35, 36] Although the disease has been reported in domestic dogs from at least seven states, the extent of the disease in this species across the country is not known. Acute and chronic infections in canines have been reported in Texas, Oklahoma, Louisiana, Virginia, South Carolina, Georgia, and Tennessee.[24, 37, 38, 39, 40, 41, 42, 43] Seroprevalence studies in domestic dogs have been published from Texas (2.6-8.8%), Oklahoma (3.6%), Louisiana (2.3-4.7%), and Georgia, in combination with other southeastern states (2%).[18, 40, 43, 44, 45]

Domestic canines in South and Central America are considered an important reservoir in the domestic transmission cycle,[46, 47] and serve as surveillance sentinels for human infection.[48] It has been shown that dogs have a higher capacity to infect triatomine bugs than humans due to persistent parasitemia, further supporting their role in the disease cycle in domestic settings.[49, 50] Although the importance of dogs as Chagas disease reservoirs in the U.S. has not been extensively studied, there is some

evidence to support their involvement in domestic transmission in this country as well. Seropositive dogs were found in close proximity to two locally-acquired human cases in the U.S.[24, 28] In the current study, multiple sources including serologic data, clinical case records, and histopathologic case records were compiled in an effort to document the magnitude of the disease among domestic dogs in Texas.

Materials and Methods

Cases of canine Chagas disease in Texas were ascertained from serology records at the Texas Veterinary Medical Diagnostic Laboratory (TVMDL) for the time period January 1, 1994 through April 1, 2006, and from necropsy records at TVMDL for the time period January 1, 1999 through October 1, 2006. Cases were also ascertained from necropsy records at the Veterinary Medical Teaching Hospital at Texas A&M University (TAMU) for the time period January 1, 2001 through October 1, 2006. Serologically positive cases were defined as dogs with serum IgG titers of ≥ 1:160 using an immunofluorescence assay (IFA), according to TVMDL protocol. *T. cruzi* antigen was whole, fixed epimastigotes maintained in serial cultures originally derived from infected dogs from Texas. Necropsy cases were defined as dogs with histopathology consistent with infection by *T. cruzi*, as determined by the pathologist.

Breed and county level location data were abstracted from both serology and necropsy records when available. Signalment, clinical presentation, clinical diagnosis, and histopathologic diagnosis were abstracted from necropsy records. Location data for

canine cases and triatomine vector records (unpublished, S. Kjos) were mapped using ArcGIS 9.1 (ESRI, Redlands, CA).

Results

A total of 553 serologically- or histopathologically-confirmed canine cases from Texas were diagnosed during the study period by TVMDL or TAMU. For the 13-year time period, 1994-2006, 463 serologically-confirmed cases were processed; and for the eight year time period, 1999-2006, 90 histopathologically-confirmed cases were processed. Little overlap between serologic and histopathologic case counts was detected. Only two histopathologically-confirmed cases reported concurrent serologic testing. Prior diagnostic testing for Chagas disease was not noted in any of the necropsy reports. It is possible that there were multiple serology reports for a single dog, because new case numbers are assigned at subsequent submissions. Canine cases were reported from 46 counties within Texas, covering most geographic regions except the far west. Both histopathologically-confirmed and serologically-confirmed cases were reported from 25 counties. The distribution of canine cases closely matches the known distribution of triatomine bug vectors in Texas. Figure 26 is a map of the distribution of canine Chagas disease cases in Texas by county with the distribution of reported triatomine bug vectors overlaid.

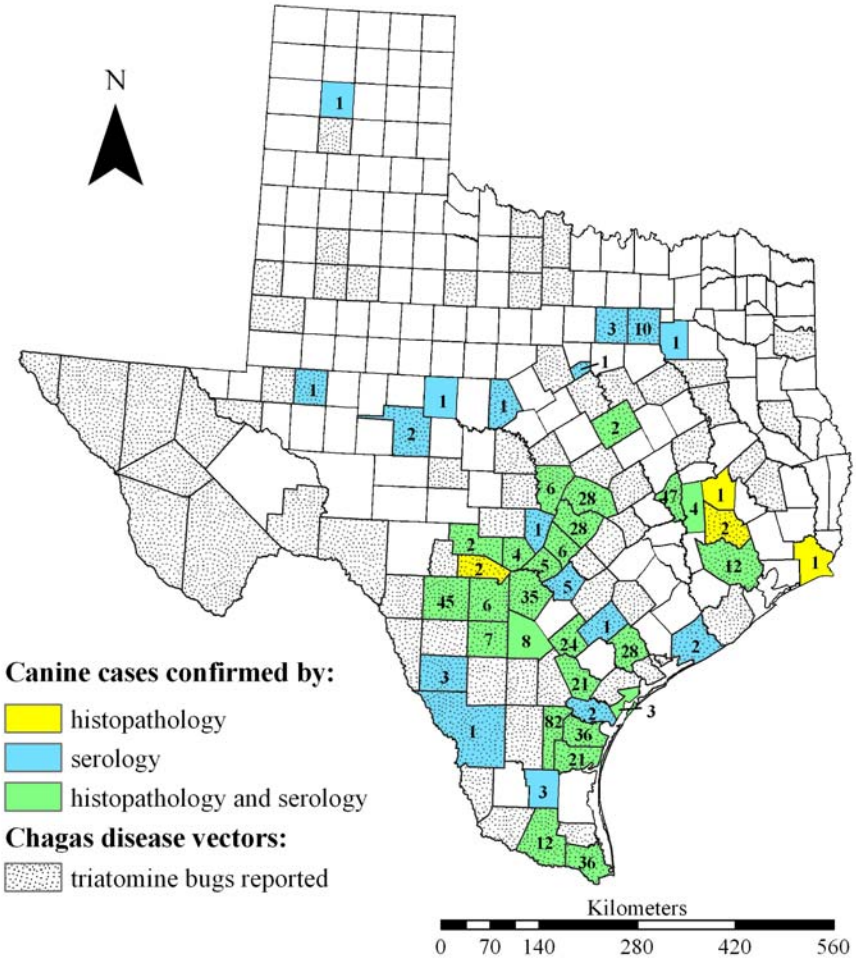

Figure 26. Distribution of canine Chagas disease cases in Texas by county as confirmed by serology (1994-2006, 463 cases) or histopathology (1999-2006, 90 cases), and distribution of triatomine bugs in Texas by county (1928-2006). The numbers within county boundaries indicate the case count.

There was information on breed for 113 cases (46/463 serologic; 67/90 histopathologic). Thirty-three different breeds were represented, including 24

sporting/working, 5 Terrier, 2 nonsporting, and 1 toy. A list of breeds and case counts is provided in Table 17.

Table 17

T. cruzi -infected dog breeds diagnosed by serology[1] or histopathology[2] in Texas, in order of frequency (# of cases)

Labrador Retriever (25)	English Springer Spaniel (2)	English Setter (1)
English Pointer (19)	Golden Retriever (2)	Fila Brasileiro (1)
Crossbreed (10)	Great Pyrenees (2)	Flat-Coated Retriever (1)
Boxer (6)	Rottweiler (2)	Great Dane (1)
Mastiff (6)	Weimaraner (2)	Jack Russell Terrier (1)
Walker Hound (4)	Yorkshire Terrier (2)	Papillon (1)
Belgian Malinois (3)	Australian Heeler (1)	Pit Bull Terrier (1)
Blue Heeler (3)	Bulldog (1)	Poodle (1)
Boston Terrier (3)	Catahoula Leopard Dog (1)	Rat Terrier (1)
German Shepherd (3)	Dachshund (1)	Rhodesian Ridgeback (1)
German Shorthair Pointer (3)	Doberman Pinscher (1)	Siberian Husky (1)

[1]46 of 463 (1994-2006) serologically-confirmed cases included information on breed

[2]67 of 90 (1999-2006) histopathologically-confirmed cases included information on breed

Data on signalment, clinical presentation, clinical diagnosis, and histopathologic diagnosis were available for 90 histopathologically-confirmed cases. The age of cases ranged from six weeks to 10 years, with 64% of the cases less than one year of age. Approximately 57% of cases were male. The sex ratio did not vary significantly by age group. Acute death was the predominant clinical presentation in approximately 43% of cases overall and suffered by 67% of the cases one year of age or older. In cases that did

not experience acute death, lethargy, ascites, anorexia, and dyspnea were the most common clinical signs. Other clinical signs reported in multiple cases included distended abdomen, pale or cyanotic gums, vomiting, hepatomegaly, ataxia, diarrhea, and tachycardia. Clinical signs reported in only a single case included conjunctival edema, corneal edema, lymphadenopathy, anemia, weight loss, irregular heart sounds, and epistaxis. In non-acute death cases, duration of apparent illness ranged from one day to six weeks. There were 58 different referring veterinarians for the histopathologically-confirmed cases. Half of the veterinarians assigned a clinical diagnosis (non-acute death cases) involving a cardiovascular etiology, including 20 diagnoses of suspect Chagas disease. Additional clinical diagnoses included other infectious causes (e.g., *Ehrlichia*, heartworm, *Leishmania*, *Hepatozoon*), ingestion of toxin, gastroenteritis, and heat stroke.

At necropsy, myocarditis was identified in 84 of the 90 histopathologically-confirmed cases. Almost all cases had necrosis or congestion of the liver and lungs, indicative of cardiovascular deterioration. *T. cruzi* organisms were observed in the tissues of 71 cases (90% of cases < 1 year of age; 70% of cases ≥ 1 year of age). Although the parasite was found primarily in the heart, it was occasionally isolated from other tissues including brain, lymph node, cerebrospinal fluid, liver, stomach, small intestine, esophagus, adrenal gland, and blood (Fig. 27). Co-infection was noted in a small number of cases, involving hookworm (3), tapeworm (2), heartworm (1), fleas (1), as well as exposure to West Nile Virus based on serology (1). Characteristics of the histopathologically-confirmed cases are provided in Table 18.

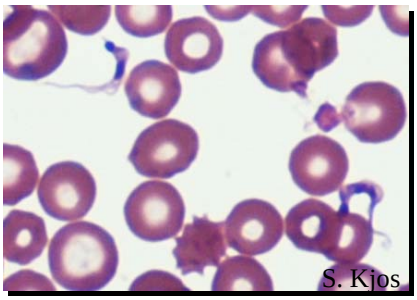

Figure 27. *T. cruzi* trypomastigotes in blood of ~6 week old crossbreed puppy from Montgomery County, Texas.

Table 18

Characteristics of *T. cruzi* histopathologically-confirmed canine cases in Texas, 1999-2006

	Total	< 1 year	≥1 year
Cases	90*	58	27
Age range	6 wks-10 yrs	6 wks-11 mo	1-10 yrs
Sex (M/F)	48/37	32/25	16/12
Acute deaths	39 (43.3%)	21 (36.2%)	18 (66.7%)
Clinical presentation:			
Lethargy	25	18	7
Ascites	16	14	2
Anorexia	16	12	4
Dyspnea	11	10	1
Distended abdomen	6	4	2
Pale gums	6	5	1
Vomiting	6	4	2
Hepatomegaly	5	4	1
Ataxia	4	2	2
Cyanotic gums	4	4	0
Diarrhea	4	3	2
Tachycardia	4	4	0
Necropsy:			
myocarditis	84	57	27
T. cruzi parasites detected	71	52	19

*Age and sex were not specified for 5 cases

Discussion

This represents the first comprehensive study of canine Chagas disease in Texas with regards to geographic distribution, signalment, and clinical and histopathologic presentation. The 553 combined serologically- or histopathologically-confirmed cases were primarily ascertained from medical records at TVMDL. Serologically-confirmed canine cases abstracted from TVMDL data have been reported previously, including ~73 cases diagnosed between 1987 and 1996[38] and 67 cases diagnosed between 1994 and 1998[45]. Issues of IFA cross reactivity to other organisms such as *Leishmania* in canines have been reported in the U.S.[241, 242] The extensive overlap in geographic distribution of histopathologically-confirmed cases with serologically-confirmed cases in this study supports serologic evidence of widespread *T. cruzi* infection among canines in Texas.

As is true with most infectious diseases, it is probable that many cases during the 13-year study period were not evaluated at a veterinary clinic. Additionally, it is possible that veterinarians diagnosing canine cases did not submit serum or tissues for analysis at diagnostic laboratories. However, it is unlikely that a significant number of cases were missed due to testing at other facilities. The TVMDL, created in 1967 by the Texas legislature, is the only full service veterinary medical diagnostic laboratory in the state. Last year alone, TVMDL provided diagnostic services for nearly 190,000 animal cases.[243] Canine Chagas disease is not a reportable condition in Texas, so additional case counts were not available through the state health authorities. The resulting case count of this study underestimates the rate of infection in dogs in Texas.

The predominant clinical presentation for histopathologically-confirmed cases was acute death, particularly for dogs one year of age or older. Myocarditis and intralesional parasites in heart tissue were observed at necropsy in the vast majority of cases. In two cases, parasites were isolated from lymph nodes and no cardiac involvement was detected. This could be a reflection of variation in host immune response or the presence of multiple strains of *T. cruzi* in Texas with varying tissue predilection.[141, 226, 227] A detailed description of one these cases has been recently published.[242]

Chagas disease was diagnosed in a wide variety of dog breeds, most were sporting/working breeds. The case numbers by breed may not be an accurate representation of the distribution, because breed information was available for only 20% of the cases. The large number of Labrador Retriever cases may be due to the popularity of the breed[244] rather than a behavioral or genetic risk for infection.

The geographic distribution of canine cases in Texas is wide spread and closely matches the distribution of the insect vector species of *Triatoma* reported from the state. In addition to the distribution determined in the present study, *T. cruzi*-infected canines have been reported from Brewster and Navarro counties, located in the far west and north east regions of Texas, respectively.[13, 37] There were seven counties from which canine cases were reported but vectors were not. This is likely due to under-reporting of the vectors rather than true absence, because all of these counties had at least one adjacent neighbor reporting presence of vectors. The closely-aligned distribution of canine cases and vector species suggests that most cases were locally-acquired, probably

due to exposure to infected vectors. *T. cruzi* prevalence rates in *Triatoma* species from Texas have been reported at 17 to 48%.[13, 14, 16, 18] Transmission typically occurs when mucous membranes or the bite wound become contaminated with infectious fecal material deposited on the host by the feeding vector. In an experimental study, it was shown that two of the most commonly-encountered vector species in Texas, *Triatoma sanguisuga* (Leconte) and *Triatoma gerstaeckeri* (Stål) (Fig. 28), defecate less frequently on their hosts while feeding than other South American species.[14] It is possible that many canine infections in Texas may be caused by ingestion of infected vectors or tissue of wild mammals rather than by the classical transmission route.[44, 245, 246] Other potential routes of transmission in canines include vertical transmission from mother to pup via intrauterine or transmammary routes and blood transfusion.[247]

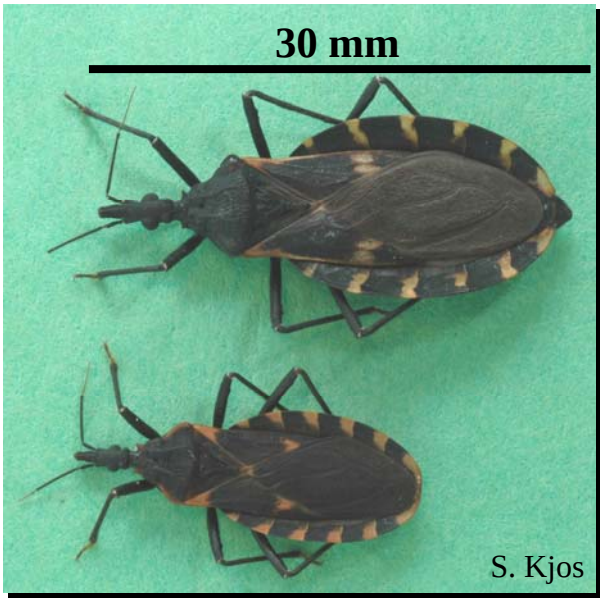

Figure 28. The two most commonly encountered *Triatoma* spp. in Texas. Top: *T. gerstaeckeri* (Stål), female. Bottom: *T. sanguisuga* (Leconte), male.

In a recent field study of triatomine bug vectors in Texas, 158 of 233 bugs were found on the external surfaces of houses or inside dog kennels (unpublished, S. Kjos). Of the bugs found exclusively in the dog kennels, *T. cruzi* was identified by PCR in the hindgut of 55.3%. At a residential field site in central Texas, the family had observed for the past few years triatomine bugs feeding on one of their dogs, which slept inside at night. After the dog died, the bugs began to feed on family members while sleeping. Two members reported itchy welts on multiple occasions after waking in the morning, and adult triatomine bugs were found in the bedrooms. *T. cruzi* was identified by PCR in 11 of 13 bugs collected from the home. Only adult bugs were collected; 12 *T. gerstaeckeri* and 1 *Triatoma indictiva* Neiva. No diagnostic tests were performed on the dog that died before or after its death. Because of the dog's advanced age, the family assumed it had died of natural causes. The family members and their remaining dog, a hunting breed that resided outside, were subsequently tested for Chagas disease. Only the dog tested positive for exposure to *T. cruzi* (personal communication, K. Vonalt, Texas Department of State Health Services, July 8, 2005). The residence was new construction (five years old) built on previously-undeveloped land in mesquite and oak woodlands.

In parts of South America, domestic dogs are the preferred blood hosts for the primary human vector species, *Triatoma infestans* (Klug).[248] Similarly, the incidence described above suggests that some U.S. species may also prefer dogs, but will readily switch hosts when dogs are not available. Due to a sustained level of parasitemia, dogs have been found to be more infective to triatomine vectors than humans[249] As a result,

the presence of infected dogs in households has been shown to increase both vector populations and prevalence of infection among vectors.[50, 250]

The results of this study provide further support for the existence of an active Chagas disease transmission cycle in Texas. U.S. strains can be pathogenic, as evidenced by the significant numbers of canine deaths documented in this study, as well as previous reports of morbidity and mortality in dogs, humans and primates[37, 38, 52, 62, 63, 64] Although domestic infestations of triatomine bugs in the U.S. is rarely reported, scenarios like the one described above may increase as Americans continue to expand into previously-undeveloped areas. Human encroachment on the enzootic life cycle of *T. cruzi* in the U.S. should be a concern, as exemplified by the relatively recent emergence of Lyme disease in the northeast and upper Midwest due to human-driven changes, including reforestation and construction of residences in and near vector habitats.[69, 70] As residential areas continue to expand into wildlife habitats, humans and their pets will be at increased risk for exposure to *T. cruzi* and other zoonotic diseases.

CHAPTER VII

SUMMARY AND CONCLUSIONS

In this dissertation, new data have been provided on several components of the Chagas disease transmission cycle in state of the Texas, including vector and parasite distribution and genetic variation, vector habitat suitability, and canine case magnitude, distribution, and clinical presentation. The distribution of triatomine bug vectors was determined from a diverse set of resources including field surveys, institution collections, health department records, and published records. Based on this data set which dates from 1928 to 2006, the triatomine bug distribution in Texas covers 97 of 254 counties. Of the 67 counties with data on *T. cruzi* testing in bug specimens, 48 had at least one positive result. The distribution of triatomine bugs in Texas is widespread. Triatomine species were found in all 12 natural regions with the greatest species diversity occurring in the South Texas Brush Country with six of the seven species reported in Texas. Three species (*Triatoma gerstaeckeri*, *T. lecticularia*, and *T. sanguisuga*) are distributed widely across the state in diverse habitats. The distribution of *T. cruzi*-infected bugs includes most geographic regions, with the exception of the northern third of the state.

In field studies, 233 bug specimens were collected from 34 counties in Texas including at least one specimen from each of the seven species. *T. gerstaeckeri* was the most commonly-collected species followed by *T. sanguisuga*. The majority of field-collected specimens were found inside or near houses and dog kennels. The *T. cruzi*

infection rate for tested specimens was 51.78% which is higher than previously reported from this area.

Using the most abundant species of triatomine bug collected in the field studies, *T. gerstaeckeri*, a spatial distribution model was developed to predict areas of suitable habitat within Texas. Geographic information systems and remote sensing methods were used to build a model based on land cover composition. The model was built and tested with field collection sites from this study. The results of the model indicate that this species has been able to adapt to a broad range of area sizes within land cover classes. Forest and rangeland were the predominant land cover classes found within the predicted *T. gerstaeckeri* habitat. Forest may be the most important land cover for *T. gerstaeckeri*, as indicated by significantly higher minimum and maximum area limits than the other land cover types evaluated. Additional characterization of land cover, using a smaller spatial scale and higher resolution imagery, may provide further insights to the ecological dynamics influencing the presence and abundance of *T. gerstaeckeri*.

Genetic characterization of all seven triatomine species from Texas was accomplished in this study by comparison of cytochrome *b* DNA sequences from 61 new specimens and previously published sequences. This was the first study to analyze the taxonomic status of *T. gerstaeckeri*, *T. indictiva*, and *T. neotomae* using molecular markers. Results suggest taxonomic links for species whose placement into subgenera complexes was uncertain and support the re-evaluation of taxonomic status for other species. Specifically, the data indicate that *T. gerstaeckeri* is closely aligned with the *phyllosoma* complex, *T. sanguisuga* is more closely related to the *phyllosoma* complex

than the *lecticularia* complex, and *T. indictiva* is a subspecies of *T. sanguisuga*. The high degree of intraspecific variation for *T. sanguisuga* and *T. gerstaeckeri* implies that significant gene flow may occur across their ranges within the state of Texas. This represents the largest phylogenetic study of U.S. *Triatoma* spp. to date.

Genetic characterization of *T. cruzi* isolates from Texas was conducted with 68 new isolates from Texas using a segment of the small subunit rRNA gene. Parasite DNA was extracted from 63 triatomine bugs of five species. Additional canine, baboon, and human isolates were also evaluated. All U.S. sequences partitioned into two groups which is in agreement with the findings of previous studies on U.S. isolates. The pattern of group partitioning among the U.S. isolates was not immediately apparent. Similar to intraspecific variation within *T. sanguisuga* and *T. gerstaeckeri*, the variation in Texas *T. cruzi* isolates does not seem to involve host species or geographic location. This represents the largest phylogenetic study of U.S. *T. cruzi* isolates to date.

The work presented here includes the first comprehensive study of canine Chagas disease in Texas with regards to geographic distribution, signalment, and clinical and histopathologic presentation. Data were compiled from over 550 serologically- or histopathologically-confirmed canine cases that were documented primarily at the Texas Veterinary Medical Diagnostic Laboratory over the past 15 years. Based on these data, the geographic distribution of canine cases in Texas is wide spread (46 counties) and closely matches the distribution of the insect vector species of *Triatoma* reported from the state. Chagas disease was diagnosed in 33 different dog breeds, primarily sporting/working breeds. The predominant clinical presentation for histopathologically-

confirmed cases was acute death, particularly for dogs one year of age or older. Myocarditis and intralesional parasites in heart tissue were observed at necropsy in the vast majority of cases.

The research presented in this dissertation should serve to increase awareness among medical entomologists, clinicians, and public health practicioners regarding the geographic extent and infection potential of the Chagas disease transmission cycle in Texas and neighboring regions. The triatomine species and canine case distribution and infection rate data can serve as a baseline for future surveillance efforts. This study provides additional evidence that the Chagas disease transmission cycle is well-established in the U.S. Additional studies to characterize insect vector-canine interactions in the U.S. are needed to further understand the peri-domestic transmission cycle and potential risk to humans. To this end, research in the following areas would be very useful: clarification of native vector feeding preferences (e.g., blood meal analysis); estimation of reservoir potential of infected U.S. dogs (e.g., quantification of parasitemia levels in infected dogs over time); determination of landscape features associated with establishment of peri-domestic transmission cycles in the U.S. (e.g., application of GIS and remote sensing methods to fine scale landscape composition, metrices, and human-induced change).

REFERENCES

1. Schmunis GA, 1999. Iniciativa del Cono Sur. Schofield CJ, Ponce C, eds. *Proceedings of the Second International Workshop on Population Biology and the Control of Triatominae*. Mexico City: INDRE, 26-31.

2. Schofield CJ, Dias JC, 1999. The Southern Cone Initiative against Chagas disease. *Adv Parasitol 42*: 1-27.

3. Chagas C, 1909. Nova a tripanozomiaze humana. *Mem. Inst. Oswaldo Cruz 1*: 1-159.

4. Ramsey JM, Schofield CJ, 2003. Control of Chagas disease vectors. *Salud Publica Mex 45*: 123-8.

5. Jansen AM, Santos de Pinho AP, Lisboa CV, Cupolillo E, Mangia RH, Fernandes O, 1999. The sylvatic cycle of *Trypanosoma cruzi*: a still unsolved puzzle. *Mem Inst Oswaldo Cruz 94 Suppl 1*: 203-4.

6. Dias J, Schofield C, 1999. The evolution of Chagas disease (American trypanosomiasis) control after 90 years since Carlos Chagas discovery. *Mem Inst Oswaldo Cruz 94 Suppl 1*: 103-21.

7. Roberts LS, Janovy JJ, 1996. *Foundations of Parasitology*. Dubuque, IA: Wm. C. Brown Publishers.

8. Schofield C, 1994. *Triatominae Biology & Control*. West Sussex, England: Eurocommunica Publications.

9. WHO, 2002. Control of Chagas disease. *World Health Organ Tech Rep Ser 905*: i-vi, 1-109, back cover.

10. Kofoid CA, McCulloch, L., 1956. On *Trypanosoma triatomae*, a new flagellate from a hemipteran bug from the nests of the wood rat *Neotoma fuscipes*. *Univ Calif Pub Zool 16*: 113-126.

11. Schofield CJ, 2000. Biosystematics and evolution of the Triatominae. *Cad Saude Publica 16 Suppl 2*: 89-92.

12. Lent H, Wygodzinski P, 1979. Revision of the Triatominae (Hemiptera: Reduviidae) and their significance as vectors of Chagas disease. *Bull Am Mus Nat Hist 163*: 123-520.

13. Ikenga JO, Richerson JV, 1984. *Trypanosoma cruzi* (Chagas) (protozoa: Kinetoplastida: Trypanosomatidae) in invertebrate and vertebrate hosts from Brewster County in Trans-Pecos Texas. *J Econ Entomol 77*: 126-9.

14. Pippin WF, 1970. The biology and vector capability of *Triatoma sanguisuga texana* Usinger and *Triatoma gerstaeckeri* (Stal) compared with *Rhodnius prolixus* (Stal) (Hemiptera: Triatominae). *J Med Entomol 7*: 30-45.

15. Wood SF, 1975. *Trypanosoma cruzi*: new foci of enzootic Chagas' disease in California. *Exp Parasitol 38*: 153-60.

16. Sullivan TD, McGregor T, Eads RB, Davis DJ, 1942. Incidence of *Trypanosoma cruzi*, Chagas, in *Triatoma* (Hemiptera, Reduviidae) in Texas. *Am J Trop Med 29*: 453-458.

17. Wood SF, Wood FD, 1964. Nocturnal aggregation and invasion of homes in southern California by insect vectors of Chagas' disease. *J Econ Entomol 57*: 775-776.

18. Burkholder JE, Allison TC, Kelly VP, 1980. *Trypanosoma cruzi* (Chagas) (Protozoa: Kinetoplastida) in invertebrate, reservoir, and human hosts of the lower Rio Grande valley of Texas. *J Parasitol 66*: 305-11.

19. Ryckman RE, Ryckman JV, 1967. Epizootiology of *Trypanosoma cruzi* in southwestern North America. XII. Does Gause's rule apply to the ectoparasitic Triatominae? (Hemiptera: Reduviidae) (Kinetoplastidae: Trypanosomidae) (Rodentia: Cricetidae). *J Med Entomol 4*: 379-86.

20. Wood SF, 1949. Additional observations on *Trypanosoma cruzi*, Chagas, from Arizona in insects, rodents, and experimentally infected animals. *Am J Trop Med 29*: 43-55.

21. Beard CB, Young DG, Butler JF, Evans DA, 1988. First isolation of *Trypanosoma cruzi* from a wild-caught *Triatoma sanguisuga* (LeConte) (Hemiptera: Triatominae) in Florida, U.S.A. *J Parasitol 74*: 343-4.

22. Pung OJ, Banks CW, Jones DN, Krissinger MW, 1995. *Trypanosoma cruzi* in wild raccoons, opossums, and triatomine bugs in southeast Georgia, U.S.A. *J Parasitol 81*: 324-6.

23. Olsen PF, Shoemaker JP, Turner HF, Hays KL, 1964. Incidence of *Trypanosoma cruzi* (Chagas) in wild vectors and reservoirs in east-central Alabama. *J Parasitol 50*: 599-603.

24. Herwaldt BL, Grijalva MJ, Newsome AL, McGhee CR, Powell MR, Nemec DG, Steurer FJ, Eberhard ML, 2000. Use of polymerase chain reaction to diagnose the fifth reported US case of autochthonous transmission of *Trypanosoma cruzi*, in Tennessee, 1998. *J Infect Dis 181*: 395-9.

25. Yaeger RG, 1961. The present status of Chagas' disease in the United States. *Bull Tulane Univ Med Fac 21*: 9-13.

26. Griffith ME, 1948. The bloodsucking conenose, or "big bedbug", *Triatoma sanguisuga* (Leconte), in an Oklahoma City household. *The Oklahoma Academy of Science 28*.

27. Woody NC, Woody, H.B., 1955. American Trypanosomiasis (Chagas' disease): First indigenous case in the United States. *JAMA 159*: 676-677.

28. Navin TR, Roberto RR, Juranek DD, Limpakarnjanarat K, Mortenson EW, Clover JR, Yescott RE, Taclindo C, Steurer F, Allain D, 1985. Human and sylvatic *Trypanosoma cruzi* infection in California. *Am J Public Health 75*: 366-9.

29. Packchanian A, 1942. Reservoir hosts of Chagas' disease in the state of Texas. Natural infection of nine-banded armadillo (*Dasypus novemcinctus texanus*), house mice (*Mus musculus*), opossum (*Didelphis virginiana*), and wood rats (*Neotoma micropus micropus*), with *Trypanosoma cruzi* in the state of Texas. *Am J Trop Med 22*: 623-631.

30. Schaffer GD, Hanson WL, Davidson WR, Nettles VF, 1978. Hematotropic parasites of translocated raccoons in the southeast. *J Am Vet Med Assoc 173*: 1148-51.

31. John DT, Hoppe KL, 1986. *Trypanosoma cruzi* from wild raccoons in Oklahoma. *Am J Vet Res 47*: 1056-9.

32. Yaeger RG, 1988. The prevalence of *Trypanosoma cruzi* infection in armadillos collected at a site near New Orleans, Louisiana. *Am J Trop Med Hyg 38*: 323-6.

33. Barr SC, Brown CC, Dennis VA, Klei TR, 1991. The lesions and prevalence of *Trypanosoma cruzi* in opossums and armadillos from southern Louisiana. *J Parasitol 77*: 624-7.

34. Telford SR, Jr., Forrester DJ, 1991. Hemoparasites of raccoons (*Procyon lotor*) in Florida. *J Wildl Dis 27*: 486-90.

35. Karsten V, Davis C, Kuhn R, 1992. *Trypanosoma cruzi* in wild raccoons and opossums in North Carolina. *J Parasitol 78*: 547-9.

36. Grogl M, Kuhn RE, Davis DS, Green GE, 1984. Antibodies to *Trypanosoma cruzi* in coyotes in texas. *J Parasitol 70*: 189-91.

37. Williams GD, Adams LG, Yaeger RG, McGrath RK, Read WK, Bilderback WR, 1977. Naturally occurring trypanosomiasis (Chagas' disease) in dogs. *J Am Vet Med Assoc 171*: 171-7.

38. Meurs KM, Anthony MA, Slater M, Miller MW, 1998. Chronic *Trypanosoma cruzi* infection in dogs: 11 cases (1987-1996). *J Am Vet Med Assoc 213*: 497-500.

39. Fox JC, Ewing SA, Buckner RG, Whitenack D, Manley JH, 1986. *Trypanosoma cruzi* infection in a dog from Oklahoma. *J Am Vet Med Assoc 189*: 1583-4.

40. Bradley KK, Bergman DK, Woods JP, Crutcher JM, Kirchhoff LV, 2000. Prevalence of American trypanosomiasis (Chagas disease) among dogs in Oklahoma. *J Am Vet Med Assoc 217*: 1853-7.

41. Barr S, Baker D, Markovits J, 1986. Trypanosomiasis and laryngeal paralysis in a dog. *J Am Vet Med Assoc 188*: 1307-9.

42. Snider TG, Yaeger RG, Dellucky J, 1980. Myocarditis caused by *Trypanosoma cruzi* in a native Louisiana dog. *J Am Vet Med Assoc 177*: 247-9.

43. Tomlinson MJ, Chapman WL, Jr., Hanson WL, Gosser HS, 1981. Occurrence of antibody to *Trypanosoma cruzi* in dogs in the southeastern United States. *Am J Vet Res 42*: 1444-6.

44. Barr SC, Dennis VA, Klei TR, 1991. Serologic and blood culture survey of *Trypanosoma cruzi* infection in four canine populations of southern Louisiana. *Am J Vet Res 52*: 570-3.

45. Shadomy SV, Waring SC, Chappell CL, 2004. Combined use of enzyme-linked immunosorbent assay and flow cytometry to detect antibodies to *Trypanosoma cruzi* in domestic canines in Texas. *Clin Diagn Lab Immunol 11*: 313-9.

46. Mott KE, Mota EA, Sherlock I, Hoff R, Muniz TM, Oliveira TS, Draper CC, 1978. *Trypanosoma cruzi* infection in dogs and cats and household seroreactivity to *T. cruzi* in a rural community in northeast Brazil. *Am J Trop Med Hyg 27*: 1123-7.

47. Gurtler RE, Cecere MC, Petersen RM, Rubel DN, Schweigmann NJ, 1993. Chagas disease in north-west Argentina: association between *Trypanosoma cruzi* parasitaemia in dogs and cats and infection rates in domestic *Triatoma infestans*. *Trans R Soc Trop Med Hyg 87*: 12-5.

48. Estrada-Franco JG, Bhatia V, Diaz-Albiter H, Ochoa-Garcia L, Barbabosa A, Vazquez-Chagoyan JC, Martinez-Perez MA, Guzman-Bracho C, Garg N, 2006. Human *Trypanosoma cruzi* infection and seropositivity in dogs, Mexico. *Emerg Infect Dis 12*: 624-30.

49. Gurtler RE, Solard ND, Lauricela MA, Haedo AS, Pietrokovski SM, Alberti AA, Wisnivesky-Colli C, 1986. Dynamics of transmission of *Trypanosoma cruzi* in a rural area of Argentina. III. Persistence of *T. cruzi* parasitemia among canine reservoirs in a two-year follow-up. *Rev Inst Med Trop Sao Paulo 28*: 213-9.

50. Gurtler RE, Cecere MC, Rubel DN, Petersen RM, Schweigmann NJ, Lauricella MA, Bujas MA, Segura EL, Wisnivesky-Colli C, 1991. Chagas disease in north-west Argentina: infected dogs as a risk factor for the domestic transmission of *Trypanosoma cruzi*. *Trans R Soc Trop Med Hyg 85*: 741-5.

51. TDH, 1956. Found: Two cases of Chagas disease. *Tex Health Bull 9*: 11-13.

52. Ochs DE, Hnilica VS, Moser DR, Smith JH, Kirchhoff LV, 1996. Postmortem diagnosis of autochthonous acute chagasic myocarditis by polymerase chain reaction amplification of a species-specific DNA sequence of *Trypanosoma cruzi*. *Am J Trop Med Hyg 54*: 526-9.

53. Dorn P, Periniciaro L, Steurer F, Lawrence G, Balsamo G, Diaz J, Wesson D, 2006. First report of autochthonous transmission of *Trypanosoma cruzi* in Louisiana and sixth in the United States. 55th annual meeting of the American Society of Tropical Medicine and Hygiene. Atlanta, GA.

54. Robinson LE, 2006. Report of new human Chagas disease case in south Texas. Harlingen: Texas Department of State Health Services, Public Health Region 11, Zoonosis Control.

55. Barrett VJ, Leiby DA, Odom JL, Otani MM, Rowe JD, Roote JT, Cox KF, Brown KR, Hoiles JA, Saez-Alquezar A, Turrens JF, 1997. Negligible prevalence of antibodies against *Trypanosoma cruzi* among blood donors in the southeastern United States. *Am J Clin Pathol 108*: 499-503.

56. Leiby DA, Herron RM, Jr., Read EJ, Lenes BA, Stumpf RJ, 2002. *Trypanosoma cruzi* in Los Angeles and Miami blood donors: impact of evolving donor demographics on seroprevalence and implications for transfusion transmission. *Transfusion 42*: 549-55.

57. Leiby DA, Read EJ, Lenes BA, Yund AJ, Stumpf RJ, Kirchhoff LV, Dodd RY, 1997. Seroepidemiology of *Trypanosoma cruzi*, etiologic agent of Chagas' disease, in US blood donors. *J Infect Dis 176*: 1047-52.

58. Woody NC, Hernandez A, Suchow B, 1965. American trypanosomiasis. III. The incidence of serologically diagnosed Chagas' disease among persons bitten by the insect vector. *Tropical Pediatrics 66*: 107-109.

59. Di Pentima MC, Hwang LY, Skeeter CM, Edwards MS, 1999. Prevalence of antibody to *Trypanosoma cruzi* in pregnant Hispanic women in Houston. *Clin Infect Dis 28*: 1281-5.

60. Betz TG, 1978. Conflicts in the study of Chagas' disease between a southwestern Indian population and the staff of a southwestern university college of medicine. Bauwens EE, ed. *The Anthropology of Health*. St. Louis: The C.V. Mosby Company, 88-94.

61. Eads RB, Trevino HA, Campos EG, 1963. *Triatoma* (Hemiptera: Reduviidae) infected with *Trypanosoma cruzi* in south Texas wood rat dens. *Southwestern Naturalist 8*: 38-42.

62. Packchanian A, 1943. The infectivity of the Texas strain of *Trypansoma cruzi* to man. *Am J Trop Med 23*: 309-314.

63. Kasa TJ, Lathrop GD, Dupuy HJ, Bonney CH, Toft JD, 1977. An endemic focus of *Trypanosoma cruzi* infection in a subhuman primate research colony. *J Am Vet Med Assoc 171*: 850-4.

64. Gleiser CA, Yaeger RG, Ghidoni JJ, 1986. *Trypanosoma cruzi* infection in a colony-born baboon. *J Am Vet Med Assoc 189*: 1225-6.

65. Lane RS, Moss RB, Hsu YP, Wei T, Mesirow ML, Kuo MM, 1999. Anti-arthropod saliva antibodies among residents of a community at high risk for Lyme disease in California. *Am J Trop Med Hyg 61*: 850-9.

66. Frazier CA, 1974. Biting insect survey: a statistical report. *Ann Allergy 32*: 200-4.

67. Lynch PJ, Pinnas JL, 1978. "Kissing bug" bites. *Triatoma* species as an important cause of insect bites in the southwest. *Cutis 22*: 585-91.

68. Moffitt JE, Venarske D, Goddard J, Yates AB, deShazo RD, 2003. Allergic reactions to *Triatoma* bites. *Ann Allergy Asthma Immunol 91*: 122-8; quiz 128-30, 194.

69. Magnarelli LA, Dumler JS, Anderson JF, Johnson RC, Fikrig E, 1995. Coexistence of antibodies to tick-borne pathogens of babesiosis, ehrlichiosis, and Lyme borreliosis in human sera. *J Clin Microbiol 33*: 3054-7.

70. Sweeney CJ, Ghassemi M, Agger WA, Persing DH, 1998. Coinfection with *Babesia microti* and *Borrelia burgdorferi* in a western Wisconsin resident. *Mayo Clin Proc 73*: 338-41.

71. Teixeira AR, Monteiro PS, Rebelo JM, Arganaraz ER, Vieira D, Lauria-Pires L, Nascimento R, Vexenat CA, Silva AR, Ault SK, Costa JM, 2001. Emerging Chagas disease: trophic network and cycle of transmission of *Trypanosoma cruzi* from palm trees in the Amazon. *Emerg Infect Dis 7*: 100-12.

72. Guzman-Bracho C, 2001. Epidemiology of Chagas disease in Mexico: an update. *Trends Parasitol 17*: 372-6.

73. Pavlovsky EN, 1966. *The Natural Nidality of Transmissible Disease, with Special Reference to the Landscape Epidemiology of Zooanthroponses*. Urbana: University of Illinois Press.

74. Kitron U, 1998. Landscape ecology and epidemiology of vector-borne diseases: tools for spatial analysis. *J Med Entomol 35*: 435-45.

75. Beck LR, Lobitz BM, Wood BL, 2000. Remote sensing and human health: new sensors and new opportunities. *Emerg Infect Dis 6*: 217-27.

76. Patz JA, Daszak P, Tabor GM, Aguirre AA, Pearl M, Epstein J, Wolfe ND, Kilpatrick AM, Foufopoulos J, Molyneux D, Bradley DJ, 2004. Unhealthy landscapes: policy recommendations on land use change and infectious disease emergence. *Environ Health Perspect 112*: 1092-8.

77. Cromley EK, 2003. GIS and disease. *Annu Rev Public Health 24*: 7-24.

78. Shililu J, Ghebremeskel T, Mengistu S, Fekadu H, Zerom M, Mbogo C, Githure J, Gu W, Novak R, Beier JC, 2003. Distribution of anopheline mosquitoes in Eritrea. *Am J Trop Med Hyg 69*: 295-302.

79. Noma M, Nwoke BE, Nutall I, Tambala PA, Enyong P, Namsenmo A, Remme J, Amazigo UV, Kale OO, Seketeli A, 2002. Rapid epidemiological mapping of onchocerciasis (REMO): its application by the African Programme for Onchocerciasis Control (APOC). *Ann Trop Med Parasitol 96 Suppl 1*: S29-39.

80. Linthicum KJ, Anyamba A, Tucker CJ, Kelley PW, Myers MF, Peters CJ, 1999. Climate and satellite indicators to forecast Rift Valley fever epidemics in Kenya. *Science 285*: 397-400.

81. Guerra M, Walker E, Jones C, Paskewitz S, Cortinas MR, Stancil A, Beck L, Bobo M, Kitron U, 2002. Predicting the risk of Lyme disease: habitat suitability

for *Ixodes scapularis* in the north central United States. *Emerg Infect Dis 8*: 289-97.

82. Peterson AT, Sanchez-Cordero V, Beard CB, Ramsey JM, 2002. Ecologic niche modeling and potential reservoirs for Chagas disease, Mexico. *Emerg Infect Dis 8*: 662-7.

83. Costa J, Peterson AT, Beard CB, 2002. Ecologic niche modeling and differentiation of populations of *Triatoma brasiliensis* Neiva, 1911, the most important Chagas' disease vector in northeastern Brazil (hemiptera, reduviidae, triatominae). *Am J Trop Med Hyg 67*: 516-20.

84. Dumonteil E, Gourbiere S, 2004. Predicting *Triatoma dimidiata* abundance and infection rate: a risk map for natural transmission of Chagas disease in the Yucatan peninsula of Mexico. *Am J Trop Med Hyg 70*: 514-9.

85. Beard CB, Pye G, Steurer FJ, Rodriguez R, Campman R, Peterson AT, Ramsey J, Wirtz RA, Robinson LE, 2003. Chagas disease in a domestic transmission cycle, southern Texas, USA. *Emerg Infect Dis 9*: 103-5.

86. Usinger RL, 1944. *The Triatominae of North and Central America and the West Indies and Their Public Health Significance*: U.S. Government Printing Office, Washington, D.C.

87. Wood SF, 1941. Notes on the distribution and habits of reduviid vectors of Chagas' disease in the southwestern United States. Part I. *The Pan-Pacific Entomologist 17*: 85-94.

88. Wood SF, 1941. Notes on the distribution and habits of reduviid vectors of Chagas' disease in the southwestern United States. Part II. *The Pan-Pacific Entomologist 17*: 115-118.

89. Wood SF, 1941. New localities for *Trypanosoma cruzi* Chagas in southwestern United States. *Am J Hyg 34*: 1-13.

90. Sullivan TD, McGregor T, Eads RB, Davis DJ, 1949. Incidence of *Trypanosoma cruzi*, Chagas, in *Triatoma* (Hemiptera: Reduviidae) in Texas. *Am J Trop Med 29*: 453-458.

91. Thurman Jr. DC, 1945. The biology of *Triatoma gerstaeckeri*. *J Econ Entomol 38*: 597-598.

92. Nasci RS, Savage HM, White DJ, Miller JR, Cropp BC, Godsey MS, Kerst AJ, Bennett P, Gottfried K, Lanciotti RS, 2001. West Nile virus in overwintering *Culex* mosquitoes, New York City, 2000. *Emerg Infect Dis 7*: 742-4.

93. Sardelis MR, Turell MJ, Dohm DJ, O'Guinn ML, 2001. Vector competence of selected North American *Culex* and *Coquillettidia* mosquitoes for West Nile virus. *Emerg Infect Dis 7*: 1018-22.

94. Theis JH, Tibayrenc M, Ault SK, Mason DT, 1985. Agent of Chagas' disease from Honduran vector capable of developing in California insects: implications for cardiologists. *Am Heart J 110*: 605-8.

95. Theis JH, Tibayrenc M, Mason DT, Ault SK, 1987. Exotic stock of *Trypanosoma cruzi* (Schizotrypanum) capable of development in and transmission by *Triatoma protracta protracta* from California: public health implications. *Am J Trop Med Hyg 36*: 523-8.

96. Kirchhoff LV, Gam AA, Gilliam FC, 1987. American trypanosomiasis (Chagas' disease) in Central American immigrants. *Am J Med 82*: 915-20.

97. Cimo PL, Luper WE, Scouros MA, 1993. Transfusion-associated Chagas' disease in Texas: report of a case. *Tex Med 89*: 48-50.

98. Leiby DA, Lenes BA, Tibbals MA, Tames-Olmedo MT, 1999. Prospective evaluation of a patient with *Trypanosoma cruzi* infection transmitted by transfusion. *N Engl J Med 341*: 1237-9.

99. Grant IH, Gold JW, Wittner M, Tanowitz HB, Nathan C, Mayer K, Reich L, Wollner N, Steinherz L, Ghavimi F, et al., 1989. Transfusion-associated acute Chagas disease acquired in the United States. *Ann Intern Med 111*: 849-51.

100. Centers for Disease Control and Prevention, 2002. Chagas disease after organ transplantation--United States, 2001. *MMWR Morb Mortal Wkly Rep 51*: 210-2.

101. Centers for Disease Control and Prevention, 2006. Chagas disease after organ transplantation--Los Angeles, California, 2006. *MMWR Morb Mortal Wkly Rep 55*: 798-800.

102. McCarthy M, 2003. American Red Cross to screen blood for Chagas' disease. *Lancet 362*: 1988.

103. FDA, 2006. Product approval information--licensing action BL 125161/0. Rockville: US FDA Center for Biologics Evaluation and Research.

104. Centers for Disease Control and Prevention, 2007. Blood donor screening for chagas disease--United States, 2006-2007. *MMWR Morb Mortal Wkly Rep 56*: 141-3.

105. Waring SC, Chappell CL, 2004. Trypanosomiasis in Texas. Texas Branch Meeting of The American Society for Microbiology. Houston, TX.

106. Monteiro FA, Escalante AA, Beard CB, 2001. Molecular tools and triatomine systematics: a public health perspective. *Trends Parasitol 17*: 344-7.

107. Dujardin JP, Cardozo L, Schofield C, 1996. Genetic analysis of *Triatoma infestans* following insecticidal control interventions in central Bolivia. *Acta Trop 61*: 263-6.

108. Garcia AL, Carrasco HJ, Schofield CJ, Stothard JR, Frame IA, Valente SA, Miles MA, 1998. Random amplification of polymorphic DNA as a tool for taxonomic studies of triatomine bugs (Hemiptera: Reduviidae). *J Med Entomol 35*: 38-45.

109. Dujardin JP, Schofield CJ, Tibayrenc M, 1998. Population structure of Andean *Triatoma infestans*: allozyme frequencies and their epidemiological relevance. *Med Vet Entomol 12*: 20-9.

110. Dujardin JP, Munoz M, Chavez T, Ponce C, Moreno J, Schofield CJ, 1998. The origin of *Rhodnius prolixus* in Central America. *Med Vet Entomol 12*: 113-5.

111. Garcia BA, Soares Barata JM, Blanco A, 1995. Enzyme polymorphism among *Triatoma infestans* (Hemiptera: Reduviidae) colonies. *J Med Entomol 32*: 126-33.

112. Lopez G, Moreno J, 1995. Genetic variability and differentiation between populations of *Rhodnius prolixus* and *R. pallescens*, vectors of Chagas' disease in Colombia. *Mem Inst Oswaldo Cruz 90*: 353-7.

113. Harry M, Galindez I, Cariou ML, 1992. Isozyme variability and differentiation between *Rhodnius prolixus, R.robustus* and *R.pictipes*, vectors of Chagas disease in Venezuela. *Med Vet Entomol 6*: 37-43.

114. Breniere SF, Bosseno MF, Vargas F, Yaksic N, Noireau F, Noel S, Dujardin JP, Tibayrenc M, 1998. Smallness of the panmictic unit of *Triatoma infestans* (Hemiptera: Reduviidae). *J Med Entomol 35*: 911-7.

115. Borges EC, Dujardin JP, Schofield CJ, Romanha AJ, Diotaiuti L, 2005. Dynamics between sylvatic, peridomestic and domestic populations of *Triatoma brasiliensis* (Hemiptera: Reduviidae) in Ceara State, Northeastern Brazil. *Acta Trop 93*: 119-126.

116. Breniere SF, Taveira B, Bosseno MF, Ordonez R, Lozano-Kasten F, Magallon-Gastelum E, Ouaissi A, Ramsey J, 2003. Preliminary results of random

amplification of polymorphic DNA among Triatominae of the *Phyllosoma* complex (Hemiptera, Reduviidae). *Mem Inst Oswaldo Cruz 98*: 1033-8.

117. Calderon CI, Dorn PL, Melgar S, Chavez JJ, Rodas A, Rosales R, Monroy CM, 2004. A preliminary assessment of genetic differentiation of *Triatoma dimidiata* (Hemiptera: Reduviidae) in Guatemala by random amplification of polymorphic DNA-polymerase chain reaction. *J Med Entomol 41*: 882-7.

118. Dorn PL, Melgar S, Rouzier V, Gutierrez A, Combe C, Rosales R, Rodas A, Kott S, Salvia D, Monroy CM, 2003. The Chagas vector, *Triatoma dimidiata* (Hemiptera: Reduviidae), is panmictic within and among adjacent villages in Guatemala. *J Med Entomol 40*: 436-40.

119. Jaramillo C, Montana MF, Castro LR, Vallejo GA, Guhl F, 2001. Differentiation and genetic analysis of *Rhodnius prolixus* and *Rhodnius colombiensis* by rDNA and RAPD amplification. *Mem Inst Oswaldo Cruz 96*: 1043-8.

120. Black WCt, 1993. PCR with arbitrary primers: approach with care. *Insect Mol Biol 2*: 1-6.

121. Garcia BA, Powell JR, 1998. Phylogeny of species of *Triatoma* (Hemiptera: Reduviidae) based on mitochondrial DNA sequences. *J Med Entomol 35*: 232-8.

122. Lyman DF, Monteiro FA, Escalante AA, Cordon-Rosales C, Wesson DM, Dujardin JP, Beard CB, 1999. Mitochondrial DNA sequence variation among triatomine vectors of Chagas' disease. *Am J Trop Med Hyg 60*: 377-86.

123. Monteiro FA, Wesson DM, Dotson EM, Schofield CJ, Beard CB, 2000. Phylogeny and molecular taxonomy of the Rhodniini derived from mitochondrial and nuclear DNA sequences. *Am J Trop Med Hyg 62*: 460-5.

124. Avise JC, Arnold J, Ball RM, Bermingham E, Lamb T, Neigel JE, Reeb CA, Saunders NC, 1987. Intraspecific phylogeography: The mitochondrial DNA bridge between population genetics and systematics. *Annu. Rev. Ecol. Syst. 18*: 489-522.

125. Hypsa V, Tietz DF, Zrzavy J, Rego RO, Galvao C, Jurberg J, 2002. Phylogeny and biogeography of Triatominae (Hemiptera: Reduviidae): molecular evidence of a New World origin of the Asiatic clade. *Mol Phylogenet Evol 23*: 447-57.

126. Sainz AC, Mauro LV, Moriyama EN, Garcia BA, 2004. Phylogeny of triatomine vectors of *Trypanosoma cruzi* suggested by mitochondrial DNA sequences. *Genetica 121*: 229-40.

127. Monteiro FA, Donnelly MJ, Beard CB, Costa J, 2004. Nested clade and phylogeographic analyses of the Chagas disease vector *Triatoma brasiliensis* in Northeast Brazil. *Mol Phylogenet Evol 32*: 46-56.

128. Garcia BA, Moriyama EN, Powell JR, 2001. Mitochondrial DNA sequences of triatomines (Hemiptera: Reduviidae): phylogenetic relationships. *J Med Entomol 38*: 675-83.

129. Giordano R, Cortez JC, Paulk S, Stevens L, 2005. Genetic diversity of *Triatoma infestans* (Hemiptera: Reduviidae) in Chuquisaca, Bolivia based on the mitochondrial cytochrome *b* gene. *Mem Inst Oswaldo Cruz 100*: 753-60.

130. Martinez FH, Villalobos GC, Cevallos AM, Torre Pde L, Laclette JP, Alejandre-Aguilar R, Espinoza B, 2006. Taxonomic study of the *Phyllosoma* complex and other triatomine (Insecta: Hemiptera: Reduviidae) species of epidemiological importance in the transmission of Chagas disease: using ITS-2 and mtCytB sequences. *Mol Phylogenet Evol 41*: 279-87.

131. Pfeiler E, Bitler BG, Ramsey JM, Palacios-Cardiel C, Markow TA, 2006. Genetic variation, population structure, and phylogenetic relationships of *Triatoma rubida* and *T. recurva* (Hemiptera: Reduviidae: Triatominae) from the Sonoran Desert, insect vectors of the Chagas' disease parasite *Trypanosoma cruzi*. *Mol Phylogenet Evol 41*: 209-21.

132. Miles MA, Toye PJ, Oswald SC, Godfrey DG, 1977. The identification by isoenzyme patterns of two distinct strain-groups of *Trypanosoma cruzi*, circulating independently in a rural area of Brazil. *Trans R Soc Trop Med Hyg 71*: 217-25.

133. Barrett TV, Hoff RH, Mott KE, Miles MA, Godfrey DG, Teixeira R, Almeida de Souza JA, Sherlock IA, 1980. Epidemiological aspects of three *Trypanosoma cruzi* zymodemes in Bahia State, Brazil. *Trans R Soc Trop Med Hyg 74*: 84-90.

134. Miles MA, 1983. The epidemiology of South American trypanosomiasis--biochemical and immunological approaches and their relevance to control. *Trans R Soc Trop Med Hyg 77*: 5-23.

135. Diotaiuti L, Pereira AS, Loiola CF, Fernandes AJ, Schofield JC, Dujardin JP, Dias JC, Chiari E, 1995. Inter-relation of sylvatic and domestic transmission of *Trypanosoma cruzi* in areas with and without domestic vectorial transmission in Minas Gerais, Brazil. *Mem Inst Oswaldo Cruz 90*: 443-8.

136. Almeida CE, Vinhaes MC, de Almeida JR, Silveira AC, Costa J, 2000. Monitoring the domiciliary and peridomiciliary invasion process of *Triatoma*

rubrovaria in the State of Rio Grande do Sul, Brazil. *Mem Inst Oswaldo Cruz 95*: 761-8.

137. Steindel M, Toma HK, Ishida MM, Murta SM, de Carvalho Pinto CJ, Grisard EC, Schlemper BR, Jr., Ribeiro-Rodrigues R, Romanha AJ, 1995. Biological and isoenzymatic characterization of *Trypanosoma cruzi* strains isolated from sylvatic reservoirs and vectors from the state of Santa Catarina, Southern Brazil. *Acta Trop 60*: 167-77.

138. Jones EM, Colley DG, Tostes S, Lopes ER, Vnencak-Jones CL, McCurley TL, 1993. Amplification of a *Trypanosoma cruzi* DNA sequence from inflammatory lesions in human chagasic cardiomyopathy. *Am J Trop Med Hyg 48*: 348-57.

139. Momen H, 1999. Taxonomy of *Trypanosoma cruzi*: a commentary on characterization and nomenclature. *Mem Inst Oswaldo Cruz 94 Suppl 1*: 181-4.

140. Maslov DA, Podlipaev SA, Lukes J, 2001. Phylogeny of the kinetoplastida: taxonomic problems and insights into the evolution of parasitism. *Mem Inst Oswaldo Cruz 96*: 397-402.

141. Macedo AM, Machado CR, Oliveira RP, Pena SD, 2004. *Trypanosoma cruzi*: genetic structure of populations and relevance of genetic variability to the pathogenesis of Chagas disease. *Mem Inst Oswaldo Cruz 99*: 1-12.

142. Anonymous, 1999. Recommendations from a satellite meeting. *Mem Inst Oswaldo Cruz 94 Suppl 1*: 429-32.

143. Brisse S, Barnabe C, Tibayrenc M, 2000. Identification of six *Trypanosoma cruzi* phylogenetic lineages by random amplified polymorphic DNA and multilocus enzyme electrophoresis. *Int J Parasitol 30*: 35-44.

144. Brisse S, Verhoef J, Tibayrenc M, 2001. Characterisation of large and small subunit rRNA and mini-exon genes further supports the distinction of six *Trypanosoma cruzi* lineages. *Int J Parasitol 31*: 1218-26.

145. Fernandes AP, Nelson K, Beverley SM, 1993. Evolution of nuclear ribosomal RNAs in kinetoplastid protozoa: perspectives on the age and origins of parasitism. *Proc Natl Acad Sci U S A 90*: 11608-12.

146. Stevens JR, Gibson W, 1999. The molecular evolution of trypanosomes. *Parasitol Today 15*: 432-7.

147. Maslov DA, Lukes J, Jirku M, Simpson L, 1996. Phylogeny of trypanosomes as inferred from the small and large subunit rRNAs: implications for the evolution

of parasitism in the trypanosomatid protozoa. *Mol Biochem Parasitol 75*: 197-205.

148. Briones MR, Souto RP, Stolf BS, Zingales B, 1999. The evolution of two *Trypanosoma cruzi* subgroups inferred from rRNA genes can be correlated with the interchange of American mammalian faunas in the Cenozoic and has implications to pathogenicity and host specificity. *Mol Biochem Parasitol 104*: 219-32.

149. Da Silva FM, Noyes H, Campaner M, Junqueira AC, Coura JR, Anez N, Shaw JJ, Stevens JR, Teixeira MM, 2004. Phylogeny, taxonomy and grouping of *Trypanosoma rangeli* isolates from man, triatomines and sylvatic mammals from widespread geographical origin based on SSU and ITS ribosomal sequences. *Parasitology 129*: 549-61.

150. Kawashita SY, Sanson GF, Fernandes O, Zingales B, Briones MR, 2001. Maximum-likelihood divergence date estimates based on rRNA gene sequences suggest two scenarios of *Trypanosoma cruzi* intraspecific evolution. *Mol Biol Evol 18*: 2250-9.

151. Souto RP, Fernandes O, Macedo AM, Campbell DA, Zingales B, 1996. DNA markers define two major phylogenetic lineages of *Trypanosoma cruzi*. *Mol Biochem Parasitol 83*: 141-52.

152. Nunes LR, de Carvalho MR, Buck GA, 1997. *Trypanosoma cruzi* strains partition into two groups based on the structure and function of the spliced leader RNA and rRNA gene promoters. *Mol Biochem Parasitol 86*: 211-24.

153. Barnabe C, Yaeger R, Pung O, Tibayrenc M, 2001. *Trypanosoma cruzi*: a considerable phylogenetic divergence indicates that the agent of Chagas disease is indigenous to the native fauna of the United States. *Exp Parasitol 99*: 73-9.

154. Pung OJ, Spratt J, Clark CG, Norton TM, Carter J, 1998. *Trypanosoma cruzi* infection of free-ranging lion-tailed macaques (*Macaca silenus*) and ring-tailed lemurs (*Lemur catta*) on St. Catherine's Island, Georgia, USA. *J Zoo Wildl Med 29*: 25-30.

155. Yabsley MJ, Noblet GP, 2002. Biological and molecular characterization of a raccoon isolate of *Trypanosoma cruzi* from South Carolina. *J Parasitol 88*: 1273-6.

156. Barr SC, Dennis VA, Klei TR, 1990. Growth characteristics in axenic and cell cultures, protein profiles, and zymodeme typing of three *Trypanosoma cruzi* isolates from Louisiana mammals. *J Parasitol 76*: 631-8.

157. Schofield CJ, 1988. Biosystematics of the Triatominae. Service MW, ed. *Systematics Association Special Volume*. Oxford: Clarendon Press, 284-312.

158. U.S. Census Bureau, 2000. TX Land area, 2000 (square miles): U.S. Census Bureau. http://quickfacts.census.gov/qfd/states/48000.html.

159. Garcia ES, De Azambuja P, 1997. Infection of triatomines with *Trypanosoma cruzi*. Crampton JM, Beard CB, Louis C, eds. *Molecular Biology of Disease Vectors*. New York: Chapman & Hall, 146-155.

160. Vera-Cruz JM, Magallon-Gastelum E, Grijalva G, Rincon AR, Ramos-Garcia C, Armendariz-Borunda J, 2003. Molecular diagnosis of Chagas' disease and use of an animal model to study parasite tropism. *Parasitol Res 89*: 480-6.

161. McGinnis S, Madden TL, 2004. BLAST: at the core of a powerful and diverse set of sequence analysis tools. *Nucleic Acids Res 32*: W20-5.

162. Texas Parks and Wildlife Department, 1997. natmajpy.shp. Austin: Texas Parks and Wildlife Department. http://www.tpwd.state.tx.us/landwater/land/maps/gis/data_downloads/.

163. Moore CG, Freier JE, 2005. Use of geographic information system methods in the study of vector-borne diseases. Marquardt W, ed. *Biology of Disease Vectors*. Burlington, MA: Academic Press, 207-218.

164. Pippin WF, Law PF, Gaylor MJ, 1968. *Triatoma sanguisuga texana* Usinger and *Triatoma sanguisuga indictiva* Neiva naturally infected with *Trypanosoma cruzi* Chagas in Texas (Hemiptera: Triatominae) (Kinetoplastida: Trypanosomidae). *J Med Entomol 5*: 134.

165. Schaub GA, Reduth D, Pudney M, 1990. The peculiarities of *Blastocrithidia triatomae*. *Parasitol Today 6*: 361-3.

166. Cerisola JA, Rohwedder R, Bozzini JP, Del Prado CE, 1971. *Blastocrithidia triatomae* n. sp. found in *Triatoma infestans* from Argentina. *J Protozool 18*: 503-6.

167. Cecere MC, Castanera MB, Canale DM, Chuit R, Gurtler RE, 1999. *Trypanosoma cruzi* infection in *Triatoma infestans* and other triatomines: long-term effects of a control program in rural northwestern Argentina. *Rev Panam Salud Publica 5*: 392-9.

168. Schaub GA, Losch P, 1989. Parasite/host-interrelationships of the trypanosomatids *Trypanosoma cruzi* and *Blastocrithidia triatomae* and the

reduviid bug *Triatoma infestans*: influence of starvation of the bug. *Ann Trop Med Parasitol 83*: 215-23.

169. Martinez-Ibarra JA, Galaviz-Silva L, Campos CL, Trujillo-Garcia JC, 1992. Distribucion de los triatominos asociados al domicilio humano en el municipio de general Teran, Nuevo Leon, Mexico. *Southwestern Entomologist 17*: 261-264.

170. Lane JE, Olivares-Villagomez D, Vnencak-Jones CL, McCurley TL, Carter CE, 1997. Detection of *Trypanosoma cruzi* with the polymerase chain reaction and *in situ* hybridization in infected murine cardiac tissue. *Am J Trop Med Hyg 56*: 588-95.

171. Brownstein JS, Skelly DK, Holford TR, Fish D, 2005. Forest fragmentation predicts local scale heterogeneity of Lyme disease risk. *Oecologia 146(3)*: 469-75.

172. Allan BF, Keesing F, Ostfeld RS, 2002. Effect of forest fragmentation on Lyme disease risk. *Convservation Biology 17*: 267-272.

173. Frank DH, Fish D, Moy FH, 1998. Landscape features associated with Lyme disease risk in a suburban residential environment. *Landscape ecology 13*: 27-36.

174. Wood FD, Wood SF, 1941. Present knowledge of the distribution of *Trypanosoma cruzi* in reservoir animals and vectors. *Am J Trop Med 21*: 335-345.

175. Packchanian A, 1939. Natural infection of *Triatoma gerstaeckeri* with *Trypanosoma cruzi* in Texas. *Public Health Reports 54*: 1547-1554.

176. Ryckman RE, 1979. Host reactions to bug bites (Hemiptera, Homoptera): a literature review and annotated bibiliography, part I. *Calif Vector Views 26*: 1-24.

177. Anderson JR, Hardy E, Roach J, Witmer R, 1976. *A Land-use/Land-cover Classification System for Use with Remote Sensor Data*. Washington: U.S. Geological Survey, 1-28.

178. Jensen JR, 2005. Thematic Information Extraction: Pattern Recognition. *Introductory Digital Image Processing: A Remote Sensing Perspective*. Upper Saddle River, NJ: Pearson Prentice Hall, 337-406.

179. Fitzpatrick-Lins K, 1981. Comparison of sampling procedures and data analysis for a land-use and land-cover map. *Photogrammetric Engineering & Remote Sensing 47*: 343-351.

180. Lehane MJ, Schofield CJ, 1981. Field experiments of dispersive flight by *Triatoma infestans*. *Trans R Soc Trop Med Hyg 75*: 399-400.

181. Gringorten JL, Friend WG, 1979. Wingbeat pattern in *Rhodnius prolixus* Stal (Heteroptera: Reduviidae) during exhaustive flight. *Can J Zool 57*: 391-395.

182. McGarigal KS, Cushman SA, Neel MC, Ene E, 2002. FRAGSTATS. Amherst, MA: University of Massachusetts. http://www.umass.edu/landeco/research/fragstats/fragstats.html.

183. Landis J, Koch G, 1977. The measurement of observer agreement for categorical data. *Biometrics 33*: 159-174.

184. Monroy MC, Bustamante DM, Rodas AG, Enriquez ME, Rosales RG, 2003. Habitats, dispersion and invasion of sylvatic *Triatoma dimidiata* (Hemiptera: Reduviidae: Triatominae) in Peten, Guatemala. *J Med Entomol 40*: 800-6.

185. Gustafson EJ, Parker GR, Bascks SE, 1994. Evaluating spatial pattern of wildlife habitat: a case study of the wild turkey (*Meleagris gallopavo*). *Am Midl Nat 131*: 24-33.

186. Dumonteil E, Gourbiere S, Barrera-Perez M, Rodriguez-Felix E, Ruiz-Pina H, Banos-Lopez O, Ramirez-Sierra MJ, Menu F, Rabinovich JE, 2002. Geographic distribution of *Triatoma dimidiata* and transmission dynamics of *Trypanosoma cruzi* in the Yucatan peninsula of Mexico. *Am J Trop Med Hyg 67*: 176-83.

187. Monteiro FA, Perez R, Panzera F, Dujardin JP, Galvao C, Rocha D, Noireau F, Schofield C, Beard CB, 1999. Mitochondrial DNA variation of *Triatoma infestans* populations and its implication on the specific status of *T. melanosoma*. *Mem Inst Oswaldo Cruz 94 Suppl 1*: 229-38.

188. Monteiro FA, Barrett TV, Fitzpatrick S, Cordon-Rosales C, Feliciangeli D, Beard CB, 2003. Molecular phylogeography of the Amazonian Chagas disease vectors *Rhodnius prolixus* and *R. robustus*. *Mol Ecol 12*: 997-1006.

189. Paredes EA, Miranda JV, Torres BN, Alejandre-Aguilar R, Romero RC, 2001. Vectorial importance of triatominae bugs (Hemiptera: Reduviidae) in Guaymas, Mexico. *Rev Latinoam Microbiol 43*: 119-22.

190. Ryckman RE, 1984. The Triatominae of North and Central America and the West Indies: A checklist with synonymy (Hemiptera: Reduviidae: Triatominae). *Bull Soc Vector Ecol 9*: 71-83.

191. Edgar RC, 2004. MUSCLE: a multiple sequence alignment method with reduced time and space complexity. *BMC Bioinformatics 5*: 113.

192. Edgar RC, 2004. MUSCLE: multiple sequence alignment with high accuracy and high throughput. *Nucleic Acids Res 32*: 1792-7.

193. Bininda-Edmonds O, 2006. seqConverter. pl. Institut fur Spezeille Zoologie und Evolutionsbiologie mit Phyletischem Museum, Friedrich-Schiller-Universitat Jena. http://www.personal.uni-jena.de/~b6biol2/ProgramsMain.html.

194. Maddison DR, Maddison WP, 2000. MacClade 4: *Analysis of Phylogeny and Character Evolution*. Sunderland: Sinauer Associates.

195. Swofford D, 1999. PAUP*: *Phylogenetic Analysis Using Parsimony (*and other methods)*. Sunderland: Sinauer Associates.

196. Felsenstein J, 1985. Confidence limits on phylogenies: An approach using the bootstrap. *Evolution 39*: 783-791.

197. Ronquist F, Huelsenbeck JP, 2003. MrBayes 3: Bayesian phylogenetic inference under mixed models. *Bioinformatics 19*: 1572-4.

198. Rambaut A, Drummond A, 2006. Tracer: University of Oxford, A program for analysing results from Bayesian MCMC programs such as BEAST & MrBayes. http://evolve.zoo.ox.ac.uk/software.html?id=tracer.

199. Simon C, Frati F, Beckenbach A, Crespi B, Liu H, Flook P, 1994. Evolution, weighting, and phylogenetic utility of mitochondrial gene sequences and a compilation of conserved polymerase chain reaction primers. *Ann Entomol Soc Am 87*: 651-701.

200. Kjer KM, 1995. Use of rRNA secondary structure in phylogenetic studies to identify homologous positions: An example of alignment and data presentation from the frogs. *Mol Phylogenet Evol 4*: 314-330.

201. Gillespie JJ, 2004. Characterizing regions of ambiguous alignment caused by the expansion and contraction of hairpin-stem loops in ribosomal RNA molecules. *Mol Phylogenet Evol 33*: 936-43.

202. Cannone JJ, Subramanian S, Schnare MN, Collett JR, D'Souza LM, Du Y, Feng B, Lin N, Madabusi LV, Muller KM, Pande N, Shang Z, Yu N, Gutell RR, 2002. The comparative RNA web (CRW) site: an online database of comparative sequence and structure information for ribosomal, intron, and other RNAs. *BMC Bioinformatics 3*: 2.

203. Van de Peer Y, Robbrecht E, de Hoog S, Caers A, De Rijk P, De Wachter R, 1999. Database on the structure of small subunit ribosomal RNA. *Nucleic Acids Res 27*: 179-83.

204. Wuyts J, De Rijk P, Van de Peer Y, Pison G, Rousseeuw P, De Wachter R, 2000. Comparative analysis of more than 3000 sequences reveals the existence of two pseudoknots in area V4 of eukaryotic small subunit ribosomal RNA. *Nucleic Acids Res 28*: 4698-708.

205. Alkemar G, Nygård O, 2003. A possible tertiary rRNA interaction between expansion segments ES3 and ES6 in eukaryotic 40S ribosomal subunits. *RNA 9*: 20-24.

206. Gillespie JJ, McKenna CH, Yoder MJ, Gutell RR, Johnston JS, Kathirithamby J, Cognato AI, 2005. Assessing the odd secondary structural properties of nuclear small subunit ribosomal RNA sequences (18S) of the twisted-wing parasites (Insecta: Strepsiptera). *Insect Mol Biol 14*: 625-43.

207. Gillespie JJ, Johnston JS, Cannone JJ, Gutell RR, 2006. Characteristics of the nuclear (18S, 5.8S, 28S and 5S) and mitochondrial (12S and 16S) rRNA genes of *Apis mellifera* (Insecta: Hymenoptera): structure, organization, and retrotransposable elements. *Insect Mol Biol 15*: 657-86.

208. Zuker M, mfold: Washington University. http://www.bioinfo.rpi.edu/applications/mfold/download/.

209. Mathews DH, Sabina J, Zuker M, Turner DH, 1999. Expanded sequence dependence of thermodynamic parameters improves prediction of RNA secondary structure. *J Mol Biol 288*: 911-40.

210. Zuker M, Mathews DH, Turner DH, 1999. Algorithms and theromodynamic for RNA secondary structure prediction: a practical guide. Barciszewski J, Clark BFC, eds. *RNA Biochemistry and Biotechnology*. Boston: Kluwer Academic Publications, 11-43.

211. Zuker M, 2003. Mfold web server for nucleic acid folding and hybridization prediction. *Nucleic Acids Res 31*: 3406-15.

212. Kjer KM, 1997. An alignment template for amphibian 12S rRNA, domain III: conserved primary and secondary structural motifs. *J Herpetology 31*: 559-604.

213. Smith TG, 1996. The genus *Hepatozoon* (Apicomplexa: Adeleina). *J Parasitol 82*: 565-85.

214. Craig TM, Smallwood JE, Knauer KW, McGrath JP, 1978. *Hepatozoon canis* infection in dogs: clinical, radiographic, and hematologic findings. *J Am Vet Med Assoc 173*: 967-72.

215. Mercer SH, Jones LP, Rappole JH, Twedt D, Lack LL, Craig TM, 1988. *Hepatozoon* sp. in wild carnivores in Texas. *J Wildl Dis 24*: 574-6.

216. Osimani JJ, 1942. *Haemogregarina triatomae* n. sp. from a South American lizard *Tupinambis teguixin* transmitted by the reduviid *Triatoma rubrovaria*. *J Parasitol 28*: 147-154.

217. Aguilera X, Miles MA, Apt W, 1986. *Triatoma spinolai* in Chile: a new host for *Hepatozoon triatomae*. *Trans R Soc Trop Med Hyg 80*: 492-3.

218. Bice DE, 1965. A sporozoan parasite of *Triatoma rubida uhleri*. *Rev Bio Trop 13*: 293-296.

219. Alkemar G, Nygård O, 2004. Secondary structure of two regions in expansion segments ES3 and ES6 with the potential of forming a tertiary interaction in eukaryotic 40S ribosomal subunits. *RNA* 10: 403-11.

220. Dixon MT, Hillis DM, 1993. Ribosomal RNA secondary structure: compensatory mutations and implications for phylogenetic analysis. *Mol Biol Evol 10*: 256-67.

221. Merzlyak E, Yurchenko V, Kolesnikov AA, Alexandrov K, Podlipaev SA, Maslov DA, 2001. Diversity and phylogeny of insect trypanosomatids based on small subunit rRNA genes: polyphyly of *Leptomonas* and *Blastocrithidia*. *J Eukaryot Microbiol 48*: 161-9.

222. Miles MA, Cedillos RA, Povoa MM, de Souza AA, Prata A, Macedo V, 1981. Do radically dissimilar *Trypanosoma cruzi* strains (zymodemes) cause Venezuelan and Brazilian forms of Chagas' disease? *Lancet 1*: 1338-40.

223. Mendonca MB, Nehme NS, Santos SS, Cupolillo E, Vargas N, Junqueira A, Naiff RD, Barrett TV, Coura JR, Zingales B, Fernandes O, 2002. Two main clusters within *Trypanosoma cruzi* zymodeme 3 are defined by distinct regions of the ribosomal RNA cistron. *Parasitology 124*: 177-84.

224. Clark CG, Pung OJ, 1994. Host specificity of ribosomal DNA variation in sylvatic *Trypanosoma cruzi* from North America. *Mol Biochem Parasitol 66*: 175-9.

225. Andrade LO, Machado CR, Chiari E, Pena SD, Macedo AM, 1999. Differential tissue distribution of diverse clones of *Trypanosoma cruzi* in infected mice. *Mol Biochem Parasitol 100*: 163-72.

226. Barr SC, Gossett KA, Klei TR, 1991. Clinical, clinicopathologic, and parasitologic observations of trypanosomiasis in dogs infected with North American *Trypanosoma cruzi* isolates. *Am J Vet Res 52*: 954-60.

227. Tibayrenc M, Ward P, Moya A, Ayala FJ, 1986. Natural populations of *Trypanosoma cruzi*, the agent of Chagas disease, have a complex multiclonal structure. *Proc Natl Acad Sci U S A 83*: 115-9.

228. Breniere SF, Bosseno MF, Telleria J, Carrasco R, Vargas F, Yaksic N, Noireau F, 1995. Field application of polymerase chain reaction diagnosis and strain typing of *Trypanosoma cruzi* in Bolivian triatomines. *Am J Trop Med Hyg 53*: 179-84.

229. Breniere SF, Bosseno MF, Telleria J, Bastrenta B, Yacsik N, Noireau F, Alcazar JL, Barnabe C, Wincker P, Tibayrenc M, 1998. Different behavior of two *Trypanosoma cruzi* major clones: transmission and circulation in young Bolivian patients. *Exp Parasitol 89*: 285-95.

230. Veloso VM, Romanha AJ, Lana M, Murta SM, Carneiro CM, Alves CF, Borges EC, Tafuri WL, Machado-Coelho GL, Chiari E, Bahia MT, 2005. Influence of the long-term *Trypanosoma cruzi* infection in vertebrate host on the genetic and biological diversity of the parasite. *Parasitol Res 96*: 382-9.

231. El-Sayed NM, Myler PJ, Bartholomeu DC, Nilsson D, Aggarwal G, Tran AN, Ghedin E, Worthey EA, Delcher AL, Blandin G, Westenberger SJ, Caler E, Cerqueira GC, Branche C, Haas B, Anupama A, Arner E, Aslund L, Attipoe P, Bontempi E, Bringaud F, Burton P, Cadag E, Campbell DA, Carrington M, Crabtree J, Darban H, da Silveira JF, de Jong P, Edwards K, Englund PT, Fazelina G, Feldblyum T, Ferella M, Frasch AC, Gull K, Horn D, Hou L, Huang Y, Kindlund E, Klingbeil M, Kluge S, Koo H, Lacerda D, Levin MJ, Lorenzi H, Louie T, Machado CR, McCulloch R, McKenna A, Mizuno Y, Mottram JC, Nelson S, Ochaya S, Osoegawa K, Pai G, Parsons M, Pentony M, Pettersson U, Pop M, Ramirez JL, Rinta J, Robertson L, Salzberg SL, Sanchez DO, Seyler A, Sharma R, Shetty J, Simpson AJ, Sisk E, Tammi MT, Tarleton R, Teixeira S, Van Aken S, Vogt C, Ward PN, Wickstead B, Wortman J, White O, Fraser CM, Stuart KD, Andersson B, 2005. The genome sequence of *Trypanosoma cruzi*, etiologic agent of Chagas disease. *Science 309*: 409-15.

232. Ohta T, 2000. Evolution of gene families. *Gene 259*: 45-52.

233. Stothard J, Frame I, Miles M, 1999. Genetic diversity and genetic exchange in *Trypanosoma cruzi*: dual drug-resistant "progeny" from episomal transformants. *Mem Inst Oswaldo Cruz 94 Suppl 1*: 189-93.

234. Stothard JR, 2001. Ribosomal internal transcribed spacers separate triatomines. *Trends Parasitol 17*: 213-4.

235. Stevens J, Gibson W, 2000. Reply. *Parasitol Today 16*: 173.

236. Brisse S, Henriksson J, Barnabe C, Douzery EJ, Berkvens D, Serrano M, De Carvalho MR, Buck GA, Dujardin JC, Tibayrenc M, 2003. Evidence for genetic exchange and hybridization in *Trypanosoma cruzi* based on nucleotide sequences and molecular karyotype. *Infect Genet Evol 2*: 173-83.

237. Tibayrenc M, 2003. Genetic subdivisions within *Trypanosoma cruzi* (Discrete Typing Units) and their relevance for molecular epidemiology and experimental evolution. *Kinetoplastid Biol Dis 2*: 12.

238. Westenberger SJ, Barnabe C, Campbell DA, Sturm NR, 2005. Two hybridization events define the population structure of *Trypanosoma cruzi*. *Genetics 171*: 527-43.

239. Gaunt MW, Yeo M, Frame IA, Stothard JR, Carrasco HJ, Taylor MC, Mena SS, Veazey P, Miles GA, Acosta N, de Arias AR, Miles MA, 2003. Mechanism of genetic exchange in American trypanosomes. *Nature 421*: 936-9.

240. Stothard JR, 2000. Trypanosome trees and homologies. *Parasitol Today 16*: 173.

241. Grosjean NL, Vrable RA, Murphy AJ, Mansfield LS, 2003. Seroprevalence of antibodies against *Leishmania* spp among dogs in the United States. *J Am Vet Med Assoc 222*: 603-6.

242. Nabity MB, Barnhart K, Logan KS, Santos RL, Kessell A, Melmed C, Snowden KF, 2006. An atypical case of *Trypanosoma cruzi* infection in a young English Mastiff. *Vet Parasitol 140*: 356-61.

243. 2006. Veterinary Diagnostic Laboratory, Texas: Sunset Advisory Commission, 1-54. http://www.sunset.state.tx.us/80threports/vmd/vmd.pdf.

244. AKC, 2006. American Kennel Club dog registration statistics. http://www.akc.org/reg/dogreg_stats_2006.cfm.

245. Yaeger RG, 1971. Transmission of *Trypanosoma cruzi* infection to opossums via the oral route. *J Parasitol 57*: 1375-6.

246. Reithinger R, Ceballos L, Stariolo R, Davies CR, Gurtler RE, 2005. Chagas disease control: deltamethrin-treated collars reduce *Triatoma infestans* feeding success on dogs. *Trans R Soc Trop Med Hyg 99*: 502-8.

247. Castanera MB, Lauricella MA, Chuit R, Gurtler RE, 1998. Evaluation of dogs as sentinels of the transmission of *Trypanosoma cruzi* in a rural area of north-western Argentina. *Ann Trop Med Parasitol 92*: 671-83.

248. Gurtler RE, Kravetz FO, Petersen RM, Lauricella MA, Wisnivesky-Colli C, 1990. The prevalence of *Trypanosoma cruzi* and the demography of dog populations after insecticidal spraying of houses: a predictive model. *Ann Trop Med Parasitol 84*: 313-23.

249. Gurtler RE, Cecere MC, Lauricella MA, Petersen RM, Chuit R, Segura EL, Cohen JE, 2005. Incidence of *Trypanosoma cruzi* infection among children following domestic reinfestation after insecticide spraying in rural northwestern Argentina. *Am J Trop Med Hyg 73*: 95-103.

250. Gurtler RE, Cohen JE, Cecere MC, Chuit R, 1997. Shifting host choices of the vector of Chagas disease *Triatoma infestans* in relation to the availability of hosts in houses in north-west Argentina. *J Appl Ecol 34*: 699-715.

APPENDIX A

Forest landscape metrices for each designated *T. gerstaeckeri* habitat buffer zone in Texas, 2005-2006

Zone	County	CA	PLAND	NP	LPI
1	Zavala	1,212.6	49.0	108.0	45.8
2	Burnet	1,125.9	46.3	165.0	11.9
3	Nueces	854.8	34.3	362.0	15.3
4	Kerr	587.7	24.0	282.0	5.2
5	Nueces	711.2	28.5	209.0	21.5
6	Kendall	1,183.2	48.3	191.0	30.4
7	Kleberg	496.3	19.8	434.0	3.9
8	Gillespie	321.6	13.2	388.0	2.2
9	Karnes	280.2	11.3	1,008.0	0.4
10	McMullen	575.1	23.2	1,103.0	1.7
11	Williamson	874.6	36.0	302.0	8.4
12	Lampasas	479.3	19.8	526.0	2.5
13	Cameron	1,265.4	50.0	46.0	48.0
14	LaSalle	1,219.4	49.1	184.0	30.1
15	Dimmit	978.1	39.5	187.0	23.4
16	Hidalgo	1,125.0	44.4	226.0	40.9
17	Real	963.5	39.3	263.0	16.0
18	Blanco	631.8	26.0	366.0	11.3
	MEAN	827.0	33.4	352.8	17.7
	SD	325.5	13.0	282.2	15.6
	MIN	280.2	11.3		
	MAX	1,265.4	50.0		

CA = Total class area (hectares); PLAND = Percentage of landscape

NP = number of patches; LPI = large patch index (%)

APPENDIX B

Water landscape metrices for each designated *T. gerstaeckeri* habitat buffer zone in Texas, 2005-2006

Zone	County	CA	PLAND	NP	LPI
1	Zavala	15.3	0.6	55.0	0.1
2	Burnet	423.5	17.4	122.0	14.2
3	Nueces	76.3	3.1	72.0	0.9
4	Kerr	32.5	1.3	68.0	0.3
5	Nueces	1,208.4	48.3	105.0	47.0
6	Kendall	28.0	1.1	217.0	0.1
7	Kleberg	12.4	0.5	38.0	0.1
8	Gillespie	3.1	0.1	18.0	0.0
9	Karnes	0.8	0.0	3.0	0.0
10	McMullen	19.1	0.8	6.0	0.4
11	Williamson	3.8	0.2	38.0	0.0
12	Lampasas	7.7	0.3	55.0	0.0
13	Cameron	55.0	2.2	9.0	0.7
14	LaSalle	0.2	0.0	1.0	0.0
15	Dimmit	10.8	0.4	26.0	0.1
16	Hidalgo	39.0	1.5	34.0	0.3
17	Real	9.0	0.4	46.0	0.1
18	Blanco	2.3	0.1	17.0	0.0
	MEAN	108.2	4.4	51.7	3.6
	SD	291.3	11.7	53.3	11.3
	MIN	0.2	0.0		
	MAX	1,208.4	48.3		

CA = Total class area (hectares); PLAND = Percentage of landscape

NP = number of patches; LPI = large patch index (%)

APPENDIX C

Urban landscape metrices for each designated *T. gerstaeckeri* habitat buffer zone in Texas, 2005-2006

Zone	County	CA	PLAND	NP	LPI
1	Zavala	204.8	8.3	209.0	1.7
2	Burnet	13.4	0.6	53.0	0.1
3	Nueces	14.6	0.6	18.0	0.3
4	Kerr	69.3	2.8	109.0	0.5
5	Nueces	158.0	6.3	159.0	0.9
6	Kendall	37.5	1.5	112.0	0.1
7	Kleberg	77.6	3.1	110.0	0.7
8	Gillespie	2.3	0.1	16.0	0.0
9	Karnes	3.6	0.1	11.0	0.1
10	McMullen	6.5	0.3	26.0	0.0
11	Williamson	8.3	0.3	52.0	0.0
12	Lampasas	164.6	6.8	241.0	2.7
13	Cameron	20.9	0.8	31.0	0.3
14	LaSalle	6.5	0.3	8.0	0.1
15	Dimmit	197.6	8.0	94.0	3.1
16	Hidalgo	196.0	7.7	107.0	1.3
17	Real	51.5	2.1	101.0	0.2
18	Blanco	7.7	0.3	13.0	0.2
	MEAN	68.9	2.8	81.7	0.7
	SD	77.4	3.1	69.5	0.9
	MIN	2.3	0.1		
	MAX	204.8	8.3		

CA = Total class area (hectares); PLAND = Percentage of landscape

NP = number of patches; LPI = large patch index (%)

APPENDIX D

Rangeland landscape metrices for each designated *T. gerstaeckeri* habitat buffer zone in Texas, 2005-2006

Zone	County	CA	PLAND	NP	LPI
1	Zavala	778.6	31.5	435.0	5.1
2	Burnet	454.5	18.7	352.0	8.6
3	Nueces	144.2	5.8	288.0	0.6
4	Kerr	1,532.0	62.7	128.0	47.9
5	Nueces	179.0	7.2	458.0	1.4
6	Kendall	426.2	17.4	511.0	3.1
7	Kleberg	1,002.2	40.0	546.0	9.4
8	Gillespie	1,082.4	44.4	372.0	22.6
9	Karnes	2,121.1	85.7	16.0	85.6
10	McMullen	1,858.4	74.8	20.0	74.7
11	Williamson	895.1	36.9	417.0	14.4
12	Lampasas	925.7	38.3	539.0	12.2
13	Cameron	417.3	16.5	251.0	4.3
14	LaSalle	352.5	14.2	814.0	0.7
15	Dimmit	1,067.3	43.1	244.0	17.6
16	Hidalgo	13.6	0.5	48.0	0.1
17	Real	1,309.9	53.4	174.0	32.6
18	Blanco	957.6	39.3	449.0	14.2
	MEAN	862.1	35.0	336.8	19.7
	SD	587.8	23.8	211.8	25.3
	MIN	13.6	0.5		
	MAX	2,121.1	85.7		

CA = Total class area (hectares); PLAND = Percentage of landscape

NP = number of patches; LPI = large patch index (%)

APPENDIX E

Agriculture landscape metrices for each designated *T. gerstaeckeri* habitat buffer zone in Texas, 2005-2006

Zone	County	CA	PLAND	NP	LPI
1	Zavala	264.2	10.7	255.0	1.7
2	Burnet	414.7	17.1	776.0	3.0
3	Nueces	1,403.3	56.3	223.0	41.8
4	Kerr	222.9	9.1	455.0	1.2
5	Nueces	243.0	9.7	335.0	1.0
6	Kendall	773.8	31.6	611.0	7.4
7	Kleberg	914.8	36.5	544.0	6.1
8	Gillespie	1,029.6	42.2	500.0	12.5
9	Karnes	69.2	2.8	144.0	0.3
10	McMullen	23.9	1.0	123.0	0.1
11	Williamson	644.4	26.6	933.0	2.3
12	Lampasas	840.6	34.8	686.0	7.5
13	Cameron	773.6	30.5	475.0	3.8
14	LaSalle	904.6	36.4	385.0	8.6
15	Dimmit	224.1	9.0	187.0	1.1
16	Hidalgo	1,159.9	45.8	290.0	26.4
17	Real	117.5	4.8	563.0	0.1
18	Blanco	834.4	34.3	822.0	6.7
	MEAN	603.2	24.4	461.5	7.3
	SD	414.1	16.6	240.6	10.7
	MIN	23.9	1.0		
	MAX	1,403.3	56.3		

CA = Total class area (hectares); PLAND = Percentage of landscape

NP = number of patches; LPI = large patch index (%)

VITA

Name: Sonia Alane Kjos

Address: Department of Entomology, TAMU 2475, Texas A&M University, College Station, TX 77843-2475

Email Address: skjos@tamu.edu

Education: B.S., University of Minnesota, Minneapolis, 1986
M.S., University of Texas School of Public Health, Houston, 2000
Ph.D., Texas A&M University, College Station, 2007